

# CITATION REPORT

List of articles citing

## Black phosphorus field-effect transistors

DOI: 10.1038/nnano.2014.35

Nature Nanotechnology, 2014, 9, 372-7.

**Source:** <https://exaly.com/paper-pdf/58813012/citation-report.pdf>

**Version:** 2024-04-25

This report has been generated based on the citations recorded by exaly.com for the above article. For the latest version of this publication list, visit the link given above.

The third column is the impact factor (IF) of the journal, and the fourth column is the number of citations of the article.

#	Paper	IF	Citations
2298	Interaction of Black Phosphorus with Oxygen and Water.		
2297	.		
2296	Photocharge Trapping in Two-Sheet Reduced Graphene Oxide/Ti <sub>0.87</sub> O <sub>2</sub> Heterostructures and Their Photoreduction and Photomemory Applications.		
2295	Synthesis, Characterization, and Device Application of Antimony-Substituted Violet Phosphorus: A Layered Material.		
2294	Tunable Photoinduced Carrier Transport of a Black Phosphorus Transistor with Extended Stability Using a Light-Sensitized Encapsulated Layer.		
2293	Retraction of Few-Layer Antimonene: Large Yield Synthesis, Exact Atomical Structure, and Outstanding Optical Limiting.		
2292	Anomalous Temperature Dependence in Metal/Black Phosphorus Contact.		
2291	Impact of Organic Molecule-Induced Charge Transfer on Operating Voltage Control of Both nMoS <sub>2</sub> and pMoTe <sub>2</sub> Transistors.		
2290	Long-Term Stability and Reliability of Black Phosphorus Field-Effect Transistors.		
2289	The Rise of Elemental Two-Dimensional Materials Beyond Graphene. <b>2014</b> , 67, 1370		22
2288	Anisotropic charged impurity-limited carrier mobility in monolayer phosphorene. <b>2014</b> , 116, 214505		26
2287	Chemical scissors cut phosphorene nanostructures. <b>2014</b> , 1, 045041		17
2286	Electronic, phononic, and thermoelectric properties of graphyne sheets. <b>2014</b> , 105, 223108		58
2285	Electron-doped phosphorene: A potential monolayer superconductor. <b>2014</b> , 108, 67004		74
2284	Dirac fermions in blue-phosphorus. <b>2014</b> , 1, 031002		29
2283	Temporal and Thermal Stability of Al <sub>2</sub> O <sub>3</sub> -Passivated Phosphorene MOSFETs. <b>2014</b> , 35, 1314-1316		68
2282	Towards high-performance two-dimensional black phosphorus optoelectronic devices: the role of metal contacts. <b>2014</b> ,		12

2281	Phosphorene nanoribbons. <b>2014</b> , 108, 47005	118
2280	Two-dimensional flexible nanoelectronics. <b>2014</b> , 5, 5678	1201
2279	A theoretical study of blue phosphorene nanoribbons based on first-principles calculations. <b>2014</b> , 116, 073704	67
2278	Edge effects on the electronic properties of phosphorene nanoribbons. <b>2014</b> , 116, 144301	133
2277	High Stability of Faceted Nanotubes and Fullerenes of Multiphase Layered Phosphorus: A Computational Study. <b>2014</b> , 113, 226801	73
2276	Tiling phosphorene. <b>2014</b> , 8, 12763-8	109
2275	Two-dimensional material nanophotonics. <b>2014</b> , 8, 899-907	1805
2274	The extended stability range of phosphorus allotropes. <b>2014</b> , 53, 11629-33	113
2273	Lattice vibrational modes and Raman scattering spectra of strained phosphorene. <b>2014</b> , 105, 083120	140
2272	Coexistence of size-dependent and size-independent thermal conductivities in phosphorene. <b>2014</b> , 90,	159
2271	Device Perspective on 2D Materials. <b>2014</b> ,	
2270	First principles study of metal contacts to monolayer black phosphorous. <b>2014</b> , 116, 204302	27
2269	Ultrahigh sensitivity and gain white light photodetector based on GaTe/Sn:CdS nanoflake/nanowire heterostructures. <b>2014</b> , 25, 445202	15
2268	Strain-engineering the anisotropic electrical conductance of few-layer black phosphorus. <b>2014</b> , 14, 2884-9	984
2267	Two-dimensional crystals: phosphorus joins the family. <i>Nature Nanotechnology</i> , <b>2014</b> , 9, 330-1	28.7 444
2266	Theoretical prediction of hydrogen storage on Li-decorated monolayer black phosphorus. <b>2014</b> , 47, 465302	35
2265	The potential application of phosphorene as an anode material in Li-ion batteries. <b>2014</b> , 2, 19046-19052	254
2264	Few-layer black phosphorus field-effect transistors with reduced current fluctuation. <b>2014</b> , 8, 11753-62	245

2263	Black phosphorus radio-frequency transistors. <b>2014</b> , 14, 6424-9	270
2262	Hinge-like structure induced unusual properties of black phosphorus and new strategies to improve the thermoelectric performance. <b>2014</b> , 4, 6946	181
2261	Magnetism of zigzag edge phosphorene nanoribbons. <b>2014</b> , 105, 113105	85
2260	Die erweiterte Stabilitätsreihe der Phosphorallotrope. <b>2014</b> , 126, 11813-11817	30
2259	The Effect of Dielectric Capping on Few-Layer Phosphorene Transistors: Tuning the Schottky Barrier Heights. <b>2014</b> , 35, 795-797	142
2258	Theoretical Prediction of Carrier Mobility in Few-Layer BC <sub>2</sub> N. <b>2014</b> , 5, 4073-7	68
2257	Effective passivation of exfoliated black phosphorus transistors against ambient degradation. <b>2014</b> , 14, 6964-70	1117
2256	Black phosphorus photodetector for multispectral, high-resolution imaging. <b>2014</b> , 14, 6414-7	495
2255	Topological origin of quasi-flat edge band in phosphorene. <b>2014</b> , 16, 115004	134
2254	Performance Limits Projection of Black Phosphorous Field-Effect Transistors. <b>2014</b> , 35, 963-965	79
2253	Electronic bandgap and edge reconstruction in phosphorene materials. <b>2014</b> , 14, 6400-6	365
2252	Proton intercalated two-dimensional WO <sub>3</sub> nano-flakes with enhanced charge-carrier mobility at room temperature. <b>2014</b> , 6, 15029-36	53
2251	Strong Thermal Transport Anisotropy and Strain Modulation in Single-Layer Phosphorene. <b>2014</b> , 118, 25272-25277	219
2250	Investigations on V <sub>2</sub> C and V <sub>2</sub> CX <sub>2</sub> (X = F, OH) Monolayer as a Promising Anode Material for Li Ion Batteries from First-Principles Calculations. <b>2014</b> , 118, 24274-24281	215
2249	Electronic structure of black phosphorus studied by angle-resolved photoemission spectroscopy. <b>2014</b> , 90,	73
2248	Prediction of silicon-based layered structures for optoelectronic applications. <b>2014</b> , 136, 15992-7	36
2247	Towards intrinsic charge transport in monolayer molybdenum disulfide by defect and interface engineering. <b>2014</b> , 5, 5290	448
2246	Tuning of the electronic and optical properties of single-layer black phosphorus by strain. <b>2014</b> , 90,	235

2245	Mechanical and electronic properties of monolayer and bilayer phosphorene under uniaxial and isotropic strains. <b>2014</b> , 25, 455703	56
2244	Strain Engineering for Phosphorene: The Potential Application as a Photocatalyst. <b>2014</b> , 118, 26560-26568	314
2243	Simulation of phosphorene Schottky-barrier transistors. <b>2014</b> , 105, 163511	25
2242	Enhanced thermoelectric efficiency via orthogonal electrical and thermal conductances in phosphorene. <b>2014</b> , 14, 6393-9	571
2241	Ambipolar phosphorene field effect transistor. <b>2014</b> , 8, 11730-8	299
2240	Two-dimensional heterostructures: fabrication, characterization, and application. <b>2014</b> , 6, 12250-72	266
2239	Origin of photoresponse in black phosphorus phototransistors. <b>2014</b> , 90,	154
2238	Excitons in anisotropic two-dimensional semiconducting crystals. <b>2014</b> , 90,	108
2237	Electronic Properties of Edge-Hydrogenated Phosphorene Nanoribbons: A First-Principles Study. <b>2014</b> , 118, 22368-22372	108
2236	Tunable optical properties of multilayer black phosphorus thin films. <b>2014</b> , 90,	496
2235	Back gated multilayer InSe transistors with enhanced carrier mobilities via the suppression of carrier scattering from a dielectric interface. <b>2014</b> , 26, 6587-93	331
2234	Strain-engineered direct-indirect band gap transition and its mechanism in two-dimensional phosphorene. <b>2014</b> , 90,	675
2233	Electrons and holes in phosphorene. <b>2014</b> , 90,	126
2232	High-mobility transport anisotropy and linear dichroism in few-layer black phosphorus. <b>2014</b> , 5, 4475	2892
2231	Phosphorene as a Superior Gas Sensor: Selective Adsorption and Distinct I-V Response. <b>2014</b> , 5, 2675-81	723
2230	Enhanced thermoelectric performance of phosphorene by strain-induced band convergence. <b>2014</b> , 90,	213
2229	Polarized photocurrent response in black phosphorus field-effect transistors. <b>2014</b> , 6, 8978-83	279
2228	Bilayer Phosphorene: Effect of Stacking Order on Bandgap and Its Potential Applications in Thin-Film Solar Cells. <b>2014</b> , 5, 1289-93	659

2227	Interface engineering for CVD graphene: current status and progress. <b>2014</b> , 10, 4443-54	25
2226	Rediscovering black phosphorus as an anisotropic layered material for optoelectronics and electronics. <b>2014</b> , 5, 4458	2389
2225	Black phosphorus-monolayer MoS <sub>2</sub> van der Waals heterojunction p-n diode. <b>2014</b> , 8, 8292-9	979
2224	Photovoltaic effect in few-layer black phosphorus PN junctions defined by local electrostatic gating. <b>2014</b> , 5, 4651	555
2223	Superior mechanical flexibility of phosphorene and few-layer black phosphorus. <b>2014</b> , 104, 251915	727
2222	Ab initio studies of thermodynamic and electronic properties of phosphorene nanoribbons. <b>2014</b> , 90,	112
2221	Tunable exciton funnel using Moiré superlattice in twisted van der Waals bilayer. <b>2014</b> , 14, 5350-7	49
2220	Access and in situ growth of phosphorene-precursor black phosphorus. <b>2014</b> , 405, 6-10	249
2219	Enabling silicon for solar-fuel production. <b>2014</b> , 114, 8662-719	274
2218	Tunable transport gap in phosphorene. <b>2014</b> , 14, 5733-9	578
2217	Phosphorene nanoribbon as a promising candidate for thermoelectric applications. <b>2014</b> , 4, 6452	244
2216	Ballistic Transport in Monolayer Black Phosphorus Transistors. <b>2014</b> , 61, 3871-3876	64
2215	Nonlinear valley and spin currents from Fermi pocket anisotropy in 2D crystals. <b>2014</b> , 113, 156603	64
2214	Two-dimensional mono-elemental semiconductor with electronically inactive defects: the case of phosphorus. <b>2014</b> , 14, 6782-6	170
2213	Stability and properties of 2D porous nanosheets based on tetraoxa[8]circulene analogues. <b>2014</b> , 6, 14962-70	25
2212	Modulation of the Electronic Properties of Ultrathin Black Phosphorus by Strain and Electrical Field. <b>2014</b> , 118, 23970-23976	218
2211	Electronics based on two-dimensional materials. <i>Nature Nanotechnology</i> , <b>2014</b> , 9, 768-79	28.7 1953
2210	Anisotropic elastic behaviour and one-dimensional metal in phosphorene. <b>2014</b> , 8, 939-942	24

2209	Formation of stable phosphorus-carbon bond for enhanced performance in black phosphorus nanoparticle-graphite composite battery anodes. <b>2014</b> , 14, 4573-80	627
2208	Fast and broadband photoresponse of few-layer black phosphorus field-effect transistors. <b>2014</b> , 14, 3347-52	1305
2207	Strain and orientation modulated bandgaps and effective masses of phosphorene nanoribbons. <b>2014</b> , 14, 4607-14	275
2206	Layer-controlled band gap and anisotropic excitons in few-layer black phosphorus. <b>2014</b> , 89,	1650
2205	Electrical contacts to monolayer black phosphorus: A first-principles investigation. <b>2014</b> , 90,	107
2204	Isolation and characterization of few-layer black phosphorus. <b>2014</b> , 1, 025001	1163
2203	Phase coexistence and metal-insulator transition in few-layer phosphorene: a computational study. <b>2014</b> , 113, 046804	451
2202	Extraordinary photoluminescence and strong temperature/angle-dependent Raman responses in few-layer phosphorene. <b>2014</b> , 8, 9590-6	529
2201	Structure and stability of two dimensional phosphorene with O or NH functionalization. <b>2014</b> , 4, 48017-48021	63
2200	Plasmons and screening in monolayer and multilayer black phosphorus. <b>2014</b> , 113, 106802	405
2199	Phosphorene Nanoribbons, Phosphorus Nanotubes, and van der Waals Multilayers. <b>2014</b> , 118, 14051-14059	467
2198	Quasiparticle band structure and tight-binding model for single- and bilayer black phosphorus. <b>2014</b> , 89,	484
2197	NH <sub>3</sub> Adsorption on Arsenene: A First Principle Study. <b>2015</b> ,	4
2196	Phonon-limited performance of single-layer, single-gate black phosphorus n- and p-type field-effect transistors. <b>2015</b> ,	13
2195	The challenging promise of 2D materials for electronics. <b>2015</b> ,	3
2194	Layered Black Phosphorus as a Selective Vapor Sensor. <b>2015</b> , 54, 14317-20	162
2193	Simulation Evidence of Hexagonal-to-Tetragonal ZnSe Structure Transition: A Monolayer Material with a Wide-Range Tunable Direct Bandgap. <b>2015</b> , 2, 1500290	38
2192	Collective modes in anisotropic double-layer systems. <b>2015</b> , 91,	23

2191	Electric field induced gap modification in ultrathin blue phosphorus. <b>2015, 91,</b>	111
2190	Atomically thin dilute magnetism in Co-doped phosphorene. <b>2015, 91,</b>	109
2189	Topologically protected Dirac cones in compressed bulk black phosphorus. <b>2015, 91,</b>	74
2188	Single-layer crystalline phases of antimony: Antimonenes. <b>2015, 91,</b>	224
2187	Effective-mass theory for the anisotropic exciton in two-dimensional crystals: Application to phosphorene. <b>2015, 91,</b>	39
2186	Magneto-optical transport properties of monolayer phosphorene. <b>2015, 92,</b>	49
2185	Structural phase transitions of phosphorene induced by applied strains. <b>2015, 92,</b>	26
2184	TiS3 nanoribbons: Width-independent band gap and strain-tunable electronic properties. <b>2015, 92,</b>	51
2183	Landau levels of single-layer and bilayer phosphorene. <b>2015, 92,</b>	84
2182	Thermal properties of black and blue phosphorenes from a first-principles quasiharmonic approach. <b>2015, 92,</b>	111
2181	Toward a realistic description of multilayer black phosphorus: From GW approximation to large-scale tight-binding simulations. <b>2015, 92,</b>	146
2180	Van Hove singularity and ferromagnetic instability in phosphorene. <b>2015, 92,</b>	29
2179	Excitons in one-dimensional van der Waals materials: Sb2S3 nanoribbons. <b>2015, 92,</b>	21
2178	Prediction of a two-dimensional crystalline structure of nitrogen atoms. <b>2015, 92,</b>	99
2177	Significant effect of stacking on the electronic and optical properties of few-layer black phosphorus. <b>2015, 92,</b>	135
2176	Aspects of anisotropic fractional quantum Hall effect in phosphorene. <b>2015, 92,</b>	18
2175	Symmetry, distorted band structure, and spin-orbit coupling of group-III metal-monochalcogenide monolayers. <b>2015, 92,</b>	40
2174	Pressure-Induced Electronic Transition in Black Phosphorus. <b>2015, 115, 186403</b>	118



2173	Enhanced stability of black phosphorus field-effect transistors with SiO <sub>2</sub> passivation. <b>2015</b> , 26, 435702	83
2172	Anisotropic exciton Stark shift in black phosphorus. <b>2015</b> , 91,	85
2171	Ab initio study of electron-phonon interaction in phosphorene. <b>2015</b> , 91,	137
2170	Design for a spin-Seebeck diode based on two-dimensional materials. <b>2015</b> , 92,	49
2169	Magnetoelectronic properties of multilayer black phosphorus. <b>2015</b> , 92,	34
2168	Interpreting core-level spectra of oxidizing phosphorene: Theory and experiment. <b>2015</b> , 92,	31
2167	Excitonic effects in two-dimensional semiconductors: Path integral Monte Carlo approach. <b>2015</b> , 92,	41
2166	Topological currents in black phosphorus with broken inversion symmetry. <b>2015</b> , 92,	35
2165	Analyzing Longitudinal Magnetoresistance Asymmetry to Quantify Doping Gradients: Generalization of the van der Pauw Method. <b>2015</b> , 115, 186804	3
2164	Stacked bilayer phosphorene: strain-induced quantum spin Hall state and optical measurement. <b>2015</b> , 5, 13927	55
2163	Strain-driven band inversion and topological aspects in Antimonene. <b>2015</b> , 5, 16108	166
2162	Polarization and Thickness Dependent Absorption Properties of Black Phosphorus: New Saturable Absorber for Ultrafast Pulse Generation. <b>2015</b> , 5, 15899	225
2161	Strain induced piezoelectric effect in black phosphorus and MoS <sub>2</sub> van der Waals heterostructure. <b>2015</b> , 5, 16448	73
2160	Anomalous Quantum Transport Properties in Semimetallic Black Phosphorus. <b>2015</b> , 84, 073708	16
2159	Decay and the double-decay properties of edge bands of phosphorene ribbons. <b>2015</b> , 102, 610-615	3
2158	Synthesis of Extended Atomically Perfect Zigzag Graphene - Boron Nitride Interfaces. <b>2015</b> , 5, 16741	27
2157	Device performance simulations of multilayer black phosphorus tunneling transistors. <b>2015</b> , 107, 203501	25
2156	DGDFPT: A massively parallel method for large scale density functional theory calculations. <b>2015</b> , 143, 124110	42

2155	Gap state analysis in electric-field-induced band gap for bilayer graphene. <b>2015</b> , 5, 15789	33
2154	Effect of stacking order on device performance of bilayer black phosphorene-field-effect transistor. <b>2015</b> , 118, 224501	8
2153	Stacking sequence determines Raman intensities of observed interlayer shear modes in 2D layered materials--A general bond polarizability model. <b>2015</b> , 5, 14565	46
2152	Ultrafast recovery time and broadband saturable absorption properties of black phosphorus suspension. <b>2015</b> , 107, 091905	138
2151	Mechanical properties of phosphorene nanoribbons and oxides. <b>2015</b> , 118, 234304	26
2150	Tuning magnetotransport in a compensated semimetal at the atomic scale. <b>2015</b> , 6, 8892	109
2149	GeSe monolayer semiconductor with tunable direct band gap and small carrier effective mass. <b>2015</b> , 107, 122107	116
2148	Thermal effects on the Raman phonon of few-layer phosphorene. <b>2015</b> , 3, 126104	9
2147	Thermal conductivity of penta-graphene from molecular dynamics study. <b>2015</b> , 143, 154703	68
2146	Temperature coefficients of phonon frequencies and thermal conductivity in thin black phosphorus layers. <b>2015</b> , 107, 071905	41
2145	Understanding the Unique Electronic Properties of Nano Structures Using Photoemission Theory. <b>2015</b> , 5, 17834	4
2144	Performance change of few layer black phosphorus transistors in ambient. <b>2015</b> , 5, 107112	19
2143	(Invited) Microscopic Studies of Black Phosphorus and Its Field-Effect Transistors. <b>2015</b> , 69, 93-104	
2142	Synthesis of Atomically Thin Boron Films on Copper Foils. <b>2015</b> , 54, 15473-7	166
2141	Effects of interlayer interaction in van der Waals layered black phosphorus for sub-10 nm FET. <b>2015</b> , ,	5
2140	Field-effect transistors based on amorphous black phosphorus ultrathin films by pulsed laser deposition. <b>2015</b> , 27, 3748-54	222
2139	Anisotropic Thermal Conductivity of Exfoliated Black Phosphorus. <b>2015</b> , 27, 8017-22	178
2138	Black phosphorus saturable absorber for ultrafast mode-locked pulse laser via evanescent field interaction. <b>2015</b> , 527, 770-776	93

2137	The Cytotoxicity of Layered Black Phosphorus. <b>2015</b> , 21, 13991-5	143
2136	High Performance Polymer Nanowire Field-Effect Transistors with Distinct Molecular Orientations. <b>2015</b> , 27, 4963-8	68
2135	Synthesis of Atomically Thin Boron Films on Copper Foils. <b>2015</b> , 127, 15693-15697	55
2134	Electrochemically Exfoliated Black Phosphorus Nanosheets [Prospective Field Emitters. <b>2015</b> , 2015, 3102-3107	69
2133	Nonvolatile Floating-Gate Memories Based on Stacked Black Phosphorus/Boron Nitride/MoS <sub>2</sub> Heterostructures. <b>2015</b> , 25, 7360-7365	95
2132	From Black Phosphorus to Phosphorene: Basic Solvent Exfoliation, Evolution of Raman Scattering, and Applications to Ultrafast Photonics. <b>2015</b> , 25, 6996-7002	725
2131	Drying-Mediated Self-Assembled Growth of Transition Metal Dichalcogenide Wires and their Heterostructures. <b>2015</b> , 27, 4142-9	27
2130	Black Arsenic-Phosphorus: Layered Anisotropic Infrared Semiconductors with Highly Tunable Compositions and Properties. <b>2015</b> , 27, 4423-4429	282
2129	Black Phosphorus Terahertz Photodetectors. <b>2015</b> , 27, 5567-72	212
2128	Broadband Black Phosphorus Optical Modulator in the Spectral Range from Visible to Mid-Infrared. <b>2015</b> , 3, 1787-1792	91
2127	Black Phosphorus/Polymer Composites for Pulsed Lasers. <b>2015</b> , 3, 1447-1453	192
2126	Titanium Trisulfide Monolayer: Theoretical Prediction of a New Direct-Gap Semiconductor with High and Anisotropic Carrier Mobility. <b>2015</b> , 127, 7682-7686	58
2125	Diaceno[a,e]pentalenes: An Excellent Molecular Platform for High-Performance Organic Semiconductors. <b>2015</b> , 21, 17016-22	36
2124	Van der Waals p-n Junction Based on an Organic/Inorganic Heterostructure. <b>2015</b> , 25, 5865-5871	76
2123	Titanium trisulfide monolayer: theoretical prediction of a new direct-gap semiconductor with high and anisotropic carrier mobility. <b>2015</b> , 54, 7572-6	189
2122	Two-Dimensional Materials for Sensing: Graphene and Beyond. <b>2015</b> , 4, 651-687	232
2121	First-Principles Study on Electronic and Optical Properties of Graphene-Like Boron Phosphide Sheets. <b>2015</b> , 28, 588-594	36
2120	Highly stable two-dimensional silicon phosphides: Different stoichiometries and exotic electronic properties. <b>2015</b> , 91,	41

2119	Black Phosphorus p-MOSFETs With 7-nm HfO <sub>2</sub> Gate Dielectric and Low Contact Resistance. <b>2015</b> , 36, 411-413	68
2118	A Small Signal Amplifier Based on Ionic Liquid Gated Black Phosphorous Field Effect Transistor. <b>2015</b> , 36, 621-623	11
2117	Electronic Properties of Phosphorene/Graphene and Phosphorene/Hexagonal Boron Nitride Heterostructures. <b>2015</b> , 119, 13929-13936	244
2116	Exceptional and Anisotropic Transport Properties of Photocarriers in Black Phosphorus. <b>2015</b> , 9, 6436-42	139
2115	The structure and elastic properties of phosphorene edges. <b>2015</b> , 26, 235707	55
2114	Unexpected buckled structures and tunable electronic properties in arsenic nanosheets: insights from first-principles calculations. <b>2015</b> , 27, 225304	32
2113	Chemical modifications and stability of phosphorene with impurities: a first principles study. <b>2015</b> , 17, 15209-17	66
2112	Dynamical Evolution of Anisotropic Response in Black Phosphorus under Ultrafast Photoexcitation. <b>2015</b> , 15, 4650-6	113
2111	A first-principles study of sodium adsorption and diffusion on phosphorene. <b>2015</b> , 17, 16398-404	65
2110	A new phase of phosphorus: the missed tricycle type red phosphorene. <b>2015</b> , 27, 265301	33
2109	Simulated scanning tunneling microscopy images of few-layer phosphorus capped by graphene and hexagonal boron nitride monolayers. <b>2015</b> , 91,	27
2108	Group theory for structural analysis and lattice vibrations in phosphorene systems. <b>2015</b> , 91,	71
2107	Polarization-sensitive broadband photodetector using a black phosphorus vertical p-n junction. <i>Nature Nanotechnology</i> , <b>2015</b> , 10, 707-13	28.7 785
2106	Black Phosphorus Quantum Dots. <b>2015</b> , 127, 3724-3728	73
2105	Anomalous doping effect in black phosphorene using first-principles calculations. <b>2015</b> , 17, 16351-8	93
2104	Raman spectra of few-layer phosphorene studied from first-principles calculations. <b>2015</b> , 27, 185302	29
2103	Photooxidation and quantum confinement effects in exfoliated black phosphorus. <b>2015</b> , 14, 826-32	949
2102	Thermoelectric effects in graphene nanostructures. <b>2015</b> , 27, 133204	90

2101	Electrostatically Reversible Polarity of Ambipolar $\text{HMoTe}_2$ Transistors. <b>2015</b> , 9, 5976-83	89
2100	Flexible phosphorene devices and circuits. <b>2015</b> ,	
2099	A first-principles study on the magnetic properties of nonmetal atom doped phosphorene monolayers. <b>2015</b> , 17, 16341-50	75
2098	Graphene and beyond: two-dimensional materials for transistor applications. <b>2015</b> ,	4
2097	Functionalized graphene and other two-dimensional materials for photovoltaic devices: device design and processing. <b>2015</b> , 44, 5638-79	238
2096	Two-dimensional Kagome phosphorus and its edge magnetism: a density functional theory study. <b>2015</b> , 27, 255006	12
2095	Electric double-layer transistors: a review of recent progress. <b>2015</b> , 50, 5641-5673	126
2094	Theoretical predictions on the electronic structure and charge carrier mobility in 2D phosphorus sheets. <b>2015</b> , 5, 9961	153
2093	Layered Black Phosphorus as a Selective Vapor Sensor. <b>2015</b> , 127, 14525-14528	32
2092	Size and edge roughness effects on thermal conductivity of pristine antimonene allotropes. <b>2015</b> , 641, 169-172	46
2091	Probing 2D black phosphorus by quantum capacitance measurements. <b>2015</b> , 26, 485704	11
2090	2D materials via liquid exfoliation: a review on fabrication and applications. <b>2015</b> , 60, 1994-2008	180
2089	News Feature: Beyond graphene. <b>2015</b> , 112, 13128-30	16
2088	Large-Scale, Highly Efficient, and Green Liquid-Exfoliation of Black Phosphorus in Ionic Liquids. <b>2015</b> , 7, 27608-12	142
2087	Phase transition for edge band emergence induced by the edge relaxation of phosphorene ribbons. <b>2015</b> , 102, 290-294	1
2086	Analysing black phosphorus transistors using an analytic Schottky barrier MOSFET model. <b>2015</b> , 6, 8948	114
2085	Thulium/holmium-doped fiber laser passively mode locked by black phosphorus nanoplatelets-based saturable absorber. <b>2015</b> , 54, 10290-4	71
2084	Structural evolution and optoelectronic applications of multilayer silicene. <b>2015</b> , 92,	22

2083	Screening and plasmons in pure and disordered single- and bilayer black phosphorus. <b>2015</b> , 92,	31
2082	Elastic bending modulus for single-layer black phosphorus. <b>2015</b> , 48, 455305	21
2081	The mechanical exfoliation mechanism of black phosphorus to phosphorene: A first-principles study. <b>2015</b> , 112, 37003	24
2080	Quasiparticle energies, excitons, and optical spectra of few-layer black phosphorus. <b>2015</b> , 2, 044014	55
2079	Magnetic response at visible and near-infrared frequencies from black phosphorus sheet arrays. <b>2015</b> , 23, 30667-80	4
2078	Two-dimensional materials for nanophotonics application. <b>2015</b> , 4, 128-142	76
2077	Bandgap engineering in van der Waals heterostructures of blue phosphorene and MoS <sub>2</sub> : A first principles calculation. <b>2015</b> , 231, 64-69	48
2076	Defect-induced faceted blue phosphorene nanotubes. <b>2015</b> , 92,	20
2075	Optical Properties of Atomically Thin Layered Transition Metal Dichalcogenide. <b>2015</b> , 84, 121009	10
2074	Anomalous magneto-optical response of black phosphorus thin films. <b>2015</b> , 92,	47
2073	Photogalvanic effect in monolayer black phosphorus. <b>2015</b> , 26, 455202	71
2072	Gate tunable quantum oscillations in air-stable and high mobility few-layer phosphorene heterostructures. <b>2015</b> , 2, 011001	172
2071	Anisotropic intrinsic lattice thermal conductivity of phosphorene from first principles. <b>2015</b> , 17, 4854-8	296
2070	Layer-by-layer dielectric breakdown of hexagonal boron nitride. <b>2015</b> , 9, 916-21	120
2069	Scaling laws of band gaps of phosphorene nanoribbons: A tight-binding calculation. <b>2015</b> , 91,	93
2068	Ultrafast and directional diffusion of lithium in phosphorene for high-performance lithium-ion battery. <b>2015</b> , 15, 1691-7	512
2067	Microwave near-field imaging of two-dimensional semiconductors. <b>2015</b> , 15, 1122-7	34
2066	Small molecules make big differences: molecular doping effects on electronic and optical properties of phosphorene. <b>2015</b> , 26, 095201	136

2065	Van der Waals heterostructure of phosphorene and graphene: tuning the Schottky barrier and doping by electrostatic gating. <b>2015</b> , 114, 066803	372
2064	Edge State and Intrinsic Hole Doping in Bilayer Phosphorene. <b>2015</b> , 84, 013703	8
2063	Strongly anisotropic in-plane thermal transport in single-layer black phosphorene. <b>2015</b> , 5, 8501	378
2062	Giant Phononic Anisotropy and Unusual Anharmonicity of Phosphorene: Interlayer Coupling and Strain Engineering. <b>2015</b> , 25, 2230-2236	169
2061	Solid-State Reaction Synthesis of a InSe/CuInSe <sub>2</sub> Lateral p-n Heterojunction and Application in High Performance Optoelectronic Devices. <b>2015</b> , 27, 983-989	45
2060	In Situ Thermal Decomposition of Exfoliated Two-Dimensional Black Phosphorus. <b>2015</b> , 6, 773-8	172
2059	Environmental instability of few-layer black phosphorus. <b>2015</b> , 2, 011002	683
2058	Strain-induced semiconductor to metal transition in few-layer black phosphorus from first principles. <b>2015</b> , 622, 109-114	32
2057	Energetics, Charge Transfer, and Magnetism of Small Molecules Physisorbed on Phosphorene. <b>2015</b> , 119, 3102-3110	283
2056	Low Schottky barrier black phosphorus field-effect devices with ferromagnetic tunnel contacts. <b>2015</b> , 11, 2209-16	102
2055	Identifying the Crystalline Orientation of Black Phosphorus Using Angle-Resolved Polarized Raman Spectroscopy. <b>2015</b> , 127, 2396-2399	91
2054	Oxygen defects in phosphorene. <b>2015</b> , 114, 046801	432
2053	Native point defects in few-layer phosphorene. <b>2015</b> , 91,	96
2052	Thermoelectric power of bulk black-phosphorus. <b>2015</b> , 106, 022102	112
2051	Identifying the crystalline orientation of black phosphorus using angle-resolved polarized Raman spectroscopy. <b>2015</b> , 54, 2366-9	242
2050	Semiconductor to metal transition in bilayer phosphorene under normal compressive strain. <b>2015</b> , 26, 075701	75
2049	Silicene field-effect transistors operating at room temperature. <i>Nature Nanotechnology</i> , <b>2015</b> , 10, 227-318.7	1161
2048	Van der Waals heterostructures: Stacked 2D materials shed light. <b>2015</b> , 14, 264-5	167

2047	High-quality black phosphorus atomic layers by liquid-phase exfoliation. <b>2015</b> , 27, 1887-92	603
2046	Switching a normal insulator into a topological insulator via electric field with application to phosphorene. <b>2015</b> , 15, 1222-8	343
2045	A black phosphorus heterostructure for efficient visible-light-driven photocatalysis. <b>2015</b> , 3, 3285-3288	199
2044	Geometric and electronic structures of mono- and di-vacancies in phosphorene. <b>2015</b> , 26, 065705	48
2043	Van der Waals interactions in selected allotropes of phosphorus. <b>2015</b> , 230,	50
2042	Black phosphorus quantum dots. <b>2015</b> , 54, 3653-7	491
2041	Atomically thin arsenene and antimonene: semimetal-semiconductor and indirect-direct band-gap transitions. <b>2015</b> , 54, 3112-5	994
2040	Atomically Thin Arsenene and Antimonene: Semimetal Semiconductor and Indirect Direct Band-Gap Transitions. <b>2015</b> , 127, 3155-3158	323
2039	Photoluminescence quenching and charge transfer in artificial heterostacks of monolayer transition metal dichalcogenides and few-layer black phosphorus. <b>2015</b> , 9, 555-63	145
2038	A First-Principles Study on Electron Donor and Acceptor Molecules Adsorbed on Phosphorene. <b>2015</b> , 119, 2871-2878	137
2037	Single-layer MoS2 electronics. <b>2015</b> , 48, 100-10	329
2036	Stacked functionalized silicene: a powerful system to adjust the electronic structure of silicene. <b>2015</b> , 17, 5393-402	37
2035	CaFeAs2: A staggered intercalation of quantum spin Hall and high-temperature superconductivity. <b>2015</b> , 91,	35
2034	A Stillinger-Weber potential for single-layered black phosphorus, and the importance of cross-pucker interactions for a negative Poisson's ratio and edge stress-induced bending. <b>2015</b> , 7, 6059-68	69
2033	Compressive straining of bilayer phosphorene leads to extraordinary electron mobility at a new conduction band edge. <b>2015</b> , 15, 2006-10	37
2032	Thermal conduction in single-layer black phosphorus: highly anisotropic?. <b>2015</b> , 26, 055701	50
2031	Arsenene: Two-dimensional buckled and puckered honeycomb arsenic systems. <b>2015</b> , 91,	590
2030	Two-dimensional dichalcogenides for light-harvesting applications. <b>2015</b> , 10, 128-137	165



2029	Flexible black phosphorus ambipolar transistors, circuits and AM demodulator. <b>2015</b> , 15, 1883-90	341
2028	Waveguide-integrated black phosphorus photodetector with high responsivity and low dark current. <b>2015</b> , 9, 247-252	600
2027	Temperature dependent phonon shifts in few-layer black phosphorus. <b>2015</b> , 7, 5857-62	139
2026	Surface transfer doping induced effective modulation on ambipolar characteristics of few-layer black phosphorus. <b>2015</b> , 6, 6485	285
2025	Al <sub>2</sub> O <sub>3</sub> on Black Phosphorus by Atomic Layer Deposition: An in Situ Interface Study. <b>2015</b> , 7, 13038-43	71
2024	Electric-Field Tunable Band Offsets in Black Phosphorus and MoS <sub>2</sub> van der Waals p-n Heterostructure. <b>2015</b> , 6, 2483-8	153
2023	Thin-layer black phosphorus/GaAs heterojunction p-n diodes. <b>2015</b> , 106, 233110	48
2022	Electronic transport properties of transition metal dichalcogenide field-effect devices: surface and interface effects. <b>2015</b> , 44, 7715-36	282
2021	Manipulation of Magnetic State in Armchair Black Phosphorene Nanoribbon by Charge Doping. <b>2015</b> , 7, 14423-30	31
2020	Step-Edge-Guided Nucleation and Growth of Aligned WSe <sub>2</sub> on Sapphire via a Layer-over-Layer Growth Mode. <b>2015</b> , 9, 8368-75	130
2019	Revealing the importance of surface morphology of nanomaterials to biological responses: Adsorption of the villin headpiece onto graphene and phosphorene. <b>2015</b> , 94, 895-902	53
2018	Designing Isoelectronic Counterparts to Layered Group V Semiconductors. <b>2015</b> , 9, 8284-90	115
2017	Synthesis of thin-film black phosphorus on a flexible substrate. <b>2015</b> , 2, 031002	96
2016	Modelling of stacked 2D materials and devices. <b>2015</b> , 2, 032003	51
2015	Effects of stacking order, layer number and external electric field on electronic structures of few-layer C <sub>2</sub> N-h <sub>2</sub> D. <b>2015</b> , 7, 14062-70	147
2014	Controllable Growth of Vertical Heterostructure GaTe(x)Se(1-x)/Si by Molecular Beam Epitaxy. <b>2015</b> , 9, 8592-8	41
2013	Liquid-Phase Exfoliation of Phosphorene: Design Rules from Molecular Dynamics Simulations. <b>2015</b> , 9, 8255-68	137
2012	Edge reconstruction in armchair phosphorene nanoribbons revealed by discontinuous Galerkin density functional theory. <b>2015</b> , 17, 31397-404	34

2011	Colossal Ultraviolet Photoresponsivity of Few-Layer Black Phosphorus. <b>2015</b> , 9, 8070-7	175
2010	Graphene-Based Platform for Infrared Near-Field Nanospectroscopy of Water and Biological Materials in an Aqueous Environment. <b>2015</b> , 9, 7968-75	60
2009	Characterization of a Hexagonal Phosphorus Adlayer on Platinum (111). <b>2015</b> , 119, 12291-12297	4
2008	High-performance n-type black phosphorus transistors with type control via thickness and contact-metal engineering. <b>2015</b> , 6, 7809	192
2007	Recent developments in black phosphorus transistors. <b>2015</b> , 3, 8760-8775	128
2006	Electronic Structure and Carrier Mobility of Two-Dimensional Arsenic Phosphide. <b>2015</b> , 119, 20210-20216	55
2005	Transport and optical properties of single- and bilayer black phosphorus with defects. <b>2015</b> , 91,	90
2004	Single layer of MX <sub>2</sub> (M = Ti, Zr; X = S, Se, Te): a new platform for nano-electronics and optics. <b>2015</b> , 17, 18665-9	93
2003	Alloy-Based Anode Materials. <b>2015</b> , 189-229	2
2002	Quality Heterostructures from Two-Dimensional Crystals Unstable in Air by Their Assembly in Inert Atmosphere. <b>2015</b> , 15, 4914-21	289
2001	Magnetic evolution and anomalous Wilson transition in diagonal phosphorene nanoribbons driven by strain. <b>2015</b> , 26, 295402	4
2000	Two-dimensional magnetotransport in a black phosphorus naked quantum well. <b>2015</b> , 6, 7702	135
1999	Plasma-Assisted Synthesis of High-Mobility Atomically Layered Violet Phosphorus. <b>2015</b> , 7, 13723-7	35
1998	Two-Dimensional Pnictogen Honeycomb Lattice: Structure, On-Site Spin-Orbit Coupling and Spin Polarization. <b>2015</b> , 5, 11512	76
1997	Electron-Hole Confinement Symmetry in Silicon Quantum Dots. <b>2015</b> , 15, 5336-41	16
1996	Direction dependent thermal conductivity of monolayer phosphorene: Parameterization of Stillinger-Weber potential and molecular dynamics study. <b>2015</b> , 117, 214308	56
1995	The deformation and failure behaviour of phosphorene nanoribbons under uniaxial tensile strain. <b>2015</b> , 2, 035007	35
1994	Optical tuning of exciton and trion emissions in monolayer phosphorene. <b>2015</b> , 4, e312-e312	226

1993	Gate tunable MoS <sub>2</sub> Black phosphorus heterojunction devices. <b>2015</b> , 2, 034009	55
1992	Hybrid functional studies on the electronic properties of ultrathin black phosphorus under normal strain. <b>2015</b> , 109, 20-24	21
1991	Anisotropic Particle-Hole Excitations in Black Phosphorus. <b>2015</b> , 115, 026404	59
1990	Thermal Oxidation of WSe <sub>2</sub> Nanosheets Adhered on SiO <sub>2</sub> /Si Substrates. <b>2015</b> , 15, 4979-84	68
1989	Theoretical study of phosphorene tunneling field effect transistors. <b>2015</b> , 106, 083509	37
1988	Phosphorene: Fabrication, Properties, and Applications. <b>2015</b> , 6, 2794-805	545
1987	Toward air-stable multilayer phosphorene thin-films and transistors. <b>2015</b> , 5, 8989	308
1986	Synthesis, properties and applications of 2D non-graphene materials. <b>2015</b> , 26, 292001	82
1985	Creating a Stable Oxide at the Surface of Black Phosphorus. <b>2015</b> , 7, 14557-62	258
1984	Electronic Structure and Carrier Mobilities of Arsenene and Antimonene Nanoribbons: A First-Principle Study. <b>2015</b> , 10, 955	117
1983	Prediction of superconductivity in Li-intercalated bilayer phosphorene. <b>2015</b> , 106, 113107	50
1982	Electro-mechanical anisotropy of phosphorene. <b>2015</b> , 7, 9746-51	157
1981	Manifestation of unexpected semiconducting properties in few-layer orthorhombic arsenene. <b>2015</b> , 8, 055201	106
1980	Structural, Electronic, and Magnetic Properties of Adatom Adsorptions on Black and Blue Phosphorene: A First-Principles Study. <b>2015</b> , 119, 10610-10622	167
1979	Photocurrent generation with two-dimensional van der Waals semiconductors. <b>2015</b> , 44, 3691-718	608
1978	Highly anisotropic and robust excitons in monolayer black phosphorus. <i>Nature Nanotechnology</i> , <b>2015</b> , 10, 517-21	28.7 999
1977	Broadband nonlinear optical response in multi-layer black phosphorus: an emerging infrared and mid-infrared optical material. <b>2015</b> , 23, 11183-94	541
1976	Transition Metal Doped Phosphorene: First-Principles Study. <b>2015</b> , 119, 9198-9204	199

1975	First-principle study on the optical response of phosphorene. <b>2015</b> , 10, 1-9	22
1974	Tunable Magnetism in Transition-Metal-Decorated Phosphorene. <b>2015</b> , 119, 10059-10063	96
1973	Pristine and defect-containing phosphorene as promising anode materials for rechargeable Li batteries. <b>2015</b> , 3, 11246-11252	112
1972	Two-dimensional materials and their prospects in transistor electronics. <b>2015</b> , 7, 8261-83	415
1971	Grain boundary in phosphorene and its unique roles on C and O doping. <b>2015</b> , 109, 47003	10
1970	Tunable bandgap of monolayer black phosphorus by using vertical electric field: A DFT study. <b>2015</b> , 66, 1031-1034	7
1969	Strain-induced metal-semiconductor transition in monolayers and bilayers of gray arsenic: A computational study. <b>2015</b> , 91,	159
1968	Design of black phosphorus 2D nanomechanical resonators by exploiting the intrinsic mechanical anisotropy. <b>2015</b> , 2, 021001	34
1967	Beyond Graphene: Progress in Novel Two-Dimensional Materials and van der Waals Solids. <b>2015</b> , 45, 1-27	430
1966	Determination of formation and ionization energies of charged defects in two-dimensional materials. <b>2015</b> , 114, 196801	63
1965	Anisotropic thermal transport in phosphorene: effects of crystal orientation. <b>2015</b> , 7, 10648-54	90
1964	Electron-Transport Properties of Few-Layer Black Phosphorus. <b>2015</b> , 6, 1996-2002	61
1963	Single crystalline nitrogen-doped InP nanowires for low-voltage field-effect transistors and photodetectors on rigid silicon and flexible mica substrates. <b>2015</b> , 15, 293-302	18
1962	Strain-induced gap transition and anisotropic Dirac-like cones in monolayer and bilayer phosphorene. <b>2015</b> , 117, 124302	61
1961	Ultrahigh-sensitivity sensors based on thin-film coated long period gratings with reduced diameter, in transition mode and near the dispersion turning point. <b>2015</b> , 23, 8389-98	75
1960	Strain and the optoelectronic properties of nonplanar phosphorene monolayers. <b>2015</b> , 112, 5888-92	44
1959	Prediction of half-semiconductor antiferromagnets with vanishing net magnetization. <b>2015</b> , 5, 46640-46647	17
1958	Quantum oscillations in a two-dimensional electron gas in black phosphorus thin films. <i>Nature Nanotechnology</i> , <b>2015</b> , 10, 608-13	28.7 245

1957	Integrated digital inverters based on two-dimensional anisotropic ReS <sub>2</sub> field-effect transistors. <b>2015</b> , 6, 6991	417
1956	Controlled van der Waals epitaxy of monolayer MoS <sub>2</sub> triangular domains on graphene. <b>2015</b> , 7, 5265-73	106
1955	Solvent exfoliation of electronic-grade, two-dimensional black phosphorus. <b>2015</b> , 9, 3596-604	561
1954	Ultimate thin vertical p-n junction composed of two-dimensional layered molybdenum disulfide. <b>2015</b> , 6, 6564	231
1953	Nanostructured two-dimensional materials. <b>2015</b> , 477-524	
1952	Phosphorus Rich d10 Ion Polyphosphides and Selected Materials. <b>2015</b> , 641, 304-310	18
1951	Stable semiconductor black phosphorus (BP)@titanium dioxide (TiO <sub>2</sub> ) hybrid photocatalysts. <b>2015</b> , 5, 8691	196
1950	Unusual angular dependence of the Raman response in black phosphorus. <b>2015</b> , 9, 4270-6	255
1949	Unexpected magnetic semiconductor behavior in zigzag phosphorene nanoribbons driven by half-filled one dimensional band. <b>2015</b> , 5, 8921	80
1948	Air-stable transport in graphene-contacted, fully encapsulated ultrathin black phosphorus-based field-effect transistors. <b>2015</b> , 9, 4138-45	393
1947	The renaissance of black phosphorus. <b>2015</b> , 112, 4523-30	900
1946	TiS <sub>3</sub> transistors with tailored morphology and electrical properties. <b>2015</b> , 27, 2595-601	144
1945	Theoretical Prediction of Phosphorene and Nanoribbons As Fast-Charging Li Ion Battery Anode Materials. <b>2015</b> , 119, 6923-6928	83
1944	The electronic origin of shear-induced direct to indirect gap transition and anisotropy diminution in phosphorene. <b>2015</b> , 26, 215205	21
1943	Interfacing graphene and related 2D materials with the 3D world. <b>2015</b> , 27, 133203	22
1942	Low-Frequency Interlayer Breathing Modes in Few-Layer Black Phosphorus. <b>2015</b> , 15, 4080-8	154
1941	Ultrathin Single-Crystalline Boron Nanosheets for Enhanced Electro-Optical Performances. <b>2015</b> , 2, 1500023	60
1940	Black phosphorus gas sensors. <b>2015</b> , 9, 5618-24	497

1939	Single-charge transport in ambipolar silicon nanoscale field-effect transistors. <b>2015</b> , 106, 172101	7
1938	Homostructured negative differential resistance device based on zigzag phosphorene nanoribbons. <b>2015</b> , 5, 40358-40362	26
1937	Intrinsic Electron Mobility Exceeding $10^4 \text{ cm}^2/(\text{V s})$ in Multilayer InSe FETs. <b>2015</b> , 15, 3815-9	278
1936	Phosphorene as an anode material for Na-ion batteries: a first-principles study. <b>2015</b> , 17, 13921-8	267
1935	Tunable Schottky contacts in hybrid graphene-phosphorene nanocomposites. <b>2015</b> , 3, 4756-4761	104
1934	Ambipolar insulator-to-metal transition in black phosphorus by ionic-liquid gating. <b>2015</b> , 9, 3192-8	155
1933	Plasmonics in strained monolayer black phosphorus. <b>2015</b> , 117, 113105	25
1932	Transport properties of ultrathin black phosphorus on hexagonal boron nitride. <b>2015</b> , 106, 083505	77
1931	Effects of extrinsic point defects in phosphorene: B, C, N, O, and F adatoms. <b>2015</b> , 106, 173104	57
1930	Band-gap tunability and dynamical instability in strained monolayer and bilayer phosphorenes. <b>2015</b> , 27, 175006	7
1929	Determination of the Schottky barrier height of ferromagnetic contacts to few-layer phosphorene. <b>2015</b> , 106, 103108	22
1928	Large Frequency Change with Thickness in Interlayer Breathing Mode--Significant Interlayer Interactions in Few Layer Black Phosphorus. <b>2015</b> , 15, 3931-8	85
1927	An Atomically Layered InSe Avalanche Photodetector. <b>2015</b> , 15, 3048-55	201
1926	First-Principles Study of Metal Adatom Adsorption on Black Phosphorene. <b>2015</b> , 119, 8199-8207	182
1925	Carbon-Based Sorbents with Three-Dimensional Architectures for Water Remediation. <b>2015</b> , 11, 3319-36	136
1924	Reversible conversion of dominant polarity in ambipolar polymer/graphene oxide hybrids. <b>2015</b> , 5, 9446	15
1923	Structural and Electronic Properties of Layered Arsenic and Antimony Arsenide. <b>2015</b> , 119, 6918-6922	184
1922	Tuning the Electronic and Magnetic Properties of Phosphorene by Vacancies and Adatoms. <b>2015</b> , 119, 6530-6538	103

1921	Nine new phosphorene polymorphs with non-honeycomb structures: a much extended family. <b>2015</b> , 15, 3557-62	247
1920	Transport properties of pristine few-layer black phosphorus by van der Waals passivation in an inert atmosphere. <b>2015</b> , 6, 6647	394
1919	Band-gap modulation of two-dimensional saturable absorbers for solid-state lasers. <b>2015</b> , 3, A10	21
1918	The strain effect on superconductivity in phosphorene: a first-principles prediction. <b>2015</b> , 17, 035008	56
1917	Theoretical Prediction of Anode Materials in Li-Ion Batteries on Layered Black and Blue Phosphorus. <b>2015</b> , 119, 8662-8670	147
1916	Tunable p-type doping of Si nanostructures for near infrared light photodetector application. <b>2015</b> , 5, 19020-19026	8
1915	Strain effects on thermoelectric properties of two-dimensional materials. <b>2015</b> , 91, 382-398	103
1914	Anisotropic Ripple Deformation in Phosphorene. <b>2015</b> , 6, 1509-13	88
1913	Surface and interfacial study of half cycle atomic layer deposited Al <sub>2</sub> O <sub>3</sub> on black phosphorus. <b>2015</b> , 147, 1-4	13
1912	Preparation of Gallium Sulfide Nanosheets by Liquid Exfoliation and Their Application As Hydrogen Evolution Catalysts. <b>2015</b> , 27, 3483-3493	144
1911	Stable and Selective Humidity Sensing Using Stacked Black Phosphorus Flakes. <b>2015</b> , 9, 9898-905	176
1910	Aluminene as highly hole-doped graphene. <b>2015</b> , 17, 083014	62
1909	First-Principles Prediction of the Charge Mobility in Black Phosphorus Semiconductor Nanoribbons. <b>2015</b> , 6, 4141-7	46
1908	Electrochemistry of Nanostructured Layered Transition-Metal Dichalcogenides. <b>2015</b> , 115, 11941-66	606
1907	Nonlocal Response and Anamorphosis: The Case of Few-Layer Black Phosphorus. <b>2015</b> , 15, 6991-5	36
1906	Electronic properties of monolayer and bilayer arsenene under in-plane biaxial strains. <b>2015</b> , 86, 501-507	47
1905	Engineering Graphene Conductivity for Flexible and High-Frequency Applications. <b>2015</b> , 7, 22246-55	19
1904	Single-Layer ReS <sub>2</sub> Two-Dimensional Semiconductor with Tunable In-Plane Anisotropy. <b>2015</b> , 9, 11249-57	286

1903	Environmental, thermal, and electrical susceptibility of black phosphorus field effect transistors. <b>2015</b> , 33, 052202	18
1902	Black phosphorus as saturable absorber for the Q-switched Er:ZBLAN fiber laser at 2.8 $\mu\text{m}$ . <b>2015</b> , 23, 24713-8	222
1901	Graphene nanophotonic sensors. <b>2015</b> , 2, 032005	15
1900	Effect of high-k dielectric and ionic liquid gate on nanolayer black-phosphorus field effect transistors. <b>2015</b> , 107, 113103	17
1899	Mechanical and Electrical Anisotropy of Few-Layer Black Phosphorus. <b>2015</b> , 9, 11362-70	199
1898	Phosphorene: Overcoming the Oxidation Barrier. <b>2015</b> , 1, 289-91	18
1897	The electronic structures of group-V-group-IV hetero-bilayer structures: a first-principles study. <b>2015</b> , 17, 27769-76	45
1896	Nonvolatile Ferroelectric Memory Circuit Using Black Phosphorus Nanosheet-Based Field-Effect Transistors with P(VDF-TrFE) Polymer. <b>2015</b> , 9, 10394-401	109
1895	Characterization of nonlinear properties of black phosphorus nanoplatelets with femtosecond pulsed Z-scan measurements. <b>2015</b> , 40, 3480-3	80
1894	Ultrathin Two-Dimensional Nanomaterials. <b>2015</b> , 9, 9451-69	1342
1893	Observing the semiconducting band-gap alignment of MoS <sub>2</sub> layers of different atomic thicknesses using a MoS <sub>2</sub> /SiO <sub>2</sub> /Si heterojunction tunnel diode. <b>2015</b> , 107, 053101	7
1892	Magnetism in phosphorene: Interplay between vacancy and strain. <b>2015</b> , 107, 072401	38
1891	Modulation of the electronic property of phosphorene by wrinkle and vertical electric field. <b>2015</b> , 107, 112103	12
1890	Mechanically exfoliated black phosphorus as a new saturable absorber for both Q-switching and Mode-locking laser operation. <b>2015</b> , 23, 12823-33	734
1889	Microfiber-based few-layer black phosphorus saturable absorber for ultra-fast fiber laser. <b>2015</b> , 23, 20030-9	322
1888	Boron based two-dimensional crystals: theoretical design, realization proposal and applications. <b>2015</b> , 7, 18863-71	47
1887	The Nature of the Interlayer Interaction in Bulk and Few-Layer Phosphorus. <b>2015</b> , 15, 8170-5	205
1886	Interlayer interactions in anisotropic atomically thin rhenium diselenide. <b>2015</b> , 8, 3651-3661	133



1885	Filling the Gaps between Graphene Oxide: A General Strategy toward Nanolayered Oxides. <b>2015</b> , 25, 5683-5690	27
1884	Electronic Structure and the Properties of Phosphorene and Few-Layer Black Phosphorus. <b>2015</b> , 84, 121004	49
1883	Ultrahigh sensitivity and layer-dependent sensing performance of phosphorene-based gas sensors. <b>2015</b> , 6, 8632	491
1882	Air-Stable Black Phosphorus Devices for Ion Sensing. <b>2015</b> , 7, 24396-402	125
1881	Self-screened high performance multi-layer MoS <sub>2</sub> transistor formed by using a bottom graphene electrode. <b>2015</b> , 7, 19273-81	27
1880	Recent Advances in Two-Dimensional Materials beyond Graphene. <b>2015</b> , 9, 11509-39	1581
1879	Prediction of spin-orbital coupling effects on the electronic structure of two dimensional van der Waals heterostructures. <b>2015</b> , 17, 31253-9	15
1878	Anomalous polarization dependence of Raman scattering and crystallographic orientation of black phosphorus. <b>2015</b> , 7, 18708-15	139
1877	Control of Light-Matter Interaction in 2D Atomic Crystals Using Microcavities. <b>2015</b> , 51, 1-8	4
1876	Remarkably low-energy one-dimensional fault line defects in single-layered phosphorene. <b>2015</b> , 7, 19073-9	14
1875	2D MATERIALS. Observation of tunable band gap and anisotropic Dirac semimetal state in black phosphorus. <b>2015</b> , 349, 723-6	597
1874	Exciton binding energies and luminescence of phosphorene under pressure. <b>2015</b> , 91,	41
1873	Phosphorene: Synthesis, Scale-Up, and Quantitative Optical Spectroscopy. <b>2015</b> , 9, 8869-84	365
1872	Tunable photoluminescence from sheet-like black phosphorus crystal by electrochemical oxidation. <b>2015</b> , 107, 021901	28
1871	Atomic and electronic structure of exfoliated black phosphorus. <b>2015</b> , 33, 060604	60
1870	Linear Scaling of the Exciton Binding Energy versus the Band Gap of Two-Dimensional Materials. <b>2015</b> , 115, 066403	137
1869	Intrinsic Defects, Fluctuations of the Local Shape, and the Photo-Oxidation of Black Phosphorus. <b>2015</b> , 1, 320-7	61
1868	Landau levels and magneto-transport property of monolayer phosphorene. <b>2015</b> , 5, 12295	114

1867	Two-Dimensional Atomic Crystals: Paving New Ways for Nanoelectronics. <b>2015</b> , 44, 4080-4097	5
1866	Electronic structure and magnetic properties of zigzag blue phosphorene nanoribbons. <b>2015</b> , 118, 054301	18
1865	. <b>2015</b> ,	2
1864	Localized charge carriers in graphene nanodevices. <b>2015</b> , 2, 031301	62
1863	Thermal conductivity of a two-dimensional phosphorene sheet: a comparative study with graphene. <b>2015</b> , 7, 18716-24	107
1862	Anisotropic in-plane thermal conductivity observed in few-layer black phosphorus. <b>2015</b> , 6, 8572	426
1861	Highly anisotropic physics in phosphorene. <b>2015</b> , 603, 012006	13
1860	Scaling Limit of Bilayer Phosphorene FETs. <b>2015</b> , 36, 978-980	16
1859	Anisotropic Effective Mass, Optical Property, and Enhanced Band Gap in BN/Phosphorene/BN Heterostructures. <b>2015</b> , 7, 23489-95	50
1858	Liquid exfoliation of solvent-stabilized few-layer black phosphorus for applications beyond electronics. <b>2015</b> , 6, 8563	764
1857	A Black Phosphorus FET Integrated on a Silicon Waveguide for High Speed, Low Dark Current Photodetection. <b>2015</b> ,	
1856	Noncovalent Molecular Doping of Two-Dimensional Materials. <b>2015</b> , 1, 542-557	35
1855	Anisotropic in-plane thermal conductivity of black phosphorus nanoribbons at temperatures higher than 100 K. <b>2015</b> , 6, 8573	249
1854	Black Phosphorus: Narrow Gap, Wide Applications. <b>2015</b> , 6, 4280-91	515
1853	Strain modulated variations in monolayer phosphorene n-MOSFET. <b>2015</b> ,	0
1852	Memristive phase switching in two-dimensional 1T-TaS <sub>2</sub> crystals. <b>2015</b> , 1, e1500606	156
1851	Anisotropic photocurrent response at black phosphorus-MoS <sub>2</sub> p-n heterojunctions. <b>2015</b> , 7, 18537-41	92
1850	Two-dimensional transition metal dichalcogenide alloys: preparation, characterization and applications. <b>2015</b> , 7, 18392-401	157

1849	Buckled honeycomb lattice materials and unconventional magnetic responses. <b>2015</b> , 5, 83350-83360	4
1848	Plasma-Treated Thickness-Controlled Two-Dimensional Black Phosphorus and Its Electronic Transport Properties. <b>2015</b> , 9, 8729-36	135
1847	Hydrogenated arsenenes as planar magnet and Dirac material. <b>2015</b> , 107, 022102	122
1846	Two-dimensional octagon-structure monolayer of nitrogen group elements and the related nano-structures. <b>2015</b> , 110, 109-114	27
1845	Monolayer transition metal dichalcogenide and black phosphorus transistors for low power robust SRAM design. <b>2015</b> ,	1
1844	Structural Transition in Layered As(1-x)P(x) Compounds: A Computational Study. <b>2015</b> , 15, 6042-6	63
1843	Ultrashort Channel Length Black Phosphorus Field-Effect Transistors. <b>2015</b> , 9, 9236-43	122
1842	High-quality sandwiched black phosphorus heterostructure and its quantum oscillations. <b>2015</b> , 6, 7315	369
1841	Carrier dynamics and transient photobleaching in thin layers of black phosphorus. <b>2015</b> , 107, 081103	60
1840	Defects in Phosphorene. <b>2015</b> , 119, 20474-20480	183
1839	Ultrathin Black Phosphorus Nanosheets for Efficient Singlet Oxygen Generation. <b>2015</b> , 137, 11376-82	715
1838	Not your familiar two dimensional transition metal disulfide: structural and electronic properties of the PdS <sub>2</sub> monolayer. <b>2015</b> , 3, 9603-9608	93
1837	Vertical heterostructures of MoS <sub>2</sub> and graphene nanoribbons grown by two-step chemical vapor deposition for high-gain photodetectors. <b>2015</b> , 17, 25210-5	19
1836	Temperature-dependent mechanical properties of monolayer black phosphorus by molecular dynamics simulations. <b>2015</b> , 107, 023107	64
1835	Unique electron transport in ultrathin black phosphorene: Ab-initio study. <b>2015</b> , 356, 881-887	29
1834	Dual Gate Black Phosphorus Field Effect Transistors on Glass for NOR Logic and Organic Light Emitting Diode Switching. <b>2015</b> , 15, 5778-83	76
1833	3D Band Diagram and Photoexcitation of 2D-3D Semiconductor Heterojunctions. <b>2015</b> , 15, 5919-25	26
1832	Probing the anisotropic behaviors of black phosphorus by transmission electron microscopy, angular-dependent Raman spectra, and electronic transport measurements. <b>2015</b> , 107, 021906	39

1831	Single layer lead iodide: computational exploration of structural, electronic and optical properties, strain induced band modulation and the role of spin-orbital-coupling. <b>2015</b> , 7, 15168-74	67
1830	The third principal direction besides armchair and zigzag in single-layer black phosphorus. <b>2015</b> , 26, 365702	11
1829	Few-layer black phosphorus based saturable absorber mirror for pulsed solid-state lasers. <b>2015</b> , 23, 22643-8	203
1828	High-Mobility Holes in Dual-Gated WSe <sub>2</sub> Field-Effect Transistors. <b>2015</b> , 9, 10402-10	180
1827	Power Dissipation and Electrical Breakdown in Black Phosphorus. <b>2015</b> , 15, 6785-8	11
1826	Bandgap Engineering of Phosphorene by Laser Oxidation toward Functional 2D Materials. <b>2015</b> , 9, 10411-21	102
1825	Functional inks of graphene, metal dichalcogenides and black phosphorus for photonics and (opto)electronics. <b>2015</b> ,	20
1824	Controlled Synthesis of High-Quality Monolayered Hn <sub>2</sub> Se <sub>3</sub> via Physical Vapor Deposition. <b>2015</b> , 15, 6400-5	169
1823	Epitaxial growth of hetero-nanostructures based on ultrathin two-dimensional nanosheets. <b>2015</b> , 137, 12162-74	198
1822	Graphene stabilized high- $\epsilon$ dielectric Y <sub>2</sub> O <sub>3</sub> (111) monolayers and their interfacial properties. <b>2015</b> , 5, 83588-83593	14
1821	Esaki Diodes in van der Waals Heterojunctions with Broken-Gap Energy Band Alignment. <b>2015</b> , 15, 5791-8	237
1820	A phosphorene-graphene hybrid material as a high-capacity anode for sodium-ion batteries. <i>Nature Nanotechnology</i> , <b>2015</b> , 10, 980-5	28.7 1114
1819	Indirect-direct band gap transition of two-dimensional arsenic layered semiconductors Cousins of black phosphorus. <b>2015</b> , 58, 1	21
1818	Next generation field-effect transistors based on 2D black phosphorus crystal. <b>2015</b> ,	1
1817	Thickness-dependent Raman spectra, transport properties and infrared photoresponse of few-layer black phosphorus. <b>2015</b> , 3, 10974-10980	85
1816	Geometry, electronic structures and optical properties of phosphorus nanotubes. <b>2015</b> , 26, 415702	33
1815	Electronic and transport properties of phosphorene nanoribbons. <b>2015</b> , 92,	105
1814	First-Principles Study of Phosphorene and Graphene Heterostructure as Anode Materials for Rechargeable Li Batteries. <b>2015</b> , 6, 5002-8	215

1813	Strain-induced band structure and mobility modulation in graphitic blue phosphorus. <b>2015</b> , 356, 626-630	27
1812	Enhanced Raman Scattering on In-Plane Anisotropic Layered Materials. <b>2015</b> , 137, 15511-7	97
1811	Phosphorene FETs [Promising transistors based on a few layers of phosphorus atoms. <b>2015</b> ,	3
1810	A new two-dimensional material: Phosphorene. <b>2015</b> ,	
1809	Luminescent monolayer MoS2 quantum dots produced by multi-exfoliation based on lithium intercalation. <b>2015</b> , 359, 130-136	97
1808	Emergence of Two-Dimensional Massless Dirac Fermions, Chiral Pseudospins, and Berry's Phase in Potassium Doped Few-Layer Black Phosphorus. <b>2015</b> , 15, 7788-93	72
1807	Gate Modulation of Threshold Voltage Instability in Multilayer InSe Field Effect Transistors. <b>2015</b> , 7, 26691-5	38
1806	Variable electronic properties of lateral phosphorene-graphene heterostructures. <b>2015</b> , 17, 31685-92	14
1805	Electronic and magneto-optical properties of monolayer phosphorene quantum dots. <b>2015</b> , 2, 045012	54
1804	Dielectric material for monolayer black phosphorus transistors: A first-principles investigation. <b>2015</b> ,	2
1803	The study of interaction and charge transfer at black phosphorus/metal interfaces. <b>2015</b> , 48, 445101	10
1802	Focus on silicene and other 2D materials. <b>2015</b> , 17, 090201	14
1801	Size, vacancy and temperature effects on Young's modulus of silicene nanoribbons. <b>2015</b> , 5, 96052-96061	19
1800	Role of Interlayer Coupling on the Evolution of Band Edges in Few-Layer Phosphorene. <b>2015</b> , 6, 4876-83	34
1799	Electrical contacts to two-dimensional semiconductors. <b>2015</b> , 14, 1195-205	980
1798	Spin filtering in a magnetized zigzag phosphorene nanoribbon. <b>2015</b> , 48, 485301	11
1797	High-performance a MoS2 nanosheet-based nonvolatile memory transistor with a ferroelectric polymer and graphene source-drain electrode. <b>2015</b> , 67, 1499-1503	22
1796	Surface Charge Transfer Doping of Monolayer Phosphorene via Molecular Adsorption. <b>2015</b> , 6, 4701-10	61

1795	Black phosphorus nanoelectromechanical resonators vibrating at very high frequencies. <b>2015</b> , 7, 877-84	105
1794	Voltammetry of Layered Black Phosphorus: Electrochemistry of Multilayer Phosphorene. <b>2015</b> , 2, 324-327	83
1793	Significant enhancement of the thermoelectric performance of phosphorene through the application of tensile strain. <b>2015</b> , 8, 015202	18
1792	Performance improvement of multilayer InSe transistors with optimized metal contacts. <b>2015</b> , 17, 3653-8	92
1791	Band engineering for novel two-dimensional atomic layers. <b>2015</b> , 11, 1868-84	79
1790	Optoelectronic memory using two-dimensional materials. <b>2015</b> , 15, 259-65	128
1789	Simulation of Phosphorene Field-Effect Transistor at the Scaling Limit. <b>2015</b> , 62, 659-665	43
1788	Spectral properties of Dirac electron system. <b>2015</b> , 460, 253-256	1
1787	Layer-dependent band alignment and work function of few-layer phosphorene. <b>2014</b> , 4, 6677	594
1786	Elemental analogues of graphene: silicene, germanene, stanene, and phosphorene. <b>2015</b> , 11, 640-52	597
1785	Dimensionality of intermolecular interactions in layered crystals by electronic-structure theory and geometric analysis. <b>2015</b> , 54, 956-62	18
1784	Phosphorene nanoribbons: Passivation effect on bandgap and effective mass. <b>2015</b> , 324, 640-644	25
1783	Adsorption of metal adatoms on single-layer phosphorene. <b>2015</b> , 17, 992-1000	246
1782	Phosphorene oxide: stability and electronic properties of a novel two-dimensional material. <b>2015</b> , 7, 524-31	151
1781	Semiconducting black phosphorus: synthesis, transport properties and electronic applications. <b>2015</b> , 44, 2732-43	1031
1780	Science and technology roadmap for graphene, related two-dimensional crystals, and hybrid systems. <b>2015</b> , 7, 4598-810	2015
1779	Photonic Structure-Integrated Two-Dimensional Material Optoelectronics. <b>2016</b> , 5, 93	12
1778	Black phosphorus-based one-dimensional photonic crystals and microcavities. <b>2016</b> , 55, 9288-9292	8

1777	Zigzag phosphorene nanoribbons: one-dimensional resonant channels in two-dimensional atomic crystals. <b>2016</b> , 7, 1983-1990	3
1776	Optical Phase Anisotropy in Layered Black Phosphorus. <b>2016</b> ,	
1775	Graphene against Other Two-Dimensional Materials: A Comparative Study on the Basis of Electronic Applications. <b>2016</b> ,	3
1774	A Filmy Black-Phosphorus Polyimide Saturable Absorber for Q-Switched Operation in an Erbium-Doped Fiber Laser. <b>2016</b> , 9,	16
1773	Computational Search for Two-Dimensional MX <sub>2</sub> Semiconductors with Possible High Electron Mobility at Room Temperature. <b>2016</b> , 9,	90
1772	Atomic Layer Deposition of Silicon Nitride Thin Films: A Review of Recent Progress, Challenges, and Outlooks. <b>2016</b> , 9,	59
1771	Two-Dimensional Semiconductor Optoelectronics Based on van der Waals Heterostructures. <b>2016</b> , 6,	79
1770	Black Phosphorus: Critical Review and Potential for Water Splitting Photocatalyst. <b>2016</b> , 6,	60
1769	Application of 2D Non-Graphene Materials and 2D Oxide Nanostructures for Biosensing Technology. <b>2016</b> , 16, 223	97
1768	Optical properties of black phosphorus. <b>2016</b> , 8, 618	143
1767	Vector soliton fiber laser passively mode locked by few layer black phosphorus-based optical saturable absorber. <b>2016</b> , 24, 25933-25942	163
1766	Dual-wavelength Q-switched Er:SrF <sub>2</sub> laser with a black phosphorus absorber in the mid-infrared region. <b>2016</b> , 24, 30289-30295	79
1765	Probing phonon and electrical anisotropy in black phosphorus for device alignment. <b>2016</b> , 6, 1751	9
1764	Size-dependent saturable absorption and mode-locking of dispersed black phosphorus nanosheets. <b>2016</b> , 6, 3159	33
1763	Ultrafast nonlinear absorption and nonlinear refraction in few-layer oxidized black phosphorus. <b>2016</b> , 4, 286	52
1762	Effect of SiBi Bonds in Silicon-Doped Phosphorene Bilayers: Two-Dimensional Layers and One-Dimensional Nanoribbons. <b>2016</b> , 120, 17106-17114	5
1761	Structural and Electrical Irregularities Caused by Selected Dopants in Black-Phosphorus. <b>2016</b> , 5, Q3026-Q3032	16
1760	Strain- and twist-engineered optical absorption of few-layer black phosphorus. <b>2016</b> , 59, 1	11

1759	Atomic vacancies significantly degrade the mechanical properties of phosphorene. <b>2016</b> , 27, 315704	44
1758	A Dewetting-Induced Assembly Strategy for Precisely Patterning Organic Single Crystals in OFETs. <b>2016</b> , 8, 18978-84	16
1757	Visualizing Light Scattering in Silicon Waveguides with Black Phosphorus Photodetectors. <b>2016</b> , 28, 7162-6	26
1756	Heterostructured hBN-BP-hBN Nanodetectors at Terahertz Frequencies. <b>2016</b> , 28, 7390-6	72
1755	Atomically Resolved Elucidation of the Electrochemical Covalent Molecular Grafting Mechanism of Single Layer Graphene. <b>2016</b> , 3, 1600196	11
1754	An Air-Stable Densely Packed Phosphorene-Graphene Composite Toward Advanced Lithium Storage Properties. <b>2016</b> , 6, 1600453	131
1753	Layered Black Phosphorus: Strongly Anisotropic Magnetic, Electronic, and Electron-Transfer Properties. <b>2016</b> , 128, 3443-3447	24
1752	A General Method for Growing Two-Dimensional Crystals of Organic Semiconductors by Solution Epitaxy. <b>2016</b> , 128, 9671-9675	22
1751	Direct CVD Graphene Growth on Semiconductors and Dielectrics for Transfer-Free Device Fabrication. <b>2016</b> , 28, 4956-75	90
1750	Revealing the Origins of 3D Anisotropic Thermal Conductivities of Black Phosphorus. <b>2016</b> , 2, 1600040	64
1749	Facile Conversion of Red Phosphorus into Soluble Polyphosphide Anions by Reaction with Potassium Ethoxide. <b>2016</b> , 128, 3972-3976	9
1748	Doping behaviors of adatoms adsorbed on phosphorene. <b>2016</b> , 253, 1156-1166	16
1747	Effect of inplane strain on the electronic structure of mono- and bilayer black phosphorus. <b>2016</b> , 253, 1729-1733	2
1746	First-principles prediction of a novel hexagonal phosphorene allotrope. <b>2016</b> , 10, 563-565	18
1745	Visualizing Optical Phase Anisotropy in Black Phosphorus. <b>2016</b> , 3, 1176-1181	68
1744	Quantum capacitance measurement for a black phosphorus field-effect transistor. <b>2016</b> , 27, 042501	2
1743	Robust large-gap quantum spin Hall insulators in chemically decorated arsenene films. <b>2016</b> , 18, 033026	18
1742	Selenium-Doped Black Phosphorus for High-Responsivity 2D Photodetectors. <b>2016</b> , 12, 5000-5007	132



1741	Group IVB transition metal trichalcogenides: a new class of 2D layered materials beyond graphene. <b>2016</b> , 6, 211-222	73
1740	Flexible All-Solid-State Supercapacitors based on Liquid-Exfoliated Black-Phosphorus Nanoflakes. <b>2016</b> , 28, 3194-201	249
1739	Nanoscopy of Black Phosphorus Degradation. <b>2016</b> , 3, 1600121	56
1738	Controllable Growth Orientation of SnS <sub>2</sub> Flakes for Low-Noise, High-Photoswitching Ratio, and Ultrafast Phototransistors. <b>2016</b> , 4, 419-426	31
1737	Layered Black Phosphorus: Strongly Anisotropic Magnetic, Electronic, and Electron-Transfer Properties. <b>2016</b> , 55, 3382-6	111
1736	An Elemental Phosphorus Photocatalyst with a Record High Hydrogen Evolution Efficiency. <b>2016</b> , 55, 9580-5	148
1735	Tuning the Schottky contacts in the phosphorene and graphene heterostructure by applying strain. <b>2016</b> , 18, 19918-25	49
1734	Electronic structures of p-type impurity in ZrS <sub>2</sub> monolayer. <b>2016</b> , 6, 58325-58328	3
1733	Chemical Wet Etching of an Optical Fiber Using a Hydrogen Fluoride-Free Solution for a Saturable Absorber Based on the Evanescent Field Interaction. <b>2016</b> , 34, 3776-3784	35
1732	Black phosphorus-assisted laser desorption ionization mass spectrometry for the determination of low-molecular-weight compounds in biofluids. <b>2016</b> , 408, 6223-33	10
1731	Anomalously enhanced thermal stability of phosphorene via metal adatom doping: An experimental and first-principles study. <b>2016</b> , 9, 2687-2695	25
1730	Photoactivity and electronic properties of graphene-like materials and TiO <sub>2</sub> composites using first-principles calculations. <b>2016</b> , 6, 65315-65321	12
1729	The electronic structure and spin-orbit-induced spin splitting in antimonene with vacancy defects. <b>2016</b> , 6, 66140-66146	32
1728	Superior Chemical Sensing Performance of Black Phosphorus: Comparison with MoS <sub>2</sub> and Graphene. <b>2016</b> , 28, 7020-8	267
1727	Black Phosphorus Schottky Diodes: Channel Length Scaling and Application as Photodetectors. <b>2016</b> , 2, 1500346	43
1726	A General Method for Growing Two-Dimensional Crystals of Organic Semiconductors by "Solution Epitaxy". <b>2016</b> , 55, 9519-23	125
1725	Nonvolatile Charge Injection Memory Based on Black Phosphorous 2D Nanosheets for Charge Trapping and Active Channel Layers. <b>2016</b> , 26, 5701-5707	44
1724	Semiconducting Group 15 Monolayers: A Broad Range of Band Gaps and High Carrier Mobilities. <b>2016</b> , 128, 1698-1701	254

1723	Acute mechano-electronic responses in twisted phosphorene nanoribbons. <b>2016</b> , 8, 14778-84	6
1722	Enhancing Charge Separation in Metallic Photocatalysts: A Case Study of the Conducting Molybdenum Dioxide. <b>2016</b> , 26, 4445-4455	109
1721	Scalable Clean Exfoliation of High-Quality Few-Layer Black Phosphorus for a Flexible Lithium Ion Battery. <b>2016</b> , 28, 510-7	289
1720	Enhanced Photoresponse from Phosphorene-Phosphorene-Suboxide Junction Fashioned by Focused Laser Micromachining. <b>2016</b> , 28, 4090-6	35
1719	Flexible 3D Graphene Transistors with Ionogel Dielectric for Low-Voltage Operation and High Current Carrying Capacity. <b>2016</b> , 2, 1500355	16
1718	Wet-Chemical Processing of Phosphorus Composite Nanosheets for High-Rate and High-Capacity Lithium-Ion Batteries. <b>2016</b> , 6, 1502409	173
1717	High pressure Raman study of layered Mo <sub>0.5</sub> W <sub>0.5</sub> S <sub>2</sub> ternary compound. <b>2016</b> , 3, 025003	13
1716	Spin dynamics, electronic, and thermal transport properties of two-dimensional CrPS <sub>4</sub> single crystal. <b>2016</b> , 119, 043902	29
1715	Dephasing in strongly anisotropic black phosphorus. <b>2016</b> , 94,	13
1714	The thermal and electrical properties of the promising semiconductor MXene Hf <sub>2</sub> CO <sub>2</sub> . <b>2016</b> , 6, 27971	115
1713	A reliable way of mechanical exfoliation of large scale two dimensional materials with high quality. <b>2016</b> , 6, 125201	42
1712	Incorporation of black phosphorus into P3HT:PCBM/n-type Si devices resulting in improvement in electrical and optoelectronic performances. <b>2016</b> , 122, 1	5
1711	Theoretical impurity-limited carrier mobility of monolayer black phosphorus. <b>2016</b> , 108, 033508	12
1710	Positive magnetoconductance and dephasing in strongly localized black phosphorus. <b>2016</b> , 10, 819-823	
1709	Novel electronic and photonic properties of low-symmetry two-dimensional materials. <b>2016</b> ,	0
1708	Communication: Effect of accidental mode degeneracy on Raman intensity in 2D materials: Hybrid functional study of bilayer phosphorene. <b>2016</b> , 145, 021102	5
1707	A possible high-mobility signal in bulk MoTe <sub>2</sub> : Temperature independent weak phonon decay. <b>2016</b> , 6, 115207	6
1706	Theoretical Study of Carrier Mobility in Two-Dimensional Tetragonal Carbon Allotrope from Porous Graphene. <b>2016</b> , 33, 083101	5

1705	Edge plasmons in monolayer black phosphorus. <b>2016</b> , 109, 241902	36
1704	Highly anisotropic electronic transport properties of monolayer and bilayer phosphorene from first principles. <b>2016</b> , 109, 053108	24
1703	Spin-polarized quantum transport properties through flexible phosphorene. <b>2016</b> , 109, 142409	17
1702	Prediction of spin-dependent electronic structure in 3d-transition-metal doped antimonene. <b>2016</b> , 109, 022103	34
1701	Anisotropic Mechanical Properties of Black Phosphorus Nanoribbons. <b>2016</b> , 120, 29491-29497	46
1700	Molecular Structure and Dynamics of Water on Pristine and Strained Phosphorene: Wetting and Diffusion at Nanoscale. <b>2016</b> , 6, 38327	24
1699	Tinselenidene: a Two-dimensional Auxetic Material with Ultralow Lattice Thermal Conductivity and Ultrahigh Hole Mobility. <b>2016</b> , 6, 19830	119
1698	Enhanced hydrogen storage by using lithium decoration on phosphorene. <b>2016</b> , 120, 024305	33
1697	First-principles study of the defected phosphorene under tensile strain. <b>2016</b> , 120, 165104	16
1696	Strain control of vibrational properties of few layer phosphorene. <b>2016</b> , 120, 194305	8
1695	The study of ambipolar behavior in phosphorene field-effect transistors. <b>2016</b> , 120, 215701	5
1694	Mobility anisotropy of two-dimensional semiconductors. <b>2016</b> , 94,	110
1693	Monolayer borophene electrode for effective elimination of both the Schottky barrier and strong electric field effect. <b>2016</b> , 109, 061601	20
1692	Enhanced superconductivity by strain and carrier-doping in borophene: A first principles prediction. <b>2016</b> , 109, 122604	75
1691	Auxetic nanomaterials: Recent progress and future development. <b>2016</b> , 3, 041101	71
1690	Heterostructures of phosphorene and transition metal dichalcogenides for excitonic solar cells: A first-principles study. <b>2016</b> , 108, 122105	69
1689	Elastic properties of suspended black phosphorus nanosheets. <b>2016</b> , 108, 013104	52
1688	Strong electrically tunable MoTe <sub>2</sub> /graphene van der Waals heterostructures for high-performance electronic and optoelectronic devices. <b>2016</b> , 109, 193111	39

1687	A new structure of two-dimensional allotropes of group V elements. <b>2016</b> , 6, 25423	32
1686	Superhigh moduli and tension-induced phase transition of monolayer gamma-boron at finite temperatures. <b>2016</b> , 6, 23233	5
1685	Magnetism and magnetocrystalline anisotropy in single-layer PtSe <sub>2</sub> : Interplay between strain and vacancy. <b>2016</b> , 120, 013904	39
1684	Computational prediction of the diversity of monolayer boron phosphide allotropes. <b>2016</b> , 109, 153107	26
1683	Field-effect transistors of high-mobility few-layer SnSe <sub>2</sub> . <b>2016</b> , 109, 203104	55
1682	Boundary conditions for phosphorene nanoribbons in the continuum approach. <b>2016</b> , 94,	16
1681	Stable single-layer structure of group-V elements. <b>2016</b> , 94,	88
1680	Nanoelectromechanical systems based on low dimensional nanomaterials: Beyond carbon nanotube and graphene nanomechanical resonators—brief review. <b>2016</b> ,	0
1679	Tunable electronic structure of black phosphorus/blue phosphorus van der Waals p-n heterostructure. <b>2016</b> , 108, 083101	91
1678	Thermoelectric properties of phosphorene at the nanoscale. <b>2016</b> , 31, 3179-3186	17
1677	Large anisotropic thermal transport properties observed in bulk single crystal black phosphorus. <b>2016</b> , 108, 092102	22
1676	Design strategy of two-dimensional material field-effect transistors: Engineering the number of layers in phosphorene FETs. <b>2016</b> , 119, 214312	25
1675	An array of layers in silicon sulfides: Chainlike and monolayer. <b>2016</b> , 94,	3
1674	Hexagonal boron-nitride nanomesh magnets. <b>2016</b> , 109, 133110	11
1673	Black Phosphorus Based Field Effect Transistors with Simultaneously Achieved Near Ideal Subthreshold Swing and High Hole Mobility at Room Temperature. <b>2016</b> , 6, 24920	31
1672	Evolution of electronic structure of few-layer phosphorene from angle-resolved photoemission spectroscopy of black phosphorous. <b>2016</b> , 94,	37
1671	Modification of Electronic and Vibrational Properties of Doped Black-P Films. <b>2016</b> , 1, 2285-2290	1
1670	Few-layer HfS <sub>2</sub> transistors. <b>2016</b> , 6, 22277	102

1669	Decoupled electron and phonon transports in hexagonal boron nitride-silicene bilayer heterostructure. <b>2016</b> , 119, 065102	25
1668	Current crowding in two-dimensional black-phosphorus field-effect transistors. <b>2016</b> , 108, 103109	10
1667	Effect of front and back gates on $\alpha$ -Ga <sub>2</sub> O <sub>3</sub> nano-belt field-effect transistors. <b>2016</b> , 109, 062102	79
1666	A class of monolayer metal halogenides MX <sub>2</sub> : Electronic structures and band alignments. <b>2016</b> , 108, 132104	32
1665	First principles calculation of two dimensional antimony and antimony arsenide. <b>2016</b> ,	13
1664	Invited Talk1. <b>2016</b> ,	
1663	Strain engineering band gap, effective mass and anisotropic Dirac-like cone in monolayer arsenene. <b>2016</b> , 6, 035204	51
1662	d <sub>0</sub> ferromagnetism in black phosphorous oxide caused by surface P-O bonds. <b>2016</b> , 108, 091602	4
1661	Spin density waves predicted in zigzag puckered phosphorene, arsenene and antimonene nanoribbons. <b>2016</b> , 6, 045318	16
1660	Integration of 2D materials on a silicon photonics platform for optoelectronics applications. <b>2016</b> , 6, 1205-1218	55
1659	Recent advances in 2D thermoelectric materials. <b>2016</b> ,	4
1658	First-principles simulations of 2-D semiconductor devices: Mobility, I-V characteristics, and contact resistance. <b>2016</b> ,	18
1657	Few-layer black phosphorous PMOSFETs with BN/Al <sub>2</sub> O <sub>3</sub> bilayer gate dielectric: Achieving $I_{on}=850A/in$ , $g_m=340S/in$ , and $R_c=0.58k/in$ . <b>2016</b> ,	9
1656	Physics of electronic transport in two-dimensional materials for future FETs. <b>2016</b> ,	1
1655	Performance predictions of single-layer In-V double-gate n- and p-type field-effect transistors. <b>2016</b> ,	1
1654	Effects of Al <sub>2</sub> O <sub>3</sub> capping layers on the thermal properties of thin black phosphorus. <b>2016</b> , 109, 261901	18
1653	Strain-Induced Energy Band Gap Opening in Two-Dimensional Bilayered Silicon Film. <b>2016</b> , 45, 5040-5047	3
1652	Thickness tunable transport in alloyed WSSe field effect transistors. <b>2016</b> , 109, 142101	25

1651	Multipurpose Black-Phosphorus/hBN Heterostructures. <b>2016</b> , 16, 2586-94	108
1650	High-Performance p-Type Black Phosphorus Transistor with Scandium Contact. <b>2016</b> , 10, 4672-7	96
1649	The Critical Role of Substrate in Stabilizing Phosphorene Nanoflake: A Theoretical Exploration. <b>2016</b> , 138, 4763-71	59
1648	Photonics and optoelectronics of 2D semiconductor transition metal dichalcogenides. <b>2016</b> , 10, 216-226	1997
1647	Why all the fuss about 2D semiconductors?. <b>2016</b> , 10, 202-204	205
1646	High-Performance Field Effect Transistors Using Electronic Inks of 2D Molybdenum Oxide Nanoflakes. <b>2016</b> , 26, 91-100	140
1645	Electric Field Induced Reversible Phase Transition in Li Doped Phosphorene: Shape Memory Effect and Superelasticity. <b>2016</b> , 138, 4772-8	19
1644	Chiral phosphorus nanotubes: structure, bonding, and electronic properties. <b>2016</b> , 18, 12414-8	15
1643	Black phosphorus nonvolatile transistor memory. <b>2016</b> , 8, 9107-12	34
1642	Remarkable reduction of thermal conductivity in phosphorene phononic crystal. <b>2016</b> , 28, 175401	10
1641	Probing the electronic states and impurity effects in black phosphorus vertical heterostructures. <b>2016</b> , 3, 015012	15
1640	Fast Photoresponse from 1T Tin Diselenide Atomic Layers. <b>2016</b> , 26, 137-145	125
1639	Ab Initio Study of Phosphorus Anodes for Lithium- and Sodium-Ion Batteries. <b>2016</b> , 28, 2011-2021	139
1638	Electrical and Thermoelectric Transport by Variable Range Hopping in Thin Black Phosphorus Devices. <b>2016</b> , 16, 3969-75	57
1637	Passivated ambipolar black phosphorus transistors. <b>2016</b> , 8, 12773-9	70
1636	Coulomb drag in anisotropic systems: a theoretical study on a double-layer phosphorene. <b>2016</b> , 28, 285301	8
1635	Charge-transport anisotropy in black phosphorus: critical dependence on the number of layers. <b>2016</b> , 18, 16345-52	14
1634	Q-Switched Ytterbium-Doped Fiber Laser Using Black Phosphorus as Saturable Absorber. <b>2016</b> , 33, 054206	33

1633	Black phosphorus polycarbonate polymer composite for pulsed fibre lasers. <b>2016</b> , 4, 17-23	74
1632	Nanostructured Black Phosphorus/Ketjenblack-Multiwalled Carbon Nanotubes Composite as High Performance Anode Material for Sodium-Ion Batteries. <b>2016</b> , 16, 3955-65	208
1631	Preparation of large size, few-layer black phosphorus nanosheets via phytic acid-assisted liquid exfoliation. <b>2016</b> , 52, 8107-10	72
1630	Two-dimensional GeS with tunable electronic properties via external electric field and strain. <b>2016</b> , 27, 274001	68
1629	Transport studies in 2D transition metal dichalcogenides and black phosphorus. <b>2016</b> , 28, 263002	10
1628	Lateral black phosphorene PN junctions formed via chemical doping for high performance near-infrared photodetector. <b>2016</b> , 25, 34-41	126
1627	Vertically Oriented Arrays of ReS <sub>2</sub> Nanosheets for Electrochemical Energy Storage and Electrocatalysis. <b>2016</b> , 16, 3780-7	201
1626	Van der Waals stacked 2D layered materials for optoelectronics. <b>2016</b> , 3, 022001	161
1625	Prediction of the electronic structure of single-walled black phosphorus nanotubes. <b>2016</b> , 18, 15177-81	8
1624	Controlled Sculpture of Black Phosphorus Nanoribbons. <b>2016</b> , 10, 5687-95	84
1623	Exfoliated $\alpha$ -Ga <sub>2</sub> O <sub>3</sub> nano-belt field-effect transistors for air-stable high power and high temperature electronics. <b>2016</b> , 18, 15760-4	111
1622	Emerging and potential opportunities for 2D flexible nanoelectronics. <b>2016</b> ,	
1621	Strong Modulation of Optical Properties in Black Phosphorus through Strain-Engineered Rippling. <b>2016</b> , 16, 2931-7	159
1620	Electric Field Effects on Spin Splitting of Two-Dimensional van der Waals Arsenene/FeCl <sub>2</sub> Heterostructures. <b>2016</b> , 120, 5613-5618	35
1619	Fundamental Limits on the Subthreshold Slope in Schottky Source/Drain Black Phosphorus Field-Effect Transistors. <b>2016</b> , 10, 3791-800	55
1618	Prediction of a new graphenelike Si <sub>2</sub> BN solid. <b>2016</b> , 93,	46
1617	Performance Enhancement of Black Phosphorus Field-Effect Transistors by Chemical Doping. <b>2016</b> , 37, 429-432	49
1616	Structural Variation in Surface-Supported Synthesis by Adjusting the Stoichiometric Ratio of the Reactants. <b>2016</b> , 10, 4228-35	41

1615	Graphene nano-heterostructures for quantum devices. <b>2016</b> , 19, 375-381	11
1614	Transport properties through hexagonal boron nitride clusters embedded in graphene nanoribbons. <b>2016</b> , 27, 185203	5
1613	Immunity of electronic and transport properties of phosphorene nanoribbons to edge defects. <b>2016</b> , 9, 1723-1734	24
1612	A theoretical investigation on the magnetic and transport properties of the phosphorus nanoribbons with tetragons at the edges. <b>2016</b> , 652, 1-5	4
1611	Atomic structures and electronic properties of phosphorene grain boundaries. <b>2016</b> , 3, 025008	42
1610	Intrinsic Ferroelasticity and/or Multiferroicity in Two-Dimensional Phosphorene and Phosphorene Analogues. <b>2016</b> , 16, 3236-41	350
1609	Lattice Mismatch Dominant Yet Mechanically Tunable Thermal Conductivity in Bilayer Heterostructures. <b>2016</b> , 10, 5431-9	35
1608	Stable aqueous dispersions of optically and electronically active phosphorene. <b>2016</b> , 113, 11688-11693	179
1607	Ab initio studies of phosphorene island single electron transistor. <b>2016</b> , 28, 195302	12
1606	Degradation of phosphorene in air: understanding at atomic level. <b>2016</b> , 3, 025011	187
1605	Humidity Sensing and Photodetection Behavior of Electrochemically Exfoliated Atomically Thin-Layered Black Phosphorus Nanosheets. <b>2016</b> , 8, 11548-56	232
1604	Development of two-dimensional materials for electronic applications. <b>2016</b> , 59, 1	8
1603	Dynamics and Mechanisms of Exfoliated Black Phosphorus Sublimation. <b>2016</b> , 7, 1667-74	32
1602	Novel Excitonic Solar Cells in Phosphorene-TiO <sub>2</sub> Heterostructures with Extraordinary Charge Separation Efficiency. <b>2016</b> , 7, 1880-7	41
1601	Two-dimensional stanane: strain-tunable electronic structure, high carrier mobility, and pronounced light absorption. <b>2016</b> , 18, 14638-43	26
1600	Analysis of tunneling currents in multilayer black phosphorous and (hbox {MoS}_{2}) non-volatile flash memory cells. <b>2016</b> , 15, 129-137	6
1599	Thickness-controlled multilayer hexagonal boron nitride film prepared by plasma-enhanced chemical vapor deposition. <b>2016</b> , 16, 1229-1235	12
1598	Gate-Tunable Atomically Thin Lateral MoS <sub>2</sub> Schottky Junction Patterned by Electron Beam. <b>2016</b> , 16, 3788-94	82



1597	Localized Surface Plasmons in Nanostructured Monolayer Black Phosphorus. <b>2016</b> , 16, 3457-62	199
1596	Stability, electronic structure and magnetic properties of vacancy and nonmetallic atom-doped buckled arsenene: first-principles study. <b>2016</b> , 6, 43794-43801	25
1595	Growth of 2D black phosphorus film from chemical vapor deposition. <b>2016</b> , 27, 215602	192
1594	Spin-dependent Seebeck effect in zigzag black phosphorene nanoribbons. <b>2016</b> , 6, 44019-44023	9
1593	Tuning electronic and magnetic properties of blue phosphorene by doping Al, Si, As and Sb atom: A DFT calculation. <b>2016</b> , 242, 36-40	60
1592	Covalent functionalization and passivation of exfoliated black phosphorus via aryl diazonium chemistry. <b>2016</b> , 8, 597-602	574
1591	Nonradiative Relaxation of Photoexcited Black Phosphorus Is Reduced by Stacking with MoS <sub>2</sub> : A Time Domain ab Initio Study. <b>2016</b> , 7, 1830-5	29
1590	Facile one-step and high-yield synthesis of few-layered and hierarchically porous boron nitride nanosheets. <b>2016</b> , 6, 45402-45409	7
1589	Femtosecond solid-state laser based on a few-layered black phosphorus saturable absorber. <b>2016</b> , 41, 1945-8	47
1588	Electronic and Magnetic Properties of Transition-Metal-Doped Monolayer Black Phosphorus by Defect Engineering. <b>2016</b> , 120, 9773-9779	34
1587	Single-Layered Hittorf's Phosphorus: A Wide-Bandgap High Mobility 2D Material. <b>2016</b> , 16, 2975-80	153
1586	Synthesis and structure determination of the first lead arsenide phosphide Pb <sub>2</sub> As <sub>x</sub> P <sub>14-x</sub> (x ~ 3.7). <b>2016</b> , 71, 603-609	2
1585	Experimental study and modeling of atomic-scale friction in zigzag and armchair lattice orientations of MoS. <b>2016</b> , 17, 189-199	25
1584	Black Phosphorus-Based Nanodevices. <b>2016</b> , 95, 279-303	1
1583	Thermal conductivity and mechanical properties of nitrogenated holey graphene. <b>2016</b> , 106, 1-8	101
1582	Two-Dimensional Phosphorus Porous Polymorphs with Tunable Band Gaps. <b>2016</b> , 138, 7091-8	96
1581	Thickness dependence of surface energy and contact angle of water droplets on ultrathin MoS <sub>2</sub> films. <b>2016</b> , 18, 14449-53	22
1580	Germanium sulfide nanosheet: a universal anode material for alkali metal ion batteries. <b>2016</b> , 4, 8905-8912	139

- 1579 Nonorthogonal [Formula: see text] tight-binding parameterization of single-layer phosphorene under biaxial strain and application to FETs. **2016**, 27, 245202 2
- 1578 Sensitive Electronic-Skin Strain Sensor Array Based on the Patterned Two-Dimensional  $\text{In}_2\text{Se}_3$ . **2016**, 28, 4278-4283 112
- 1577 On the stability of surfactant-stabilised few-layer black phosphorus in aqueous media. **2016**, 6, 86955-86958 30
- 1576 Dirac and Weyl Materials: Fundamental Aspects and Some Spintronics Applications. **2016**, 06, 1640003 76
- 1575 Light-Matter Interactions in Phosphorene. **2016**, 49, 1806-15 89
- 1574 Tuning the electronic and optical properties of graphane/silicane and  $\text{hBN}$ /silicane nanosheets via interfacial dihydrogen bonding and electrical field control. **2016**, 4, 8962-8972 15
- 1573 Anisotropic Ballistic Transport through a Potential Barrier on Monolayer Phosphorene. **2016**, 33, 057301 9
- 1572 Te-Doped Black Phosphorus Field-Effect Transistors. **2016**, 28, 9408-9415 195
- 1571 Luminescent transition metal dichalcogenide nanosheets through one-step liquid phase exfoliation. **2016**, 3, 035014 32
- 1570 Stabilization and strengthening effects of functional groups in two-dimensional titanium carbide. **2016**, 94, 103
- 1569 A promising two-dimensional solar cell donor: Black arsenic phosphorus monolayer with 1.54 eV direct bandgap and mobility exceeding  $14,000 \text{ cm}^2\text{V}^{-1}\text{s}^{-1}$ . **2016**, 28, 433-439 152
- 1568 Onset of exciton-exciton annihilation in single-layer black phosphorus. **2016**, 94, 32
- 1567 Structure and properties of phosphorene-like IV-VI 2D materials. **2016**, 27, 415203 41
- 1566 Energy spectrum of pristine and compressed black phosphorus in the presence of a magnetic field. **2016**, 94, 12
- 1565 Versatile Titanium Silicide Monolayers with Prominent Ferromagnetic, Catalytic, and Superconducting Properties: Theoretical Prediction. **2016**, 7, 3723-3729 24
- 1564 Weak localization and electron-electron interactions in few layer black phosphorus devices. **2016**, 3, 034003 13
- 1563 A graphene-like  $\text{MgN}$  monolayer: high stability, desirable direct band gap and promising carrier mobility. **2016**, 18, 30379-30384 24
- 1562 2D Structures Beyond Graphene: The Brave New World of Layered Materials and How Computers Can Help Discover Them. **2016**, 95, 1-33 8

1561	Two-dimensional van der Waals nanosheet devices for future electronics and photonics. <b>2016</b> , 11, 626-643	64
1560	Slow and fast absorption saturation of black phosphorus: experiment and modelling. <b>2016</b> , 8, 17374-17382	33
1559	Phonon thermal conduction in novel 2D materials. <b>2016</b> , 28, 483001	54
1558	Surface chemistry of black phosphorus under a controlled oxidative environment. <b>2016</b> , 27, 434002	90
1557	Directional-dependent thickness and bending rigidity of phosphorene. <b>2016</b> , 94,	14
1556	Theoretical insight into structure stability, elastic property and carrier mobility of monolayer arsenene under biaxial strains. <b>2016</b> , 100, 324-334	18
1555	Band-gap control in phosphorene/BN structures from first-principles calculations. <b>2016</b> , 94,	8
1554	Strained monolayer germanene with 1 $\times$ lattice on Sb(111). <b>2016</b> , 3, 045005	48
1553	Inverse Funnel Effect of Excitons in Strained Black Phosphorus. <b>2016</b> , 6,	29
1552	First-Principles Prediction of the Electronic Structure and Carrier Mobility in Hexagonal Boron Phosphide Sheet and Nanoribbons. <b>2016</b> , 120, 25037-25042	66
1551	Environmental effects in mechanical properties of few-layer black phosphorus. <b>2016</b> , 3, 031007	34
1550	Electric response of edge bands and their decay property of phosphorene ribbons. <b>2016</b> , 380, 3832-3835	2
1549	Synthesis, properties, and optical applications of low-dimensional perovskites. <b>2016</b> , 52, 13637-13655	212
1548	Long-Term Stability and Reliability of Black Phosphorus Field-Effect Transistors. <b>2016</b> , 10, 9543-9549	120
1547	Black Phosphorus Nanoparticle Labels for Immunoassays via Hydrogen Evolution Reaction Mediation. <b>2016</b> , 88, 10074-10079	118
1546	Layered crystalline ZnInS nanosheets: CVD synthesis and photo-electrochemical properties. <b>2016</b> , 8, 18197-18203	25
1545	Impact of edge states on device performance of phosphorene heterojunction tunneling field effect transistors. <b>2016</b> , 8, 18180-18186	18
1544	Epitaxy of Ultrathin SnSe Single Crystals on Polydimethylsiloxane: In-Plane Electrical Anisotropy and Gate-Tunable Thermopower. <b>2016</b> , 2, 1600292	23

1543	Black phosphorus transistors with enhanced hole transport and subthreshold swing using ultra-thin HfO <sub>2</sub> high-k gate dielectric. <b>2016</b> ,	7
1542	. <b>2016</b> ,	
1541	Auxetic Black Phosphorus: A 2D Material with Negative Poisson's Ratio. <b>2016</b> , 16, 6701-6708	135
1540	A Broadband Optical Modulator Based on a Graphene Hybrid Plasmonic Waveguide. <b>2016</b> , 34, 4948-4953	47
1539	A first-principles study of transition metal doped arsenene. <b>2016</b> , 100, 131-141	20
1538	Electronic, elastic, and optical properties of monolayer BC <sub>2</sub> N. <b>2016</b> , 244, 120-128	20
1537	Transition metal dichalcogenides based saturable absorbers for pulsed laser technology. <b>2016</b> , 60, 601-617	49
1536	Gate-Tuned Thermoelectric Power in Black Phosphorus. <b>2016</b> , 16, 4819-24	84
1535	2D Black Phosphorus/SrTiO <sub>3</sub> -Based Programmable Photoconductive Switch. <b>2016</b> , 28, 7768-73	44
1534	Strain engineering of magnetic state in vacancy-doped phosphorene. <b>2016</b> , 380, 3270-3277	21
1533	Incorporation of black phosphorus into poly(3-hexylthiophene)/n-type Si devices resulting improvement in rectifying and optoelectronic performances. <b>2016</b> , 220, 538-542	5
1532	2D nanosheets-based novel architectures: Synthesis, assembly and applications. <b>2016</b> , 11, 483-520	76
1531	Recent Advances in Doping of Molybdenum Disulfide: Industrial Applications and Future Prospects. <b>2016</b> , 28, 9024-9059	129
1530	Electronic properties of red and black phosphorous and their potential application as photocatalysts. <b>2016</b> , 6, 80872-80884	27
1529	Anisotropic Thermoelectric Response in Two-Dimensional Puckered Structures. <b>2016</b> , 120, 18841-18849	71
1528	Valence-force model and nanomechanics of single-layer phosphorene. <b>2016</b> , 18, 23312-9	7
1527	Unveiling the atomic structure and electronic properties of atomically thin boron sheets on an Ag(111) surface. <b>2016</b> , 8, 16284-16291	50
1526	Preparation of black phosphorus-PEDOT:PSS hybrid semiconductor composites with good film-forming properties and environmental stability in water containing oxygen. <b>2016</b> , 6, 76174-76182	26

1525	Transition Metal Dichalcogenide Schottky Barrier Transistors: A Device Analysis and Material Comparison. <b>2016</b> , 223-256	
1524	Nanostructured Aptamer-Functionalized Black Phosphorus Sensing Platform for Label-Free Detection of Myoglobin, a Cardiovascular Disease Biomarker. <b>2016</b> , 8, 22860-8	164
1523	Strain-controlled fundamental gap and structure of bulk black phosphorus. <b>2016</b> , 94,	31
1522	The realization of half-metal and spin-semiconductor for metal adatoms on arsenene. <b>2016</b> , 390, 60-67	22
1521	Application of silicene, germanene and stanene for Na or Li ion storage: A theoretical investigation. <b>2016</b> , 213, 865-870	171
1520	Tunable electronic structures of germanium monochalcogenide nanosheets via light non-metallic atom functionalization: a first-principles study. <b>2016</b> , 18, 23080-8	16
1519	2D materials and van der Waals heterostructures. <b>2016</b> , 353, aac9439	3469
1518	The Role of Water in the Preparation and Stabilization of High-Quality Phosphorene Flakes. <b>2016</b> , 3, 1500441	56
1517	Promising thermoelectric properties of phosphorenes. <b>2016</b> , 27, 355705	35
1516	MnPSe Monolayer: A Promising 2D Visible-Light Photohydrolytic Catalyst with High Carrier Mobility. <b>2016</b> , 3, 1600062	216
1515	Phosphorene: what can we know from computations?. <b>2016</b> , 6, 5-19	112
1514	Tunable electronic and magnetic properties of two-dimensional materials and their one-dimensional derivatives. <b>2016</b> , 6, 324-350	49
1513	Number-of-layer, pressure, and temperature resolved bond-phonon-photon cooperative relaxation of layered black phosphorus. <b>2016</b> , 47, 1304-1309	8
1512	Tunable Ambipolar Polarization-Sensitive Photodetectors Based on High-Anisotropy ReSe2 Nanosheets. <b>2016</b> , 10, 8067-77	200
1511	Charge carrier transport and lifetimes in n-type and p-type phosphorene as 2D device active materials: an ab initio study. <b>2016</b> , 18, 22706-11	11
1510	Nanotubes based on monolayer blue phosphorus. <b>2016</b> , 94,	20
1509	A promising two-dimensional channel material: monolayer antimonide phosphorus. <b>2016</b> , 59, 648-656	22
1508	Influences of Stone-Wales defects on the structure, stability and electronic properties of antimonene: A first principle study. <b>2016</b> , 503, 126-129	21

1507	Tuning anisotropic electronic transport properties of phosphorene via substitutional doping. <b>2016</b> , 18, 25869-78	33
1506	Understanding the growth of black phosphorus crystals. <b>2016</b> , 18, 7737-7744	45
1505	Pressure-induced phase transitions of lead iodide. <b>2016</b> , 6, 84604-84609	5
1504	Progress in pulsed laser deposited two-dimensional layered materials for device applications. <b>2016</b> , 4, 8859-8878	86
1503	Direct Fabrication of Functional Ultrathin Single-Crystal Nanowires from Quasi-One-Dimensional van der Waals Crystals. <b>2016</b> , 16, 6188-6195	24
1502	Ultrathin and Flat Layer Black Phosphorus Fabricated by Reactive Oxygen and Water Rinse. <b>2016</b> , 10, 8723-31	53
1501	Mechanical properties of phosphorene nanotubes: a density functional tight-binding study. <b>2016</b> , 27, 395701	33
1500	Structural, electronic, mechanical, and transport properties of phosphorene nanoribbons: Negative differential resistance behavior. <b>2016</b> , 94,	51
1499	Stability and Electronic Properties of 2D Nanomaterials Conjugated with Pyrazinamide Chemotherapeutic: A First-Principles Cluster Study. <b>2016</b> , 120, 20323-20332	27
1498	Room-temperature magnetism on the zigzag edges of phosphorene nanoribbons. <b>2016</b> , 94,	39
1497	Tunable Electrical Performance of Few-Layered Black Phosphorus by Strain. <b>2016</b> , 12, 5276-5280	11
1496	Structural, Electronic and Transport Properties of Silicene and Germanene. <b>2016</b> , 347-364	
1495	Ab initio study of carrier mobility of few-layer InSe. <b>2016</b> , 9, 035203	60
1494	Black Phosphorus Based Photocathodes in Wideband Bifacial Dye-Sensitized Solar Cells. <b>2016</b> , 28, 8937-8944	100
1493	In situ thickness control of black phosphorus field-effect transistors via ozone treatment. <b>2016</b> , 9, 3056-3065	17
1492	Gate Switchable Transport and Optical Anisotropy in 90° Twisted Bilayer Black Phosphorus. <b>2016</b> , 16, 5542-6	56
1491	Prevention of Transition Metal Dichalcogenide Photodegradation by Encapsulation with h-BN Layers. <b>2016</b> , 10, 8973-9	48
1490	The tunable electronic structure and optic absorption properties of phosphorene by a normally applied electric field. <b>2016</b> , 91, 105801	3

1489	Simple fabrication of air-stable black phosphorus heterostructures with large-area hBN sheets grown by chemical vapor deposition method. <b>2016</b> , 3, 035010	41
1488	Melting-Freezing Transition of Monolayer Water Confined by Phosphorene Plates. <b>2016</b> , 120, 9011-8	13
1487	Black Phosphorus Quantum Dots as an Efficient Saturable Absorber for Bound Soliton Operation in an Erbium Doped Fiber Laser. <b>2016</b> , 8, 1-10	25
1486	Strong Quantum Confinement Effect in the Optical Properties of Ultrathin $\text{In}_2\text{Se}_3$ . <b>2016</b> , 4, 1939-1943	67
1485	Light-Induced Ambient Degradation of Few-Layer Black Phosphorus: Mechanism and Protection. <b>2016</b> , 55, 11437-41	387
1484	Light-Induced Ambient Degradation of Few-Layer Black Phosphorus: Mechanism and Protection. <b>2016</b> , 128, 11609-11613	70
1483	New structures of bilayer germanium nanosheets predicted by a particle swarm optimization method. <b>2016</b> , 8, 16467-74	2
1482	Strain-induced topological phase transition in phosphorene and in phosphorene nanoribbons. <b>2016</b> , 94,	66
1481	Sensing Characteristics of Phosphorene Monolayers toward $\text{PH}_3$ and $\text{AsH}_3$ Gases upon the Introduction of Vacancy Defects. <b>2016</b> , 120, 20428-20436	52
1480	Temperature dependent Raman spectroscopy of electrochemically exfoliated few layer black phosphorus nanosheets. <b>2016</b> , 6, 76551-76555	36
1479	Mechanical properties of two-dimensional materials and heterostructures. <b>2016</b> , 31, 832-844	53
1478	Multiple unpinned Dirac points in group-Va single-layers with phosphorene structure. <b>2016</b> , 2,	38
1477	Electric-field tunable Dirac semimetal state in phosphorene thin films. <b>2016</b> , 94,	27
1476	Synthesis and Characterization of Hexagonal Boron Nitride as a Gate Dielectric. <b>2016</b> , 6, 30449	84
1475	Electronic, vibrational, Raman, and scanning tunneling microscopy signatures of two-dimensional boron nanomaterials. <b>2016</b> , 94,	11
1474	Degradation of black phosphorus: a real-time $^{31}\text{P}$ NMR study. <b>2016</b> , 3, 035025	46
1473	Advances in 2D Materials for Electronic Devices. <b>2016</b> , 95, 221-277	5
1472	Nanotube-terminated zigzag edges of phosphorene formed by self-rolling reconstruction. <b>2016</b> , 8, 17940-17948	48

- 1471 Chemical sensing by band modulation of a black phosphorus/molybdenum diselenide van der Waals hetero-structure. **2016**, 3, 035021 62
- 1470 Blue Phosphorene Oxide: Strain-Tunable Quantum Phase Transitions and Novel 2D Emergent Fermions. **2016**, 16, 6548-6554 91
- 1469 Flexible 2D nanoelectronics from baseband to sub-THz transistors and circuits. **2016**,
- 1468 Electronic Structures and Li-Diffusion Properties of Group IV $\bar{V}$  Layered Materials: Hexagonal Germanium Phosphide and Germanium Arsenide. **2016**, 120, 23842-23850 31
- 1467 Electrical conduction mechanisms in the temperature-dependent current-voltage characteristics of poly(3-hexylthiophene)/n-type Si devices. **2016**, 65, 60-63 6
- 1466 Lattice vibrations and Raman scattering in two-dimensional layered materials beyond graphene. **2016**, 9, 3559-3597 71
- 1465 Manipulating the magnetic moment in phosphorene by lanthanide atom doping: a first-principle study. **2016**, 6, 92048-92056 17
- 1464 Surface Charge Transfer Doping of Low-Dimensional Nanostructures toward High-Performance Nanodevices. **2016**, 28, 10409-10442 105
- 1463 Inorganic Double Helices in Semiconducting SnIP. **2016**, 28, 9783-9791 50
- 1462 Tunable Optical Transparency in Self-Assembled Three-Dimensional Polyhedral Graphene Oxide. **2016**, 10, 9586-9594 15
- 1461 Prediction of above 20 K superconductivity of blue phosphorus bilayer with metal intercalations. **2016**, 3, 035006 32
- 1460 Black phosphorus crystal as a saturable absorber for both a Q-switched and mode-locked erbium-doped fiber laser. **2016**, 6, 72692-72697 56
- 1459 Small molecule-assisted fabrication of black phosphorus quantum dots with a broadband nonlinear optical response. **2016**, 8, 15132-6 54
- 1458 Tunable Electronic Transport Properties of 2D Layered Double Hydroxide Crystalline Microsheets with Varied Chemical Compositions. **2016**, 12, 4471-6 21
- 1457 Tunable schottky barrier in blue phosphorus/graphene heterojunction with normal strain. **2016**, 55, 080306 23
- 1456 Phosphorene and Phosphorene-Based Materials - Prospects for Future Applications. **2016**, 28, 8586-8617 283
- 1455 Dual-Gate Velocity-Modulated Transistor Based on Black Phosphorus. **2016**, 5, 14
- 1454 Negative compressibility in graphene-terminated black phosphorus heterostructures. **2016**, 93, 7



1453	Emergence of Dirac and quantum spin Hall states in fluorinated monolayer As and AsSb. <b>2016</b> , 93,	25
1452	Dynamical stability and superconductivity of Li-intercalated bilayer MoS <sub>2</sub> : A first-principles prediction. <b>2016</b> , 93,	28
1451	Excitons in atomically thin black phosphorus. <b>2016</b> , 93,	57
1450	Direct band gaps in group IV-VI monolayer materials: Binary counterparts of phosphorene. <b>2016</b> , 93,	111
1449	Mermin-Wagner theorem, flexural modes, and degraded carrier mobility in two-dimensional crystals with broken horizontal mirror symmetry. <b>2016</b> , 93,	55
1448	Mobility anisotropy in monolayer black phosphorus due to scattering by charged impurities. <b>2016</b> , 93,	62
1447	First-principles cluster expansion study of functionalization of black phosphorene via fluorination and oxidation. <b>2016</b> , 93,	38
1446	Thickness and electric-field-dependent polarizability and dielectric constant in phosphorene. <b>2016</b> , 93,	48
1445	Hydrostatic pressure induced three-dimensional Dirac semimetal in black phosphorus. <b>2016</b> , 93,	39
1444	Laser-induced topological transitions in phosphorene with inversion symmetry. <b>2016</b> , 93,	42
1443	Semiconductor-topological insulator transition of two-dimensional SbAs induced by biaxial tensile strain. <b>2016</b> , 93,	111
1442	First-principles investigation of two-dimensional trichalcogenide and sesquichalcogenide monolayers. <b>2016</b> , 93,	26
1441	Quantum Hall effect and semiconductor-to-semimetal transition in biased black phosphorus. <b>2016</b> , 93,	58
1440	Band alignment of two-dimensional semiconductors for designing heterostructures with momentum space matching. <b>2016</b> , 94,	247
1439	Impurity scattering and Friedel oscillations in monolayer black phosphorus. <b>2016</b> , 94,	17
1438	Anisotropic 2D Materials for Tunable Hyperbolic Plasmonics. <b>2016</b> , 116, 066804	137
1437	Ultralow-Frequency Collective Compression Mode and Strong Interlayer Coupling in Multilayer Black Phosphorus. <b>2016</b> , 116, 087401	42
1436	Intrinsic Charge Carrier Mobility in Single-Layer Black Phosphorus. <b>2016</b> , 116, 246401	95

1435	Wafer-Size and Single-Crystal MoSe <sub>2</sub> Atomically Thin Films Grown on GaN Substrate for Light Emission and Harvesting. <b>2016</b> , 8, 20267-73	45
1434	The fracture behaviors of monolayer phosphorene with grain boundaries under tension: a molecular dynamics study. <b>2016</b> , 18, 20562-70	10
1433	Four allotropes of semiconducting layered arsenic that switch into a topological insulator via an electric field: Computational study. <b>2016</b> , 94,	50
1432	Transition metal doped arsenene: A first-principles study. <b>2016</b> , 389, 594-600	82
1431	Single and bilayer bismuthene: Stability at high temperature and mechanical and electronic properties. <b>2016</b> , 94,	224
1430	Excitons and optical spectra of phosphorene nanoribbons. <b>2016</b> , 94,	30
1429	Two-Dimensional Phosphorus Carbide: Competition between sp(2) and sp(3) Bonding. <b>2016</b> , 16, 3247-52	98
1428	Highly Itinerant Atomic Vacancies in Phosphorene. <b>2016</b> , 138, 10199-206	112
1427	2D Materials Beyond Graphene for High-Performance Energy Storage Applications. <b>2016</b> , 6, 1600671	301
1426	Competition between spin-orbit interaction and exchange coupling within a honeycomb lattice ribbon. <b>2016</b> , 49, 015305	9
1425	2D Metals by Repeated Size Reduction. <b>2016</b> , 28, 8170-8176	53
1424	Two-Dimensional Phosphorus Oxides as Energy and Information Materials. <b>2016</b> , 55, 8575-80	24
1423	Alternate to Molybdenum Disulfide: A 2D, Few-Layer Transition-Metal Thiophosphate and Its Hydrogen Evolution Reaction Activity over a Wide pH Range. <b>2016</b> , 3, 1392-1399	35
1422	Multiscale Analysis for Field-Effect Penetration through Two-Dimensional Materials. <b>2016</b> , 16, 5044-52	22
1421	Gate-induced superconductivity in two-dimensional atomic crystals. <b>2016</b> , 29, 093001	42
1420	Photoinduced Schottky Barrier Lowering in 2D Monolayer WS <sub>2</sub> Photodetectors. <b>2016</b> , 4, 1573-1581	47
1419	Tuning Surface Properties of Low Dimensional Materials via Strain Engineering. <b>2016</b> , 12, 4028-47	38
1418	Electronic properties of a pristine and NH <sub>3</sub> /NO <sub>2</sub> adsorbed buckled arsenene monolayer. <b>2016</b> , 6, 72634-72642	23

1417	Anomalous Temperature Dependence of the Band Gap in Black Phosphorus. <b>2016</b> , 16, 5095-101	64
1416	Valley physics in tin (II) sulfide. <b>2016</b> , 93,	88
1415	Disentangling bulk from surface contributions in the electronic structure of black phosphorus. <b>2016</b> , 93,	9
1414	Phosphorene confined systems in magnetic field, quantum transport, and superradiance in the quasiflat band. <b>2016</b> , 93,	30
1413	Tunable skewed edges in puckered structures. <b>2016</b> , 93,	26
1412	Ferroelectricity in Covalently Functionalized Two-dimensional Materials: Integration of High-mobility Semiconductors and Nonvolatile Memory. <b>2016</b> , 16, 7309-7315	83
1411	Effect of the edge states on the conductance and thermopower in zigzag phosphorene nanoribbons. <b>2016</b> , 94,	25
1410	Two-dimensional semiconductors for transistors. <b>2016</b> , 1,	670
1409	Interface Engineering for the Enhancement of Carrier Transport in Black Phosphorus Transistor with Ultra-Thin High-k Gate Dielectric. <b>2016</b> , 6, 26609	26
1408	Valley-engineered ultra-thin silicon for high-performance junctionless transistors. <b>2016</b> , 6, 29354	2
1407	Tunable electronic and dielectric properties of $\Gamma$ -phosphorene nanoflakes for optoelectronic applications. <b>2016</b> , 6, 101835-101845	4
1406	Two-dimensional antimonene single crystals grown by van der Waals epitaxy. <b>2016</b> , 7, 13352	633
1405	Black phosphorus as a saturable absorber for generating mode-locked fiber laser in normal dispersion regime. <b>2016</b> ,	2
1404	An atomically thin layer of Ru/MoS heterostructure: structural, electronic, and magnetic properties. <b>2016</b> , 18, 32528-32533	6
1403	Catalytic properties of group 4 transition metal dichalcogenides ( $\text{MX}_2$ ; M = Ti, Zr, Hf; X = S, Se, Te). <b>2016</b> , 4, 18322-18334	65
1402	High-performance black phosphorus top-gate ferroelectric transistor for nonvolatile memory applications. <b>2016</b> , 69, 1347-1351	4
1401	Hydrogen separation by porous phosphorene: A periodical DFT study. <b>2016</b> , 41, 23067-23074	20
1400	Phosphorus K Crystal: A New Stable Allotrope. <b>2016</b> , 6, 37528	9

1399	Graphene plasmonics: physics and potential applications. <b>2016</b> , 6, 1191-1204	72
1398	New Ferroelectric Phase in Atomic-Thick Phosphorene Nanoribbons: Existence of in-Plane Electric Polarization. <b>2016</b> , 16, 8015-8020	46
1397	Nanoscopy reveals surface-metallic black phosphorus. <b>2016</b> , 5, e16162	31
1396	Negative capacitance transistors with monolayer black phosphorus. <b>2016</b> , 1,	42
1395	Stability of single-layer and multilayer arsenene and their mechanical and electronic properties. <b>2016</b> , 94,	82
1394	Optical properties of single-layer and bilayer arsenene phases. <b>2016</b> , 94,	53
1393	Design of graphene-like gallium nitride and WS <sub>2</sub> /WSe <sub>2</sub> nanocomposites for photocatalyst applications. <b>2016</b> , 59, 1027-1036	53
1392	Low-symmetry two-dimensional materials for electronic and photonic applications. <b>2016</b> , 11, 763-777	85
1391	Room-temperature ferroelectricity in CuInP <sub>2</sub> S <sub>6</sub> ultrathin flakes. <b>2016</b> , 7, 12357	355
1390	Surface charge transfer doping of monolayer molybdenum disulfide by black phosphorus quantum dots. <b>2016</b> , 27, 505204	22
1389	Interaction of Black Phosphorus with Oxygen and Water. <b>2016</b> , 28, 8330-8339	345
1388	Screening limited switching performance of multilayer 2D semiconductor FETs: the case for SnS. <b>2016</b> , 8, 19050-19057	49
1387	Disorder effect on the anisotropic resistivity of phosphorene determined by a tight-binding model. <b>2016</b> , 94,	12
1386	Biodegradable black phosphorus-based nanospheres for in vivo photothermal cancer therapy. <b>2016</b> , 7, 12967	659
1385	Tuning the magnetoresistance of ultrathin WTe sheets by electrostatic gating. <b>2016</b> , 8, 18703-18709	17
1384	The polarization-dependent anisotropic Raman response of few-layer and bulk WTe <sub>2</sub> under different excitation wavelengths. <b>2016</b> , 6, 103830-103837	21
1383	Comparative study of phonon spectrum and thermal expansion of graphene, silicene, germanene, and blue phosphorene. <b>2016</b> , 94,	61
1382	Resonant bonding driven giant phonon anharmonicity and low thermal conductivity of phosphorene. <b>2016</b> , 94,	79

1381	Impact of CNT process imperfection on circuit-level functionality and yield. <b>2016,</b>	
1380	Mass production of two-dimensional oxides by rapid heating of hydrous chlorides. <b>2016, 7, 12543</b>	56
1379	Unexpected electronic structure of the alloyed and doped arsenene sheets: First-Principles calculations. <b>2016, 6, 29114</b>	49
1378	Electronic structure of the germanium phosphide monolayer and Li-diffusion in its bilayer. <b>2016, 18, 32458-32465</b>	54
1377	Two new phases of monolayer group-IV monochalcogenides and their piezoelectric properties. <b>2016, 18, 32514-32520</b>	59
1376	Comparative study of thermal properties of group-VA monolayers with buckled and puckered honeycomb structures. <b>2016, 94,</b>	39
1375	Two-Dimensional Phosphorus Oxides as Energy and Information Materials. <b>2016, 128, 8717-8722</b>	9
1374	Noncovalent Functionalization of Black Phosphorus. <b>2016, 128, 14777-14782</b>	59
1373	Optical anisotropy of tungsten-doped ReS <sub>2</sub> layered crystals. <b>2016, 62, 433-437</b>	1
1372	Introduction of Interfacial Charges to Black Phosphorus for a Family of Planar Devices. <b>2016, 16, 6870-6878</b>	60
1371	SnS <sub>2</sub> nanoflakes for efficient humidity and alcohol sensing at room temperature. <b>2016, 6, 105421-105427</b>	84
1370	Black Phosphorus Transistors with Near Band Edge Contact Schottky Barrier. <b>2015, 5, 18000</b>	29
1369	Nitrogen induced phosphorene formation on the boron phosphide (111) surface: a density functional theory study. <b>2016, 6, 108621-108626</b>	2
1368	Resonantly Increased Optical Frequency Conversion in Atomically Thin Black Phosphorus. <b>2016, 28, 10693-10700</b>	47
1367	Phosphorene: from theory to applications. <b>2016, 1,</b>	571
1366	Partial Oxidized Arsenene: Emerging Tunable Direct Bandgap Semiconductor. <b>2016, 6, 24981</b>	30
1365	A theoretical review on electronic, magnetic and optical properties of silicene. <b>2016, 79, 126501</b>	106
1364	Spin-orbit coupling and spin relaxation in phosphorene: Intrinsic versus extrinsic effects. <b>2016, 94,</b>	33

- 1363 Novel graphene field effect transistor with BNTM ferroelectric gate. **2016**,
- 1362 Performance of arsenene and antimonene double-gate MOSFETs from first principles. **2016**, 7, 12585 224
- 1361 Large Area Fabrication of Semiconducting Phosphorene by Langmuir-Blodgett Assembly. **2016**, 6, 34095 58
- 1360 Noncovalent Functionalization of Black Phosphorus. **2016**, 55, 14557-14562 172
- 1359 Inconsistencies in the Electronic Properties of Phosphorene Nanotubes: New Insights from Large-Scale DFT Calculations. **2016**, 7, 4340-4345 42
- 1358 Semi-metallic Be<sub>5</sub>C<sub>2</sub> monolayer global minimum with quasi-planar pentacoordinate carbons and negative Poisson's ratio. **2016**, 7, 11488 179
- 1357 Thermal transport properties of antimonene: an ab initio study. **2016**, 18, 31217-31222 53
- 1356 Interfacial thermal conductance in multilayer graphene/phosphorene heterostructure. **2016**, 49, 465301 12
- 1355 Mid-infrared time-resolved photoconduction in black phosphorus. **2016**, 3, 041006 42
- 1354 Two-dimensional hexagonal semiconductors beyond graphene. **2016**, 7, 043001 9
- 1353 Uniform Benchmarking of Low-Voltage van der Waals FETs. **2016**, 2, 28-35 16
- 1352 Covalent Functionalization of Black Phosphorus from First-Principles. **2016**, 7, 4540-4546 63
- 1351 A Dynamically Reconfigurable Ambipolar Black Phosphorus Memory Device. **2016**, 10, 10428-10435 72
- 1350 Photo-FETs: Phototransistors Enabled by 2D and 0D Nanomaterials. **2016**, 3, 2197-2210 160
- 1349 Interlayer thermal conductance within a phosphorene and graphene bilayer. **2016**, 8, 19211-19218 43
- 1348 Ferromagnetism controlled by electric field in tilted phosphorene nanoribbon. **2016**, 6, 26300 15
- 1347 Quantum spin Hall insulator in halogenated arsenene films with sizable energy gaps. **2016**, 6, 28487 31
- 1346 The electronic transport properties of transition-metal dichalcogenide lateral heterojunctions. **2016**, 4, 10962-10966 50

1345	Topological node-line semimetal in compressed black phosphorus. <b>2016</b> , 94,	89
1344	Two-dimensional wide-band-gap nitride semiconductors: Single-layer $1T\bar{X}N_2$ (X=S,Se, and Te). <b>2016</b> , 94,	14
1343	Investigation and analysis of single layer phosphorene properties based on tight-binding and green's function formalism. <b>2016</b> ,	1
1342	Phosphorene as a promising anode material for lithium-ion batteries: A first-principle study. <b>2016</b> ,	2
1341	Electronic energy loss spectra from mono-layer to few layers of phosphorene. <b>2016</b> ,	3
1340	Production of Two-Dimensional Nanomaterials via Liquid-Based Direct Exfoliation. <b>2016</b> , 12, 272-93	339
1339	Black Phosphorus Nanosheets: Synthesis, Characterization and Applications. <b>2016</b> , 12, 3480-502	267
1338	Toward High-Performance Top-Gate Ultrathin HfS <sub>2</sub> Field-Effect Transistors by Interface Engineering. <b>2016</b> , 12, 3106-11	42
1337	In silico engineering of graphene-based van der Waals heterostructured nanohybrids for electronics and energy applications. <b>2016</b> , 6, 551-570	27
1336	Facile Conversion of Red Phosphorus into Soluble Polyphosphide Anions by Reaction with Potassium Ethoxide. <b>2016</b> , 55, 3904-8	27
1335	Carrier Type Control of WSe <sub>2</sub> Field-Effect Transistors by Thickness Modulation and MoO <sub>3</sub> Layer Doping. <b>2016</b> , 26, 4223-4230	133
1334	Nanostructured Photodetectors: From Ultraviolet to Terahertz. <b>2016</b> , 28, 403-33	376
1333	Bottom-Up Preparation of Ultrathin 2D Aluminum Oxide Nanosheets by Duplicating Graphene Oxide. <b>2016</b> , 28, 1703-8	54
1332	Effect of multilayer structure, stacking order and external electric field on the electrical properties of few-layer boron-phosphide. <b>2016</b> , 18, 16229-36	53
1331	Thermal stability of a free nanotube from single-layer black phosphorus. <b>2016</b> , 27, 235703	26
1330	First-principles and angle-resolved photoemission study of lithium doped metallic black phosphorus. <b>2016</b> , 3, 025031	19
1329	Investigation of black phosphorus field-effect transistors and its stability. <b>2016</b> , 48, 1	7
1328	Tuning the electronic properties and work functions of graphane/fully hydrogenated h-BN heterobilayers via heteronuclear dihydrogen bonding and electric field control. <b>2016</b> , 18, 16386-95	36

- 1327 A first-principles study on the magnetic properties of Sc, V, Cr and Mn-doped monolayer TlS<sub>3</sub>. **2016**, 6, 55194-55202 6
- 1326 Polarized Raman spectra of phosphorene in edge and top view measuring configurations. **2016**, 6, 58003-58009
- 1325 Sub-300 femtosecond soliton tunable fiber laser with all-anomalous dispersion passively mode locked by black phosphorus. **2016**, 24, 13316-24 52
- 1324 Integration of Upconversion Nanoparticles and Ultrathin Black Phosphorus for Efficient Photodynamic Theranostics under 808 nm Near-Infrared Light Irradiation. **2016**, 28, 4724-4734 174
- 1323 Wedge energy bands of monolayer black phosphorus: a first-principles study. **2016**, 28, 305301
- 1322 Atomically thin binary  $VV$  compound semiconductor: a first-principles study. **2016**, 4, 6581-6587 98
- 1321 A Honeycomb BeN<sub>2</sub> Sheet with a Desirable Direct Band Gap and High Carrier Mobility. **2016**, 7, 2664-70 72
- 1320 Transition Metal and Vacancy Defect Complexes in Phosphorene: A Spintronic Perspective. **2016**, 120, 14991-15000 49
- 1319 High-performance photodetectors based on bandgap engineered novel layer GaSe<sub>0.5</sub>Te<sub>0.5</sub> nanoflakes. **2016**, 6, 60862-60868 9
- 1318 Weak localization in few-layer black phosphorus. **2016**, 3, 024003 15
- 1317 Universal low-temperature Ohmic contacts for quantum transport in transition metal dichalcogenides. **2016**, 3, 021007 78
- 1316 Doping enhanced ferromagnetism and induced half-metallicity in CrI<sub>3</sub> monolayer. **2016**, 114, 47001 99
- 1315 Black Phosphorus Mid-Infrared Photodetectors with High Gain. **2016**, 16, 4648-55 476
- 1314 Transition-metal-decorated germanene as promising catalyst for removing CO contamination in H<sub>2</sub>. **2016**, 107, 82-89 13
- 1313 The advent of multilayer antimonene nanoribbons with room temperature orange light emission. **2016**, 52, 8409-12 79
- 1312 Strain enhancement of acoustic phonon limited mobility in monolayer TlS<sub>3</sub>. **2016**, 18, 14434-41 24
- 1311 Electronic structure and optic absorption of phosphorene under strain. **2016**, 81, 177-181 35
- 1310 First-principles study of thermal expansion and thermomechanics of single-layer black and blue phosphorus. **2016**, 380, 2098-2104 47



1309	Strain engineering the charged-impurity-limited carrier mobility in phosphorene. <b>2016</b> , 89, 204-215	5
1308	Tunable Photoinduced Carrier Transport of a Black Phosphorus Transistor with Extended Stability Using a Light-Sensitized Encapsulated Layer. <b>2016</b> , 3, 1102-1108	16
1307	Dilute Magnetic Semiconductor and Half-Metal Behaviors in 3d Transition-Metal Doped Black and Blue Phosphorenes: A First-Principles Study. <b>2016</b> , 11, 77	78
1306	Multi-layered black phosphorus as saturable absorber for pulsed Cr:ZnSe laser at 2.4 $\mu\text{m}$ . <b>2016</b> , 24, 1598-603	37
1305	Interaction of Adatoms and Molecules with Single-Layer Arsenene Phases. <b>2016</b> , 120, 14345-14355	88
1304	Capping Black Phosphorene by h-BN Enhances Performances in Anodes for Li and Na Ion Batteries. <b>2016</b> , 1, 253-259	102
1303	High thermoelectric performance of the distorted bismuth(110) layer. <b>2016</b> , 18, 17373-9	14
1302	Unusual electronic and magnetic properties of lateral phosphorene $\text{WSe}_2$ heterostructures. <b>2016</b> , 4, 6657-6665	8
1301	Two-dimensional BX (X = P, As, Sb) semiconductors with mobilities approaching graphene. <b>2016</b> , 8, 13407-13	84
1300	Strength and stability analysis of a single-walled black phosphorus tube under axial compression. <b>2016</b> , 27, 275701	16
1299	Electronic structure engineering of various structural phases of phosphorene. <b>2016</b> , 18, 18312-22	29
1298	Black Phosphorus (BP) Nanodots for Potential Biomedical Applications. <b>2016</b> , 12, 214-9	205
1297	Spatial conductivity mapping of unprotected and capped black phosphorus using microwave microscopy. <b>2016</b> , 3, 021002	29
1296	Epitaxial Growth of Single Layer Blue Phosphorus: A New Phase of Two-Dimensional Phosphorus. <b>2016</b> , 16, 4903-8	490
1295	Type-controlled nanodevices based on encapsulated few-layer black phosphorus for quantum transport. <b>2016</b> , 3, 031001	17
1294	Liquid-Exfoliated Black Phosphorous Nanosheet Thin Films for Flexible Resistive Random Access Memory Applications. <b>2016</b> , 26, 2016-2024	137
1293	Exciton Brightening in Monolayer Phosphorene via Dimensionality Modification. <b>2016</b> , 28, 3493-8	41
1292	Broadband Black-Phosphorus Photodetectors with High Responsivity. <b>2016</b> , 28, 3481-5	293

1291	Anisotropic Black Phosphorus Synaptic Device for Neuromorphic Applications. <b>2016</b> , 28, 4991-7	217
1290	Solvothermal Synthesis and Ultrafast Photonics of Black Phosphorus Quantum Dots. <b>2016</b> , 4, 1223-1229	267
1289	Surface Coordination of Black Phosphorus for Robust Air and Water Stability. <b>2016</b> , 128, 5087-5091	92
1288	An Elemental Phosphorus Photocatalyst with a Record High Hydrogen Evolution Efficiency. <b>2016</b> , 128, 9732-9737	28
1287	Semiconducting Group 15 Monolayers: A Broad Range of Band Gaps and High Carrier Mobilities. <b>2016</b> , 55, 1666-9	535
1286	Surface Coordination of Black Phosphorus for Robust Air and Water Stability. <b>2016</b> , 55, 5003-7	406
1285	Stacking Fault Enriching the Electronic and Transport Properties of Few-Layer Phosphorenes and Black Phosphorus. <b>2016</b> , 16, 1317-22	35
1284	Producing air-stable monolayers of phosphorene and their defect engineering. <b>2016</b> , 7, 10450	358
1283	Stacking dependence of carrier transport properties in multilayered black phosphorous. <b>2016</b> , 28, 075001	12
1282	Aging of Transition Metal Dichalcogenide Monolayers. <b>2016</b> , 10, 2628-35	267
1281	Black Phosphorus-Zinc Oxide Nanomaterial Heterojunction for p-n Diode and Junction Field-Effect Transistor. <b>2016</b> , 16, 1293-8	125
1280	Novel effects of strains in graphene and other two dimensional materials. <b>2016</b> , 617, 1-54	239
1279	Fundamentals of lateral and vertical heterojunctions of atomically thin materials. <b>2016</b> , 8, 3870-87	90
1278	N- and p-type doping of antimonene. <b>2016</b> , 6, 14620-14625	48
1277	Liquid exfoliation of black phosphorus nanosheets and its application as humidity sensor. <b>2016</b> , 225, 494-503	150
1276	Tuning carrier mobility of phosphorene nanoribbons by edge passivation and strain. <b>2016</b> , 380, 614-620	20
1275	Gate-induced superconductivity in atomically thin MoS2 crystals. <i>Nature Nanotechnology</i> , <b>2016</b> , 11, 339-48.7	216
1274	Blockage of ultrafast and directional diffusion of Li atoms on phosphorene with intrinsic defects. <b>2016</b> , 8, 4001-6	65

1273	Charge trap memory based on few-layer black phosphorus. <b>2016</b> , 8, 2686-92	72
1272	Tuning the electronic and optical properties of phosphorene by transition-metal and nonmetallic atom co-doping. <b>2016</b> , 6, 10919-10929	38
1271	Substitutionally doped phosphorene: electronic properties and gas sensing. <b>2016</b> , 27, 065708	111
1270	Supercritical carbon dioxide-assisted rapid synthesis of few-layer black phosphorus for hydrogen peroxide sensing. <b>2016</b> , 80, 34-38	82
1269	Evolution of band structures in MoS <sub>2</sub> -based homo- and heterobilayers. <b>2016</b> , 49, 065304	6
1268	Optical Anisotropy of Black Phosphorus in the Visible Regime. <b>2016</b> , 138, 300-5	217
1267	2D phosphorene as a water splitting photocatalyst: fundamentals to applications. <b>2016</b> , 9, 709-728	420
1266	Novel mesoporous P-doped graphitic carbon nitride nanosheets coupled with ZnIn <sub>2</sub> S <sub>4</sub> nanosheets as efficient visible light driven heterostructures with remarkably enhanced photo-reduction activity. <b>2016</b> , 8, 3711-9	186
1265	Gate tunable WSe <sub>2</sub> -BP van der Waals heterojunction devices. <b>2016</b> , 8, 3254-8	50
1264	Mechanical strain effects on black phosphorus nanoresonators. <b>2016</b> , 8, 901-5	24
1263	Toward an Accurate Estimate of the Exfoliation Energy of Black Phosphorus: A Periodic Quantum Chemical Approach. <b>2016</b> , 7, 131-6	46
1262	Band Gap Engineering in a 2D Material for Solar-to-Chemical Energy Conversion. <b>2016</b> , 16, 74-9	111
1261	Physical vapor deposition synthesis of two-dimensional orthorhombic SnS flakes with strong angle/temperature-dependent Raman responses. <b>2016</b> , 8, 2063-70	163
1260	Simple fabrication method for atomically-thin crystal devices with polymer passivation. <b>2016</b> , 216, 98-102	0
1259	Van der Waals heterostructure of phosphorene and hexagonal boron nitride: First-principles modeling. <b>2016</b> , 25, 037302	6
1258	In situ observation of electrical property of thin-layer black phosphorus based on dry transfer method. <b>2016</b> , 9, 045202	3
1257	Black Phosphorus Flexible Thin Film Transistors at Gighertz Frequencies. <b>2016</b> , 16, 2301-6	112
1256	Black Phosphorous Thin-Film Transistor and RF Circuit Applications. <b>2016</b> , 37, 449-451	8

1255	One-pot solventless preparation of PEGylated black phosphorus nanoparticles for photoacoustic imaging and photothermal therapy of cancer. <b>2016</b> , 91, 81-89	324
1254	Generation of Mode-locked Ytterbium doped fiber ring laser using few-layer black phosphorus as a saturable absorber. <b>2016</b> , 1-1	5
1253	Calcium decorated and doped phosphorene for gas adsorption. <b>2016</b> , 377, 311-323	69
1252	Polytypism and unexpected strong interlayer coupling in two-dimensional layered ReS <sub>2</sub> . <b>2016</b> , 8, 8324-32	99
1251	Pseudo-Jahn-Teller Distortion in Two-Dimensional Phosphorus: Origin of Black and Blue Phases of Phosphorene and Band Gap Modulation by Molecular Charge Transfer. <b>2016</b> , 7, 1288-97	67
1250	Selective Ionic Transport Pathways in Phosphorene. <b>2016</b> , 16, 2240-7	68
1249	First-principles studies on substitutional doping by group IV and VI atoms in the two-dimensional arsenene. <b>2016</b> , 378, 350-356	31
1248	Optical reflection, transmission and absorption properties of single-layer black phosphorus from a model calculation. <b>2016</b> , 18, 055102	7
1247	High-pressure melt growth and transport properties of SiP, SiAs, GeP, and GeAs 2D layered semiconductors. <b>2016</b> , 443, 75-80	77
1246	Carbon phosphide monolayers with superior carrier mobility. <b>2016</b> , 8, 8819-25	97
1245	Scalable shear-exfoliation of high-quality phosphorene nanoflakes with reliable electrochemical cycleability in nano batteries. <b>2016</b> , 3, 025005	57
1244	Phosphorene as a promising anchoring material for lithium-sulfur batteries: a computational study. <b>2016</b> , 4, 6124-6130	122
1243	Chemically Tailoring Semiconducting Two-Dimensional Transition Metal Dichalcogenides and Black Phosphorus. <b>2016</b> , 10, 3900-17	192
1242	Quantum Hall effect in black phosphorus two-dimensional electron system. <i>Nature Nanotechnology</i> , <b>2016</b> , 11, 593-7	28.7 289
1241	Electronic Structures and Carrier Mobilities of Blue Phosphorus Nanoribbons and Nanotubes: A First-Principles Study. <b>2016</b> , 120, 4638-4646	69
1240	Fracture patterns and the energy release rate of phosphorene. <b>2016</b> , 8, 5728-36	36
1239	Light adatoms influences on electronic structures of the two-dimensional arsenene nanosheets. <b>2016</b> , 230, 6-10	18
1238	Review on the Raman spectroscopy of different types of layered materials. <b>2016</b> , 8, 6435-50	235

1237	Germanium monosulfide monolayer: a novel two-dimensional semiconductor with a high carrier mobility. <b>2016</b> , 4, 2155-2159	150
1236	Temperature Evolution of Phonon Properties in Few-Layer Black Phosphorus. <b>2016</b> , 120, 5265-5270	49
1235	Optoelectronic properties of atomically thin ReSSe with weak interlayer coupling. <b>2016</b> , 8, 5826-34	27
1234	Recent advances in high-pressure science and technology. <b>2016</b> , 1, 59-75	70
1233	Sustained hole inversion layer in a wide-bandgap metal-oxide semiconductor with enhanced tunnel current. <b>2016</b> , 7, 10632	14
1232	Black phosphorene/monolayer transition-metal dichalcogenides as two dimensional van der Waals heterostructures: a first-principles study. <b>2016</b> , 18, 7381-8	82
1231	Structural, electronic and magnetic properties of 3d transition metals embedded graphene-like carbon nitride sheet: A DFT + U study. <b>2016</b> , 380, 1373-1377	16
1230	Manipulation of n and p type dope black phosphorene layer: A first principles study. <b>2016</b> , 16, 506-514	10
1229	Two-dimensional tricycle arsenene with a direct band gap. <b>2016</b> , 18, 8723-9	27
1228	Electron-hole asymmetry in the electron-phonon coupling in top-gated phosphorene transistor. <b>2016</b> , 3, 015008	20
1227	Formation of a quantum spin Hall state on a Ge(111) surface. <b>2016</b> , 27, 095703	7
1226	Symmetric complementary logic inverter using integrated black phosphorus and MoS <sub>2</sub> transistors. <b>2016</b> , 3, 011006	46
1225	Edge-Modified Phosphorene Nanoflake Heterojunctions as Highly Efficient Solar Cells. <b>2016</b> , 16, 1675-82	142
1224	Electronic and magnetic properties of nonmetal atoms doped blue phosphorene: First-principles study. <b>2016</b> , 408, 121-126	38
1223	Present perspectives of broadband photodetectors based on nanobelts, nanoribbons, nanosheets and the emerging 2D materials. <b>2016</b> , 8, 6410-34	196
1222	Two-Dimensional Disorder in Black Phosphorus and Monochalcogenide Monolayers. <b>2016</b> , 16, 1704-12	82
1221	Superconductivity of bilayer phosphorene under interlayer compression. <b>2016</b> , 25, 027402	7
1220	. <b>2016</b> , 63, 1189-1194	3

1219	Low-frequency interlayer vibration modes in two-dimensional layered materials. <b>2016</b> , 80, 130-141	15
1218	Phosphorene: A new competitor for graphene. <b>2016</b> , 41, 4085-4095	81
1217	Nonradiative Electron-Hole Recombination Rate Is Greatly Reduced by Defects in Monolayer Black Phosphorus: Ab Initio Time Domain Study. <b>2016</b> , 7, 653-9	78
1216	Nonequilibrium spin injection in monolayer black phosphorus. <b>2016</b> , 18, 1601-6	37
1215	Quantum dots derived from two-dimensional materials and their applications for catalysis and energy. <b>2016</b> , 45, 2239-62	311
1214	Mid-infrared mode-locked pulse generation with multilayer black phosphorus as saturable absorber. <b>2016</b> , 41, 56-9	142
1213	Effects of interlayer coupling and electric fields on the electronic structures of graphene and MoS <sub>2</sub> heterobilayers. <b>2016</b> , 4, 1776-1781	89
1212	The stacking dependent electronic structure and optical properties of bilayer black phosphorus. <b>2016</b> , 18, 6085-91	36
1211	Interactions between lasers and two-dimensional transition metal dichalcogenides. <b>2016</b> , 45, 2494-515	49
1210	Gas adsorption on MoS <sub>2</sub> /WS <sub>2</sub> in-plane heterojunctions and the I <sub>V</sub> response: a first principles study. <b>2016</b> , 6, 17494-17503	41
1209	Long-Range Magnetic Ordering and Switching of Magnetic State by Electric Field in Porous Phosphorene. <b>2016</b> , 7, 647-52	16
1208	Monolayer PhosphoreneMetal Contacts. <b>2016</b> , 28, 2100-2109	166
1207	The electronic structure, mechanical flexibility and carrier mobility of black arsenic-phosphorus monolayers: a first principles study. <b>2016</b> , 18, 9779-87	33
1206	Tuning the electronic properties of monolayer and bilayer PtSe <sub>2</sub> via strain engineering. <b>2016</b> , 4, 3106-3112	70
1205	Multilayer Black Phosphorus as a Versatile Mid-Infrared Electro-optic Material. <b>2016</b> , 16, 1683-9	117
1204	Interaction between phosphorene and the surface of a substrate. <b>2016</b> , 3, 025013	7
1203	Periodic Modulation of the Doping Level in Striped MoS <sub>2</sub> Superstructures. <b>2016</b> , 10, 3461-8	26
1202	Thickness-Dependent Thermal Conductivity of Suspended Two-Dimensional Single-Crystal In <sub>2</sub> Se <sub>3</sub> Layers Grown by Chemical Vapor Deposition. <b>2016</b> , 120, 4753-4758	38

1201	Promising electron mobility and high thermal conductivity in Sc <sub>2</sub> CT <sub>2</sub> (T = F, OH) MXenes. <b>2016</b> , 8, 6110-7	141
1200	Characterization and sonochemical synthesis of black phosphorus from red phosphorus. <b>2016</b> , 3, 014007	50
1199	Harmonic mode-locking and wavelength-tunable Q-switching operation in the grapheneBi <sub>2</sub> Te <sub>3</sub> heterostructure saturable absorber-based fiber laser. <b>2016</b> , 55, 081314	18
1198	Strongly enhanced photoluminescence in nanostructured monolayer MoS <sub>2</sub> by chemical vapor deposition. <b>2016</b> , 27, 135706	28
1197	Observation of coupling between zero- and two-dimensional semiconductor systems based on anomalous diamagnetic effects. <b>2016</b> , 9, 306-316	15
1196	Polaronic effects in monolayer black phosphorus on polar substrates. <b>2016</b> , 93,	37
1195	Two-step heating synthesis of sub-3 millimeter-sized orthorhombic black phosphorus single crystal by chemical vapor transport reaction method. <b>2016</b> , 59, 122-134	48
1194	Bending Two-Dimensional Materials To Control Charge Localization and Fermi-Level Shift. <b>2016</b> , 16, 2444-9	57
1193	Thermal conductivity of armchair black phosphorus nanotubes: a molecular dynamics study. <b>2016</b> , 27, 155703	22
1192	Control of electronic properties of 2D carbides (MXenes) by manipulating their transition metal layers. <b>2016</b> , 1, 227-234	242
1191	Electron Doping of Ultrathin Black Phosphorus with Cu Adatoms. <b>2016</b> , 16, 2145-51	165
1190	Probing Out-of-Plane Charge Transport in Black Phosphorus with Graphene-Contacted Vertical Field-Effect Transistors. <b>2016</b> , 16, 2580-5	106
1189	Half-oxidized phosphorene: band gap and elastic properties modulation. <b>2016</b> , 28, 145501	8
1188	Optically driven black phosphorus as a saturable absorber for mode-locked laser pulse generation. <b>2016</b> , 55, 081317	21
1187	Phosphorene-based nanogenerator powered by cyclic molecular doping. <b>2016</b> , 23, 34-39	13
1186	Extraordinarily Bound Quasi-One-Dimensional Trions in Two-Dimensional Phosphorene Atomic Semiconductors. <b>2016</b> , 10, 2046-53	75
1185	Growth Mechanism and Enhanced Yield of Black Phosphorus Microribbons. <b>2016</b> , 16, 1096-1103	63
1184	Interlayer electronic hybridization leads to exceptional thickness-dependent vibrational properties in few-layer black phosphorus. <b>2016</b> , 8, 2740-50	111

1183	Out-of-plane structural flexibility of phosphorene. <b>2016</b> , 27, 055701	34
1182	Anomalous Size Dependence of Optical Properties in Black Phosphorus Quantum Dots. <b>2016</b> , 7, 370-5	78
1181	Direct Synthesis and Practical Bandgap Estimation of Multilayer Arsenene Nanoribbons. <b>2016</b> , 28, 425-429	189
1180	Second-Harmonic Generation of Spoof Surface Plasmon Polaritons Using Nonlinear Plasmonic Metamaterials. <b>2016</b> , 3, 139-146	78
1179	Tuning Phosphorene Nanoribbon Electronic Structure through Edge Oxidization. <b>2016</b> , 120, 2149-2158	25
1178	Graphene/phosphorene bilayer: High electron speed, optical property and semiconductor-metal transition with electric field. <b>2016</b> , 16, 318-323	22
1177	"Doping" pentacene with sp(2)-phosphorus atoms: towards high performance ambipolar semiconductors. <b>2016</b> , 18, 3173-8	12
1176	Anomalous Raman scattering and lattice dynamics in mono- and few-layer WTe <sub>2</sub> . <b>2016</b> , 8, 2309-16	77
1175	Tailoring magnetism of black phosphorene doped with B, C, N, O, F, S and Se atom: A DFT calculation. <b>2016</b> , 662, 528-533	48
1174	Atom-Thin SnS <sub>2</sub> -xSex with Adjustable Compositions by Direct Liquid Exfoliation from Single Crystals. <b>2016</b> , 10, 755-62	33
1173	Indiene 2D monolayer: a new nanoelectronic material. <b>2016</b> , 6, 8006-8014	30
1172	Electric field and strain tunable electronic structures in monolayer Black Phosphorus. <b>2016</b> , 112, 297-303	10
1171	Effect of incorporation of black phosphorus into PEDOT:PSS on conductivity and electron-phonon coupling. <b>2016</b> , 212, 180-185	24
1170	Al <sub>2</sub> C Monolayer Sheet and Nanoribbons with Unique Direction-Dependent Acoustic-Phonon-Limited Carrier Mobility and Carrier Polarity. <b>2016</b> , 7, 302-7	21
1169	Two-Dimensional SiS Layers with Promising Electronic and Optoelectronic Properties: Theoretical Prediction. <b>2016</b> , 16, 1110-7	110
1168	Mechanisms of current fluctuation in ambipolar black phosphorus field-effect transistors. <b>2016</b> , 8, 3572-8	26
1167	Ambipolar Black Phosphorus MOSFETs With Record n-Channel Transconductance. <b>2016</b> , 37, 103-106	28
1166	Structure and magnetism of Mn, Fe, or Co adatoms on monolayer and bilayer black phosphorus. <b>2016</b> , 401, 706-710	14



1165	Weak Van der Waals Stacking, Wide-Range Band Gap, and Raman Study on Ultrathin Layers of Metal Phosphorus Trichalcogenides. <b>2016</b> , 10, 1738-43	273
1164	Thermal conductivities of single- and multi-layer phosphorene: a molecular dynamics study. <b>2016</b> , 8, 483-91	129
1163	Layer-dependent surface potential of phosphorene and anisotropic/layer-dependent charge transfer in phosphorene-gold hybrid systems. <b>2016</b> , 8, 129-35	54
1162	First-principles study of MoS <sub>2</sub> , phosphorene and graphene based single electron transistor for gas sensing applications. <b>2016</b> , 222, 492-498	140
1161	First-principles study of two-dimensional van der Waals heterojunctions. <b>2016</b> , 112, 518-526	72
1160	Elastic and Inelastic LightMatter Interactions in 2D Materials. <b>2017</b> , 23, 206-213	6
1159	Field-effect transistor biosensors with two-dimensional black phosphorus nanosheets. <b>2017</b> , 89, 505-510	166
1158	Compact Passive Q-Switching Pr <sup>3+</sup> -Doped ZBLAN Fiber Laser With Black Phosphorus-Based Saturable Absorber. <b>2017</b> , 23, 7-12	26
1157	Generation of Mode-Locked Ytterbium Doped Fiber Ring Laser Using Few-Layer Black Phosphorus as a Saturable Absorber. <b>2017</b> , 23, 39-43	89
1156	Giant Anisotropic Raman Response of Encapsulated Ultrathin Black Phosphorus by Uniaxial Strain. <b>2017</b> , 27, 1600986	81
1155	Visualizing subsurface defects in graphite by acoustic atomic force microscopy. <b>2017</b> , 80, 66-74	11
1154	Substrate induced changes in atomically thin 2-dimensional semiconductors: Fundamentals, engineering, and applications. <b>2017</b> , 4, 011301	76
1153	Effective Doping of Monolayer Phosphorene by Surface Adsorption of Atoms for Electronic and Spintronic Applications. <b>2017</b> , 63, 205-215	39
1152	First-principle calculations of optical properties of monolayer arsenene and antimonene allotropes. <b>2017</b> , 529, 1600152	101
1151	Can a Black Phosphorus Schottky Barrier Transistor Be Good Enough?. <b>2017</b> , 9, 3959-3966	55
1150	Schwarzer Phosphor neu entdeckt: vom Volumenmaterial zu Monoschichten. <b>2017</b> , 129, 8164-8185	56
1149	Black Phosphorus Rediscovered: From Bulk Material to Monolayers. <b>2017</b> , 56, 8052-8072	315
1148	Sensitive Detection of Carcinoembryonic Antigen Using Stability-Limited Few-Layer Black Phosphorus as an Electron Donor and a Reservoir. <b>2017</b> , 13, 1603589	102

1147	Anisotropic Spectroscopy and Electrical Properties of 2D ReS <sub>2</sub> Se Alloys with Distorted 1T Structure. <b>2017</b> , 13, 1603788	57
1146	Realization of vertical and lateral van der Waals heterojunctions using two-dimensional layered organic semiconductors. <b>2017</b> , 10, 1336-1344	23
1145	Photo-responsive Bi <sub>2</sub> S <sub>3</sub> nanoflakes: Synthesis and device fabrication at ambient conditions. <b>2017</b> , 89, 108-115	9
1144	Few-layer black phosphorus: A bright future in electromagnetic absorption. <b>2017</b> , 193, 30-33	15
1143	Chemical Functionalization of Pentagermanene Leads to Stabilization and Tunable Electronic Properties by External Tensile Strain. <b>2017</b> , 2, 171-180	11
1142	As thin as it gets. <b>2017</b> , 16, 155	9
1141	Stability and electronic properties of phosphorene oxides: from 0-dimensional to amorphous 2-dimensional structures. <b>2017</b> , 9, 2428-2435	26
1140	Influence of removing PMMA residues on surface of CVD graphene using a contact-mode atomic force microscope. <b>2017</b> , 7, 6943-6949	44
1139	Strain-induced modulation on phonon and electronic properties of suspended black phosphorus field effect transistor. <b>2017</b> , 381, 792-795	6
1138	Thermal Properties of Two Dimensional Layered Materials. <b>2017</b> , 27, 1604134	96
1137	TiL-Coordinated Black Phosphorus Quantum Dots as an Efficient Contrast Agent for In Vivo Photoacoustic Imaging of Cancer. <b>2017</b> , 13, 1602896	198
1136	Infrared fingerprints of few-layer black phosphorus. <b>2017</b> , 8, 14071	179
1135	Effects of Contact Placement and Intra/Interlayer Interaction in Current Distribution of Black Phosphorus Sub-10-nm FET. <b>2017</b> , 64, 579-586	5
1134	Electronic band structure of surface-doped black phosphorus. <b>2017</b> , 219, 86-91	9
1133	Epitaxial Stitching and Stacking Growth of Atomically Thin Transition-Metal Dichalcogenides (TMDCs) Heterojunctions. <b>2017</b> , 27, 1603884	57
1132	Toward Sensitive Room-Temperature Broadband Detection from Infrared to Terahertz with Antenna-Integrated Black Phosphorus Photoconductor. <b>2017</b> , 27, 1604414	68
1131	Nonlinear Saturable and Polarization-induced Absorption of Rhenium Disulfide. <b>2017</b> , 7, 40080	86
1130	General criterion to distinguish between Schottky and Ohmic contacts at the metal/two-dimensional semiconductor interface. <b>2017</b> , 9, 2068-2073	26

1129	Emergent elemental two-dimensional materials beyond graphene. <b>2017</b> , 50, 053004	56
1128	Effective g factor in black phosphorus thin films. <b>2017</b> , 95,	19
1127	Unintentional doping effects in black phosphorus by native vacancies in h-BN supporting layer. <b>2017</b> , 402, 175-181	10
1126	Novel QCM humidity sensors using stacked black phosphorus nanosheets as sensing film. <b>2017</b> , 244, 259-264	72
1125	Recent development of two-dimensional transition metal dichalcogenides and their applications. <b>2017</b> , 20, 116-130	1250
1124	Three-Dimensional Integration of Black Phosphorus Photodetector with Silicon Photonics and Nanoplasmonics. <b>2017</b> , 17, 985-991	81
1123	Ideal strength and elastic instability in single-layer 8-Pmmn borophene. <b>2017</b> , 7, 8654-8660	40
1122	Linear and nonlinear magneto-optical properties of monolayer phosphorene. <b>2017</b> , 121, 045107	33
1121	Oxygen induced strong mobility modulation in few-layer black phosphorus. <b>2017</b> , 4, 021007	40
1120	Atomic-scale imaging of few-layer black phosphorus and its reconstructed edge. <b>2017</b> , 50, 084003	27
1119	Two-Dimensional SnS: A Phosphorene Analogue with Strong In-Plane Electronic Anisotropy. <b>2017</b> , 11, 2219-2226	184
1118	A density-functional-theory-based finite element model to study the mechanical properties of zigzag phosphorene nanotubes. <b>2017</b> , 88, 272-278	17
1117	Ambipolar transport based on CVD-synthesized ReSe 2. <b>2017</b> , 4, 025014	22
1116	Size modulation electronic and optical properties of phosphorene nanoribbons: DFT-BOLS approximation. <b>2017</b> , 19, 5304-5309	42
1115	Density functional study of metal-phosphorene interfaces. <b>2017</b> , 31, 1750077	4
1114	Structural and electronic properties of arsenic nitrogen monolayer. <b>2017</b> , 381, 1102-1106	24
1113	Ultraviolet saturable absorption and ultrafast carrier dynamics in ultrasmall black phosphorus quantum dots. <b>2017</b> , 9, 4683-4690	83
1112	In situ observation of the thermal stability of black phosphorus. <b>2017</b> , 4, 025001	29

1111	Au/La Ti O Nanostructures Sensitized with Black Phosphorus for Plasmon-Enhanced Photocatalytic Hydrogen Production in Visible and Near-Infrared Light. <b>2017</b> , 56, 2064-2068	228
1110	Two-Dimensional Metal Halide Perovskites: Theory, Synthesis, and Optoelectronics. <b>2017</b> , 1, 1600018	95
1109	Widely tunable and anisotropic charge carrier mobility in monolayer tin(II) selenide using biaxial strain: a first-principles study. <b>2017</b> , 5, 1247-1254	78
1108	Au/La <sub>2</sub> Ti <sub>2</sub> O <sub>7</sub> Nanostructures Sensitized with Black Phosphorus for Plasmon-Enhanced Photocatalytic Hydrogen Production in Visible and Near-Infrared Light. <b>2017</b> , 129, 2096-2100	49
1107	Electrocatalysis for the oxygen evolution reaction: recent development and future perspectives. <b>2017</b> , 46, 337-365	3041
1106	Black phosphorus nanoparticles as a novel fluorescent sensing platform for nucleic acid detection. <b>2017</b> , 1, 1130-1136	65
1105	Ultra-narrow blue phosphorene nanoribbons for tunable optoelectronics. <b>2017</b> , 7, 2992-3002	25
1104	Black Phosphorus Quantum Dots for Hole Extraction of Typical Planar Hybrid Perovskite Solar Cells. <b>2017</b> , 8, 591-598	139
1103	First-principles prediction of a low energy edge-reconstruction for zigzag phosphorene nanoribbons. <b>2017</b> , 50, 065304	4
1102	Universal edge bands induced by linearly polarized irradiation on phosphorene. <b>2017</b> , 19, 013004	4
1101	Phosphorus quantum dots as visible-light photocatalyst for water splitting. <b>2017</b> , 130, 56-63	47
1100	Sodium-Induced Reordering of Atomic Stacks in Black Phosphorus. <b>2017</b> , 29, 1350-1356	44
1099	2D metal carbides and nitrides (MXenes) for energy storage. <b>2017</b> , 2,	3469
1098	Synthesis and chemistry of elemental 2D materials. <b>2017</b> , 1,	475
1097	A Review of Thermal Transport in Low-Dimensional Materials Under External Perturbation: Effect of Strain, Substrate, and Clustering. <b>2017</b> , 21, 201-236	27
1096	On the stability characteristics of zigzag phosphorene nanotubes: A finite element investigation. <b>2017</b> , 702, 388-398	11
1095	Predicting a graphene-like WB nanosheet with a double Dirac cone, an ultra-high Fermi velocity and significant gap opening by spin-orbit coupling. <b>2017</b> , 19, 5449-5453	28
1094	Is the Metallic Phosphorus Carbide (MPC) Monolayer Stable? An Answer from a Theoretical Perspective. <b>2017</b> , 8, 747-754	35

1093	GeP: A Small Indirect Band Gap 2D Crystal with High Carrier Mobility and Strong Interlayer Quantum Confinement. <b>2017</b> , 17, 1833-1838	228
1092	High-Pressure Synthesis and Characterization of $\alpha$ -GeSe-A Six-Membered-Ring Semiconductor in an Uncommon Boat Conformation. <b>2017</b> , 139, 2771-2777	71
1091	A first principle study of graphene functionalized with hydroxyl, nitrile, or methyl groups. <b>2017</b> , 146, 044705	7
1090	Thermal Transport Properties of Black Phosphorus: A Topical Review. <b>2017</b> , 21, 45-57	15
1089	Advent of 2D Rhenium Disulfide (ReS <sub>2</sub> ): Fundamentals to Applications. <b>2017</b> , 27, 1606129	224
1088	Introduction to Topological Phases and Electronic Interactions in (2+1) Dimensions. <b>2017</b> , 47, 215-230	3
1087	Strain and deformations engineered germanene bilayer double gate-field effect transistor by first principles. <b>2017</b> , 418, 308-311	2
1086	Electronic structure, optical properties and band edges of layered MoO <sub>3</sub> : A first-principles investigation. <b>2017</b> , 130, 242-248	47
1085	2D Materials for Optical Modulation: Challenges and Opportunities. <b>2017</b> , 29, 1606128	256
1084	Exfoliation of black phosphorus in ionic liquids. <b>2017</b> , 28, 125603	39
1083	Emerging Low-Dimensional Materials for Nonlinear Optics and Ultrafast Photonics. <b>2017</b> , 29, 1605886	184
1082	Control of Surface and Edge Oxidation on Phosphorene. <b>2017</b> , 9, 9126-9135	102
1081	From single atoms to self-assembled quantum single-atomic nanowires: noble metal atoms on black phosphorene monolayers. <b>2017</b> , 19, 7864-7870	0
1080	Black Phosphorus Revisited: A Missing Metal-Free Elemental Photocatalyst for Visible Light Hydrogen Evolution. <b>2017</b> , 29, 1605776	309
1079	Suppressed superconductivity in substrate-supported $\sqrt{12}$ borophene by tensile strain and electron doping. <b>2017</b> , 4, 025032	63
1078	Magnetic engineering in 3d transition metals on phosphorene by strain. <b>2017</b> , 381, 1236-1240	15
1077	Temperature-Dependent Raman Responses of the Vapor-Deposited Tin Selenide Ultrathin Flakes. <b>2017</b> , 121, 4674-4679	68
1076	Franckeite as a naturally occurring van der Waals heterostructure. <b>2017</b> , 8, 14409	68

1075	Ab initio study of tunable band gap of monolayer and bilayer phosphorene by the vertical electronic field. <b>2017</b> , 32, 213-216	5
1074	Size-dependent nonlinear optical properties of black phosphorus nanosheets and their applications in ultrafast photonics. <b>2017</b> , 5, 3007-3013	121
1073	Anisotropic mechanical and optical response and negative Poisson's ratio in MoC nanomembranes revealed by first-principles simulations. <b>2017</b> , 28, 115705	41
1072	Ferroelectric FET for nonvolatile memory application with two-dimensional MoSe <sub>2</sub> channels. <b>2017</b> , 4, 025036	63
1071	Adaptively Compressed Exchange Operator for Large-Scale Hybrid Density Functional Calculations with Applications to the Adsorption of Water on Silicene. <b>2017</b> , 13, 1188-1198	21
1070	Monolayer Transistor SRAMs. <b>2017</b> , 13, 1-28	1
1069	Rapid and Large-Area Characterization of Exfoliated Black Phosphorus Using Third-Harmonic Generation Microscopy. <b>2017</b> , 8, 1343-1350	50
1068	Different-sized black phosphorus nanosheets with good cytocompatibility and high photothermal performance. <b>2017</b> , 7, 14618-14624	47
1067	Orbital Edge States in a Photonic Honeycomb Lattice. <b>2017</b> , 118, 107403	53
1066	Interfacial thermal conductance in graphene/black phosphorus heterogeneous structures. <b>2017</b> , 117, 399-410	58
1065	Optical Identification of Few-Layer Antimonene Crystals. <b>2017</b> , 4, 600-605	48
1064	Atomic Defects in Two-Dimensional Materials: From Single-Atom Spectroscopy to Functionalities in Opto-/Electronics, Nanomagnetism, and Catalysis. <b>2017</b> , 29, 1606434	146
1063	Gas adsorption on monolayer blue phosphorus: implications for environmental stability and gas sensors. <b>2017</b> , 28, 175708	67
1062	Toward high-performance two-dimensional black phosphorus electronic and optoelectronic devices. <b>2017</b> , 26, 037307	8
1061	Vastly enhancing the chemical stability of phosphorene by employing an electric field. <b>2017</b> , 9, 4219-4226	19
1060	Optical properties of phosphorene. <b>2017</b> , 26, 034201	9
1059	Chemically exfoliating large sheets of phosphorene via choline chloride urea viscosity-tuning. <b>2017</b> , 28, 155601	10
1058	Black Phosphorus: Properties, Synthesis, and Applications in Energy Conversion and Storage. <b>2017</b> , 3, 352-361	30

1057	Solution-Based Processing of Monodisperse Two-Dimensional Nanomaterials. <b>2017</b> , 50, 943-951	131
1056	Ionic Intercalation in Two-Dimensional van der Waals Materials: In Situ Characterization and Electrochemical Control of the Anisotropic Thermal Conductivity of Black Phosphorus. <b>2017</b> , 17, 1431-1438	70
1055	Epitaxial chemical vapour deposition growth of monolayer hexagonal boron nitride on a Cu(111)/sapphire substrate. <b>2017</b> , 19, 8230-8235	26
1054	Novel bonding patterns and optoelectronic properties of the two-dimensional SixCy monolayers. <b>2017</b> , 5, 3561-3567	29
1053	Phonon-limited carrier mobility in monolayer black phosphorus. <b>2017</b> , 95,	23
1052	Electronic properties of single-layer antimony: Tight-binding model, spin-orbit coupling, and the strength of effective Coulomb interactions. <b>2017</b> , 95,	28
1051	Half Layer By Half Layer Growth of a Blue Phosphorene Monolayer on a GaN(001) Substrate. <b>2017</b> , 118, 046101	118
1050	Self-assembly of electronically abrupt borophene/organic lateral heterostructures. <b>2017</b> , 3, e1602356	64
1049	Multifunctional Homogeneous Lateral Black Phosphorus Junction Devices. <b>2017</b> , 29, 3143-3151	21
1048	Nonlinear Black Phosphorus for Ultrafast Optical Switching. <b>2017</b> , 7, 43371	37
1047	Rhenium dichalcogenides (ReX <sub>2</sub> , X = S or Se): an emerging class of TMDs family. <b>2017</b> , 1, 1917-1932	42
1046	Recent progress in van der Waals heterojunctions. <b>2017</b> , 9, 4324-4365	114
1045	Prediction of phonon-mediated superconductivity in borophene. <b>2017</b> , 95,	138
1044	Many-body Effect, Carrier Mobility, and Device Performance of Hexagonal Arsenene and Antimonene. <b>2017</b> , 29, 2191-2201	194
1043	Functionalization of Single-Layer Nitrogen by Vacancy, Adatoms, and Molecules. <b>2017</b> , 121, 6329-6338	11
1042	Puckered-layer-structured germanium monosulfide for superior rechargeable Li-ion battery anodes. <b>2017</b> , 5, 5685-5689	25
1041	Hittorf's phosphorus: the missing link during transformation of red phosphorus to black phosphorus. <b>2017</b> , 19, 905-909	26
1040	Emerging Trends in Phosphorene Fabrication towards Next Generation Devices. <b>2017</b> , 4, 1600305	224

1039	Large edge magnetism in oxidized few-layer black phosphorus nanomeshes. <b>2017</b> , 10, 718-728	24
1038	Ultrafast photocurrent measurements of a black phosphorus photodetector. <b>2017</b> , 110, 051102	30
1037	Atomistic mechanisms of van der Waals epitaxy and property optimization of layered materials. <b>2017</b> , 7, e1300	10
1036	The effects of vacancy and oxidation on black phosphorus nanoresonators. <b>2017</b> , 28, 135202	13
1035	Reactivity of phosphorene with a 3d element trioxide (CrO) considering van der Waals molecular interactions: a DFT-D2 study. <b>2017</b> , 23, 49	4
1034	2D lateral heterostructures of monolayer and bilayer phosphorene. <b>2017</b> , 5, 2291-2300	21
1033	Structures and Mechanical and Electronic Properties of the Ti <sub>2</sub> CO <sub>2</sub> MXene Incorporated with Neighboring Elements (Sc, V, B and N). <b>2017</b> , 46, 2460-2466	42
1032	Strong thermal transport along polycrystalline transition metal dichalcogenides revealed by multiscale modeling for MoS <sub>2</sub> . <b>2017</b> , 7, 67-76	29
1031	Winding a nanotube from black phosphorus nanoribbon onto a CNT at low temperature: A molecular dynamics study. <b>2017</b> , 121, 406-413	25
1030	Exfoliation Energy of Black Phosphorus Revisited: A Coupled Cluster Benchmark. <b>2017</b> , 8, 1290-1294	26
1029	Generation of Anisotropic Massless Dirac Fermions and Asymmetric Klein Tunneling in Few-Layer Black Phosphorus Superlattices. <b>2017</b> , 17, 2280-2286	33
1028	High thermoelectric power factor in two-dimensional crystals of MoS <sub>2</sub> . <b>2017</b> , 95,	133
1027	Enhanced hydrophilic and conductive properties of blue phosphorene doped with Si atom. <b>2017</b> , 675, 20-26	11
1026	Effects of interlayer polarization field on the band structures of the WS <sub>2</sub> /MoS <sub>2</sub> and WSe <sub>2</sub> /MoSe <sub>2</sub> heterostructures. <b>2017</b> , 661, 1-9	7
1025	Thermoelectric transport in monolayer phosphorene. <b>2017</b> , 95,	38
1024	Ultrathin MoO <sub>2</sub> nanosheets with good thermal stability and high conductivity. <b>2017</b> , 7, 025015	24
1023	Effect of flexural phonons on the hole states in single-layer black phosphorus. <b>2017</b> , 95,	4
1022	Layer-stacking effect on electronic structures of bilayer arsenene. <b>2017</b> , 117, 27002	15



1021	Stability, electronic and thermodynamic properties of aluminene from first-principles calculations. <b>2017</b> , 409, 85-90	40
1020	Air-Stable Humidity Sensor Using Few-Layer Black Phosphorus. <b>2017</b> , 9, 10019-10026	68
1019	Phase transformation in two-dimensional crystalline silica under compressive loading. <b>2017</b> , 19, 8478-8484	3
1018	Thermal properties of two-dimensional materials. <b>2017</b> , 26, 034401	45
1017	Topological transport in Dirac electronic systems: A concise review. <b>2017</b> , 26, 037301	8
1016	Field-induced diverse quantizations in monolayer and bilayer black phosphorus. <b>2017</b> , 95,	22
1015	Conceptualization of Doped Black P Thin Films for Potential Use in Photovoltaics with Validation from First Principle Calculations. <b>2017</b> , 395-399	
1014	New Method to Determine the Schottky Barrier in Few-Layer Black Phosphorus Metal Contacts. <b>2017</b> , 9, 7873-7877	11
1013	Tensile and compressive behaviors of prestrained single-layer black phosphorus: a molecular dynamics study. <b>2017</b> , 9, 3609-3619	15
1012	The fabrication of ReS <sub>2</sub> flowers at controlled locations by chemical vapor deposition. <b>2017</b> , 89, 115-118	9
1011	Interfacial Engineering of Van der Waals Coupled 2D Layered Materials. <b>2017</b> , 4, 1601054	18
1010	Tuning Electronic Properties of Monolayer Hexagonal Boron Phosphide with Group III/IV Dopants. <b>2017</b> , 121, 4583-4592	38
1009	Gate-Tunable Giant Stark Effect in Few-Layer Black Phosphorus. <b>2017</b> , 17, 1970-1977	106
1008	Carbon-doping-induced negative differential resistance in armchair phosphorene nanoribbons. <b>2017</b> , 38, 033005	6
1007	Few-Layer Black Phosphorus Carbide Field-Effect Transistor via Carbon Doping. <b>2017</b> , 29, 1700503	95
1006	Few-Layer Phosphorene-Decorated Microfiber for All-Optical Thresholding and Optical Modulation. <b>2017</b> , 5, 1700026	106
1005	Two-dimensional semiconductors XY <sub>2</sub> (X='Ge,Sn;Y='S,Se) with promising piezoelectric properties. <b>2017</b> , 11, 33-39	9
1004	Liquid-phase exfoliation of black phosphorus and its applications. <b>2017</b> , 2, 15-37	104

1003	Controlled Synthesis of High-Mobility Atomically Thin Bismuth Oxyselenide Crystals. <b>2017</b> , 17, 3021-3026	145
1002	A microprocessor based on a two-dimensional semiconductor. <b>2017</b> , 8, 14948	200
1001	2H-1T Phase Engineering of Layered Tantalum Disulfides in Electrocatalysis: Oxygen Reduction Reaction. <b>2017</b> , 23, 8082-8091	24
1000	Black phosphorus mid-infrared photodetectors. <b>2017</b> , 123, 1	29
999	Electronic and magnetic properties of Ga, Ge, P and Sb doped monolayer arsenene. <b>2017</b> , 251, 1-6	18
998	Hierarchical self-assembly of black phosphorus quantum dots with quantum confinement effects to a centimeter-scale membrane. <b>2017</b> , 254, 1700011	6
997	Effects of external electric field on the optical and electronic properties of blue phosphorene nanoribbons: A DFT study. <b>2017</b> , 135, 43-53	21
996	Electromechanical field effect transistors based on multilayer phosphorene nanoribbons. <b>2017</b> , 381, 1962-1966	7
995	Efficient electrical control of thin-film black phosphorus bandgap. <b>2017</b> , 8, 14474	183
994	1 / f noise in van der Waals materials and hybrids. <b>2017</b> , 2, 428-449	11
993	Identification of strained black phosphorous by Raman spectroscopy. <b>2017</b> , 38, 042003	0
992	Prospects of spintronics based on 2D materials. <b>2017</b> , 7, e1313	105
991	Spectroscopic investigation of defects in two-dimensional materials. <b>2017</b> , 6, 1219-1237	53
990	Degradation pattern of black phosphorus multilayer field-effect transistors in ambient conditions: Strategy for contact resistance engineering in BP transistors. <b>2017</b> , 419, 637-641	9
989	Interlayer-State-Coupling Dependent Ultrafast Charge Transfer in MoS/WS Bilayers. <b>2017</b> , 4, 1700086	61
988	Self-Assembly of a Jammed Black Phosphorus Nanoribbon on a Fixed Carbon Nanotube. <b>2017</b> , 121, 10174-10181	6
987	Black phosphorus nanostructures: recent advances in hybridization, doping and functionalization. <b>2017</b> , 46, 3492-3509	239
986	Ballistic Transport through a Strained Region on Monolayer Phosphorene. <b>2017</b> , 34, 027302	5

985	Noble metal atoms doped phosphorene: electronic properties and gas adsorption ability. <b>2017</b> , 4, 045703	16
984	Active 2D materials for on-chip nanophotonics and quantum optics. <b>2017</b> , 6, 1329-1342	28
983	Single-layer nanosheets with exceptionally high and anisotropic hydroxyl ion conductivity. <b>2017</b> , 3, e1602629	105
982	Tetra-silicene: A Semiconducting Allotrope of Silicene with Negative Poisson's Ratios. <b>2017</b> , 121, 9627-9633	31
981	Two-Dimensional Metal-Free Organic Multiferroic Material for Design of Multifunctional Integrated Circuits. <b>2017</b> , 8, 1973-1978	58
980	Intercalant-independent transition temperature in superconducting black phosphorus. <b>2017</b> , 8, 15036	68
979	Recent progress in the application of nanomaterials in the analysis of emerging chemical contaminants. <b>2017</b> , 9, 2768-2783	23
978	Two-Dimensional Semiconductors: From Materials Preparation to Electronic Applications. <b>2017</b> , 3, 1700045	69
977	Resistive Switching Performance Improvement via Modulating Nanoscale Conductive Filament, Involving the Application of Two-Dimensional Layered Materials. <b>2017</b> , 13, 1604306	105
976	Size and strain tunable band alignment of black-blue phosphorene lateral heterostructures. <b>2017</b> , 19, 12466-12472	16
975	Recent advances in synthesis, properties, and applications of phosphorene. <b>2017</b> , 1,	183
974	Magnetism in the p-type Monolayer II-VI semiconductors SrS and SrSe. <b>2017</b> , 7, 45869	12
973	Two-step fabrication of single-layer rectangular SnSe flakes. <b>2017</b> , 4, 021026	43
972	Nanoionics-Enabled Memristive Devices: Strategies and Materials for Neuromorphic Applications. <b>2017</b> , 3, 1600510	123
971	Black Phosphorus Based All-Optical-Signal-Processing: Toward High Performances and Enhanced Stability. <b>2017</b> , 4, 1466-1476	152
970	Photothermal Effect Induced Negative Photoconductivity and High Responsivity in Flexible Black Phosphorus Transistors. <b>2017</b> , 11, 6048-6056	71
969	Strong anisotropic perfect absorption in monolayer black phosphorous and its application as tunable polarizer. <b>2017</b> , 19, 075002	44
968	Few-Layered PtS <sub>2</sub> Phototransistor on h-BN with High Gain. <b>2017</b> , 27, 1701011	133

967	Resolving the In-Plane Anisotropic Properties of Black Phosphorus. <b>2017</b> , 1, 1700143	56
966	Band offsets and metal contacts in monolayer black phosphorus. <b>2017</b> , 178, 108-111	4
965	Computational mining of photocatalysts for water splitting hydrogen production: two-dimensional InSe-family monolayers. <b>2017</b> , 7, 2744-2752	94
964	Emergence of Tertiary Dirac Points in Graphene Moiré Superlattices. <b>2017</b> , 17, 3576-3581	16
963	Fluorescent black phosphorus quantum dots as label-free sensing probes for evaluation of acetylcholinesterase activity. <b>2017</b> , 250, 601-607	74
962	Self-assembled chiral phosphorus nanotubes from phosphorene: a molecular dynamics study. <b>2017</b> , 7, 24647-24651	16
961	Probing Single Vacancies in Black Phosphorus at the Atomic Level. <b>2017</b> , 17, 3607-3612	84
960	Two-band k.p Hamiltonian of phosphorene based on the infinitesimal basis transformations approach. <b>2017</b> , 109, 330-336	5
959	Antimonene Oxides: Emerging Tunable Direct Bandgap Semiconductor and Novel Topological Insulator. <b>2017</b> , 17, 3434-3440	217
958	Growth of Quasi-Free-Standing Single-Layer Blue Phosphorus on Tellurium Monolayer Functionalized Au(111). <b>2017</b> , 11, 4943-4949	92
957	Energy spectrums of bilayer triangular phosphorene quantum dots and antidots. <b>2017</b> , 7, 045122	12
956	Flexible Device Applications of 2D Semiconductors. <b>2017</b> , 13, 1603994	113
955	Layer-dependent electronic properties of phosphorene-like materials and phosphorene-based van der Waals heterostructures. <b>2017</b> , 9, 8616-8622	36
954	Atomistic quantum transport simulation of multilayer phosphorene nanoribbon field effect transistors. <b>2017</b> , 91, 161-168	5
953	Suspended black phosphorus nanosheet gas sensors. <b>2017</b> , 250, 569-573	80
952	Few-layer selenium-doped black phosphorus: synthesis, nonlinear optical properties and ultrafast photonics applications. <b>2017</b> , 5, 6129-6135	93
951	Prediction on the light-assisted exfoliation of multilayered arsenene by the photo-isomerization of azobenzene. <b>2017</b> , 9, 7006-7011	30
950	High field transport of high performance black phosphorus transistors. <b>2017</b> , 110, 163507	18

949	Analysis of multilayer black phosphorus for photodetector applications. <b>2017,</b>	
948	Thermoelectric properties of $\Gamma$ -As, Sb and Bi monolayers. <b>2017, 7, 24537-24546</b>	51
947	A study of bilayer phosphorene stability under MoS <sub>2</sub> -passivation. <b>2017, 4, 025091</b>	33
946	Phosphorus Nanostripe Arrays on Cu(110): A Case Study to Understand the Substrate Effect on the Phosphorus thin Film Growth. <b>2017, 4, 1601167</b>	13
945	Carrier thermoelectric transport model for black phosphorus field-effect transistors. <b>2017, 678, 271-274</b>	2
944	Atomic Layer Deposition on 2D Materials. <b>2017, 29, 3809-3826</b>	119
943	Ordering and Dynamics for the Formation of Two-Dimensional Molecular Crystals on Black Phosphorene. <b>2017, 121, 10210-10223</b>	36
942	Fracture mechanisms in multilayer phosphorene assemblies: from brittle to ductile. <b>2017, 19, 13083-13092</b>	8
941	Effect of metal adatoms on hydrogen adsorption properties of phosphorene. <b>2017, 4, 045503</b>	5
940	Nanoheat Conduction Performance of Black Phosphorus Field-Effect Transistor. <b>2017, 64, 2765-2769</b>	9
939	Low-Temperature Associated Interface Influence on the Black Phosphorus Nanoflakes. <b>2017, 9, 15219-15224</b>	7
938	A type-II GeSe/SnS heterobilayer with a suitable direct gap, superior optical absorption and broad spectrum for photovoltaic applications. <b>2017, 5, 13400-13410</b>	108
937	Low-Voltage 2D Material Field-Effect Transistors Enabled by Ion Gel Capacitive Coupling. <b>2017, 29, 4008-4013</b>	12
936	Five low energy phosphorene allotropes constructed through gene segments recombination. <b>2017, 7, 46431</b>	25
935	Effects of hole doping and strain on magnetism in buckled phosphorene and arsenene. <b>2017, 4, 025107</b>	24
934	Optical properties calculations of the phosphorene-CrO <sub>3</sub> system within the G <sub>0</sub> W <sub>0</sub> and BSE approximations. <b>2017, 416, 266-272</b>	3
933	Prediction of new group IV-V-VI monolayer semiconductors based on first principle calculation. <b>2017, 135, 160-164</b>	12
932	Sensitivity enhancement by using few-layer black phosphorus-graphene/TMDCs heterostructure in surface plasmon resonance biochemical sensor. <b>2017, 249, 542-548</b>	223

931	Effects of edge reconstruction on the common groups terminated zigzag phosphorene nanoribbon. <b>2017</b> , 50, 195301	3
930	Direct Growth of AlO on Black Phosphorus by Plasma-Enhanced Atomic Layer Deposition. <b>2017</b> , 12, 282	11
929	Defining the role of humidity in the ambient degradation of few-layer black phosphorus. <b>2017</b> , 4, 015025	91
928	2D Nanoelectronics. <b>2017</b> ,	11
927	Tuning quantum electron and phonon transport in two-dimensional materials by strain engineering: a Green's function based study. <b>2017</b> , 19, 1487-1495	16
926	. <b>2017</b> , 29, 23-26	18
925	Adsorption of NO molecules on armchair phosphorene nanosheet for nano sensor applications - A first-principles study. <b>2017</b> , 75, 365-374	43
924	Thermal Conductivity and Tensile Response of Phosphorene Nanosheets with Vacancy Defects. <b>2017</b> , 121, 13876-13887	39
923	Recent progress in two-dimensional COFs for energy-related applications. <b>2017</b> , 5, 14463-14479	185
922	Water-Catalyzed Oxidation of Few-Layer Black Phosphorous in a Dark Environment. <b>2017</b> , 56, 9131-9135	115
921	Edge magnetism and electronic structure properties of zigzag nanoribbons of arsenene and antimonene. <b>2017</b> , 110, 167-172	26
920	Phosphorus adlayers on Platinum (110). <b>2017</b> , 664, 216-221	
919	Solution Processed Boron Nitride Nanosheets: Synthesis, Assemblies and Emerging Applications. <b>2017</b> , 27, 1701450	109
918	The Covalent Functionalization of Layered Black Phosphorus by Nucleophilic Reagents. <b>2017</b> , 56, 9891-9896	124
917	Surface Functionalization of Black Phosphorus via Potassium toward High-Performance Complementary Devices. <b>2017</b> , 17, 4122-4129	99
916	Protective molecular passivation of black phosphorus. <b>2017</b> , 1,	46
915	Gas sensing in 2D materials. <b>2017</b> , 4, 021304	381
914	Encapsulation and Polymerization of White Phosphorus Inside Single-Wall Carbon Nanotubes. <b>2017</b> , 129, 8256-8260	20

913	Encapsulation and Polymerization of White Phosphorus Inside Single-Wall Carbon Nanotubes. <b>2017</b> , 56, 8144-8148	52
912	Properties, preparation and application of black phosphorus/phosphorene for energy storage: a review. <b>2017</b> , 52, 10364-10386	83
911	A two-dimensional semiconductor transistor with boosted gate control and sensing ability. <b>2017</b> , 3, e1602246	51
910	Adsorption of gases on monolayer GeSe: A first principle study. <b>2017</b> ,	1
909	Controlling Thermodynamic Properties of Ferromagnetic Group-IV Graphene-Like Nanosheets by Dilute Charged Impurity. <b>2017</b> , 67, 569	4
908	Rapid and nondestructive layer number identification of two-dimensional layered transition metal dichalcogenides. <b>2017</b> , 36, 698-703	6
907	Self-Assembled Layer (SAL)-Based Doping on Black Phosphorus (BP) Transistor and Photodetector. <b>2017</b> , 4, 1822-1830	31
906	Terahertz saturable absorbers from liquid phase exfoliation of graphite. <b>2017</b> , 8, 15763	69
905	Heterostructures containing dichalcogenides-new materials with predictable nanoarchitectures and novel emergent properties. <b>2017</b> , 32, 093004	24
904	Surface transport and quantum Hall effect in ambipolar black phosphorus double quantum wells. <b>2017</b> , 3, e1603179	19
903	Electrostatic-Driven Exfoliation and Hybridization of 2D Nanomaterials. <b>2017</b> , 29, 1700326	46
902	Ultrafast nonlinear optical response in solution dispersions of black phosphorus. <b>2017</b> , 7, 3352	19
901	Ab-initio study of ReCN in the bulk and as a new two dimensional material. <b>2017</b> , 7, 2799	2
900	Electronic properties of blue phosphorene/graphene and blue phosphorene/graphene-like gallium nitride heterostructures. <b>2017</b> , 19, 17324-17330	152
899	Compressed few-layer black phosphorus nanosheets from semiconducting to metallic transition with the highest symmetry. <b>2017</b> , 9, 10741-10749	13
898	Two-dimensional black phosphorus nanosheets for theranostic nanomedicine. <b>2017</b> , 4, 800-816	127
897	Progress on Electronic and Optoelectronic Devices of 2D Layered Semiconducting Materials. <b>2017</b> , 13, 1604298	55
896	2D Black Phosphorus for Energy Storage and Thermoelectric Applications. <b>2017</b> , 13, 1700661	113

895	Black phosphorus: A promising two dimensional visible and near-infrared-activated photocatalyst for hydrogen evolution. <b>2017</b> , 217, 285-292	143
894	Effect of external strain on the charge transfer: Adsorption of gas molecules on monolayer GaSe. <b>2017</b> , 198, 49-56	9
893	Programmable graphene doping via electron beam irradiation. <b>2017</b> , 9, 8657-8664	13
892	Thermal sublimation: a scalable and controllable thinning method for the fabrication of few-layer black phosphorus. <b>2017</b> , 28, 285301	15
891	Novel Field Effect Transistor Fabrication Based on Non-Graphene 2D Materials. <b>2017</b> , 2, 3675-3684	
890	Opening Two-Dimensional Materials for Energy Conversion and Storage: A Concept. <b>2017</b> , 7, 1602684	206
889	In-Plane Uniaxial Strain in Black Phosphorus Enables the Identification of Crystalline Orientation. <b>2017</b> , 13, 1700466	22
888	Anisotropic transport of normal metal-barrier-normal metal junctions in monolayer phosphorene. <b>2017</b> , 29, 285601	11
887	Monolayer Bismuthene-Metal Contacts: A Theoretical Study. <b>2017</b> , 9, 23128-23140	55
886	Ab initio performance predictions of single-layer In-V tunnel field-effect transistors. <b>2017</b> , 19, 20121-20126	7
885	Superior selectivity and sensitivity of blue phosphorus nanotubes in gas sensing applications. <b>2017</b> , 5, 5365-5371	16
884	Photoinduced quantum spin/valley Hall effect and its electrical manipulation in silicene. <b>2017</b> , 121, 205106	6
883	Electric field effect in multilayer Cr <sub>2</sub> Ge <sub>2</sub> Te <sub>6</sub> : a ferromagnetic 2D material. <b>2017</b> , 4, 024009	126
882	Black phosphorous optoelectronic devices. <b>2017</b> ,	1
881	A Hierarchical Phosphorus Nanobarbed Nanowire Hybrid: Its Structure and Electrochemical Properties. <b>2017</b> , 17, 3376-3382	35
880	Spatial-Temporal Imaging of Anisotropic Photocarrier Dynamics in Black Phosphorus. <b>2017</b> , 17, 3675-3680	40
879	Thermal spin current in zigzag silicene nanoribbons with sp <sup>2</sup> sp <sup>3</sup> edges. <b>2017</b> , 7, 28124-28129	9
878	Strain- and Fluorination-Induced Quantum Spin Hall Insulators in Blue Phosphorene: A First-Principles Study. <b>2017</b> , 121, 12945-12952	30



877	Monolayer AgBiPSe: an atomically thin ferroelectric semiconductor with out-plane polarization. <b>2017</b> , 9, 8427-8434	71
876	Electronic and optical properties of strained graphene and other strained 2D materials: a review. <b>2017</b> , 80, 096501	252
875	Few-atomic-layered hexagonal boron nitride: CVD growth, characterization, and applications. <b>2017</b> , 20, 611-628	66
874	Black Phosphorus Quantum Dot Induced Oxidative Stress and Toxicity in Living Cells and Mice. <b>2017</b> , 9, 20399-20409	101
873	Gate-tunable black phosphorus spin valve with nanosecond spin lifetimes. <b>2017</b> , 13, 888-893	91
872	Rapid mass production of two-dimensional metal oxides and hydroxides via the molten salts method. <b>2017</b> , 8, 15630	190
871	Nanostructured Materials and Architectures for Advanced Infrared Photodetection. <b>2017</b> , 2, 1700005	59
870	The high hydrogen storage capacities of Li-decorated borophene. <b>2017</b> , 137, 119-124	54
869	Ultrafast Carrier Dynamics and Efficient Triplet Generation in Black Phosphorus Quantum Dots. <b>2017</b> , 121, 12972-12978	21
868	A Generalized Strategy for the Synthesis of Large-Size Ultrathin Two-Dimensional Metal Oxide Nanosheets. <b>2017</b> , 129, 8892-8896	17
867	A Generalized Strategy for the Synthesis of Large-Size Ultrathin Two-Dimensional Metal Oxide Nanosheets. <b>2017</b> , 56, 8766-8770	91
866	Suppression of the Charge Density Wave State in Two-Dimensional 1T-TiSe by Atmospheric Oxidation. <b>2017</b> , 56, 8981-8985	27
865	Recovery of the Pristine Surface of Black Phosphorus by Water Rinsing and Its Device Application. <b>2017</b> , 9, 21382-21389	9
864	Tunable electronic properties of arsenene/GaS van der Waals heterostructures. <b>2017</b> , 7, 28393-28398	49
863	Exotic Physics and Chemistry of Two-Dimensional Phosphorus: Phosphorene. <b>2017</b> , 8, 2909-2916	57
862	Two-dimensional non-volatile programmable p-n junctions. <i>Nature Nanotechnology</i> , <b>2017</b> , 12, 901-906 28.7	196
861	Quantum confinement in black phosphorus-based nanostructures. <b>2017</b> , 29, 283001	15
860	Mid-infrared ultrafast carrier dynamics in thin film black phosphorus. <b>2017</b> , 4, 021032	25

859	The role of contact resistance in graphene field-effect devices. <b>2017</b> , 92, 143-175	130
858	Few-Layer Black Phosphorus Nanosheets as Electrocatalysts for Highly Efficient Oxygen Evolution Reaction. <b>2017</b> , 7, 1700396	251
857	First-principles study of the structures and fundamental electronic properties of two-dimensional P <sub>0.5</sub> As <sub>0.5</sub> alloy. <b>2017</b> , 254, 1700157	5
856	New Approach for Thickness Determination of Solution-Deposited Graphene Thin Films. <b>2017</b> , 2, 2630-2638	7
855	Phosphorene □The two-dimensional black phosphorous: Properties, synthesis and applications. <b>2017</b> , 221, 17-34	133
854	Deriving phosphorus atomic chains from few-layer black phosphorus. <b>2017</b> , 10, 2519-2526	19
853	Synthesis, Characterization, and Device Application of Antimony-Substituted Violet Phosphorus: A Layered Material. <b>2017</b> , 11, 4105-4113	20
852	Buckling behaviour of composites with double walled nanotubes from carbon and phosphorus. <b>2017</b> , 19, 10922-10930	13
851	Angle-resolved photoemission spectroscopy for the study of two-dimensional materials. <b>2017</b> , 4,	24
850	High Mobility 2D Palladium Diselenide Field-Effect Transistors with Tunable Ambipolar Characteristics. <b>2017</b> , 29, 1602969	180
849	High electron mobility and quantum oscillations in non-encapsulated ultrathin semiconducting BiOSe. <i>Nature Nanotechnology</i> , <b>2017</b> , 12, 530-534	28.7 332
848	Polymorphs of two dimensional phosphorus and arsenic: insight from an evolutionary search. <b>2017</b> , 19, 11282-11288	15
847	Gate tunable magneto-resistance of ultra-thin W Te 2 devices. <b>2017</b> , 4, 021018	7
846	Lattice thermal conductivity of borophene from first principle calculation. <b>2017</b> , 7, 45986	43
845	Gate-Controlled BP-WSe Heterojunction Diode for Logic Rectifiers and Logic Optoelectronics. <b>2017</b> , 13, 1603726	66
844	Energy coupling across low-dimensional contact interfaces at the atomic scale. <b>2017</b> , 110, 827-844	20
843	Recent progress in high-mobility thin-film transistors based on multilayer 2D materials. <b>2017</b> , 50, 164001	16
842	Coulomb interactions and screening effects in few-layer black phosphorus: a tight-binding consideration beyond the long-wavelength limit. <b>2017</b> , 4, 025064	21

841	Schottky Barriers in Bilayer Phosphorene Transistors. <b>2017</b> , 9, 12694-12705	81
840	Hybrid phosphorene/graphene nanocomposite as an anode material for Na-ion batteries: a first-principles study. <b>2017</b> , 50, 165501	25
839	Calculating excitons, plasmons, and quasiparticles in 2D materials and van der Waals heterostructures. <b>2017</b> , 4, 022004	131
838	Amorphous two-dimensional black phosphorus with exceptional photocarrier transport properties. <b>2017</b> , 4, 025063	16
837	Dirac-semimetal phase diagram of two-dimensional black phosphorus. <b>2017</b> , 4, 025071	12
836	Acidic gases (CO <sub>2</sub> , NO <sub>2</sub> and SO <sub>2</sub> ) capture and dissociation on metal decorated phosphorene. <b>2017</b> , 410, 505-512	36
835	From bidirectional rectifier to polarity-controllable transistor in black phosphorus by dual gate modulation. <b>2017</b> , 4, 025056	3
834	High-Performance Black Phosphorus MOSFETs Using Crystal Orientation Control and Contact Engineering. <b>2017</b> , 38, 685-688	17
833	A first principles study of the interaction between two-dimensional black phosphorus and Al <sub>2</sub> O <sub>3</sub> dielectric. <b>2017</b> , 7, 13777-13783	5
832	Electrically Tunable Energy Bandgap in Dual-Gated Ultra-Thin Black Phosphorus Field Effect Transistors. <b>2017</b> , 34, 047304	8
831	Electronic and transport properties of n-type monolayer black phosphorus at low temperatures. <b>2017</b> , 95,	10
830	Two-dimensional materials for ultrafast lasers. <b>2017</b> , 26, 034202	16
829	Continuum thin-shell model of the anisotropic two-dimensional materials: Single-layer black phosphorus. <b>2017</b> , 15, 1-9	9
828	Tuning phase transitions in FeSe thin flakes by field-effect transistor with solid ion conductor as the gate dielectric. <b>2017</b> , 95,	64
827	Water on silicene: A hydrogen bond-autocatalyzed physisorption/hemisorption/dissociation transition. <b>2017</b> , 10, 2223-2233	14
826	Two-dimensional growth of germanium under a diffusion limited aggregation environment. <b>2017</b> , 13, 91-96	
825	First-Principles-Based Quantum Transport Simulations of Monolayer Indium Selenide FETs in the Ballistic Limit. <b>2017</b> , 64, 2129-2134	9
824	Devices and applications of van der Waals heterostructures. <b>2017</b> , 38, 031005	17

823	Single-particle excitation of core states in epitaxial silicene. <b>2017</b> , 95,	12
822	Assembly of Au Plasmonic Photothermal Agent and Iron Oxide Nanoparticles on Ultrathin Black Phosphorus for Targeted Photothermal and Photodynamic Cancer Therapy. <b>2017</b> , 27, 1700371	211
821	Black phosphorus nanodevices at terahertz frequencies: Photodetectors and future challenges. <b>2017</b> , 5, 035602	42
820	Aharonov-Bohm effect in monolayer phosphorene nanorings. <b>2017</b> , 95,	18
819	Ultra high stiffness and thermal conductivity of graphene like C3N. <b>2017</b> , 118, 25-34	182
818	Geometric stability and electronic structure of infinite and finite phosphorus atomic chains. <b>2017</b> , 26, 036803	7
817	Photodetectors based on junctions of two-dimensional transition metal dichalcogenides. <b>2017</b> , 26, 038504	44
816	Two-carrier analyses of the transport properties of black phosphorus under pressure. <b>2017</b> , 95,	21
815	Phosphorene: An emerging 2D material. <b>2017</b> , 32, 2839-2847	26
814	Two-dimensional nanosheets for electrocatalysis in energy generation and conversion. <b>2017</b> , 5, 7257-7284	186
813	Structural Complexity and Phonon Physics in 2D Arsenenes. <b>2017</b> , 8, 1375-1380	34
812	Black Phosphorus Quantum Dots with Tunable Memory Properties and Multilevel Resistive Switching Characteristics. <b>2017</b> , 4, 1600435	135
811	Recent Advances in Ultrathin Two-Dimensional Nanomaterials. <b>2017</b> , 117, 6225-6331	2919
810	Monolayer Group IV/VI Monochalcogenides: Low-Dimensional Materials for Photocatalytic Water Splitting. <b>2017</b> , 121, 7615-7624	109
809	Tailoring the electronic and magnetic properties of monolayer SnO by B, C, N, O and F adatoms. <b>2017</b> , 7, 44568	11
808	Local control of the resistivity of graphene through mechanically induced switching of a ferroelectric superlattice. <b>2017</b> , 4, 021022	8
807	Mechanical property assessment of black phosphorene nanotube using molecular dynamics simulation. <b>2017</b> , 133, 35-44	10
806	Wafer-Scale Synthesis of High-Quality Semiconducting Two-Dimensional Layered InSe with Broadband Photoresponse. <b>2017</b> , 11, 4225-4236	207

805	Raman Sensitive Degradation and Etching Dynamics of Exfoliated Black Phosphorus. <b>2017</b> , 7, 44540	35
804	Intrinsic point defects in buckled and puckered arsenene: a first-principles study. <b>2017</b> , 19, 9862-9871	36
803	Environmentally Robust Black Phosphorus Nanosheets in Solution: Application for Self-Powered Photodetector. <b>2017</b> , 27, 1606834	244
802	A density functional theory-based finite element method to study the vibrational characteristics of zigzag phosphorene nanotubes. <b>2017</b> , 123, 1	6
801	Atomically thin InSe: A high mobility two-dimensional material. <b>2017</b> , 60, 1121-1122	4
800	Cyclical Thinning of Black Phosphorus with High Spatial Resolution for Heterostructure Devices. <b>2017</b> , 9, 12654-12662	10
799	Elemental two-dimensional nanosheets beyond graphene. <b>2017</b> , 46, 2127-2157	220
798	Two-dimensional Material based Printed Photonics: A Review.	1
797	Smart Synthetic and Surface-Engineering Approaches to Functionalize 2D Black Phosphorus for Real-Setting Applications. 2102149	0
796	Enhanced absorption in black phosphorene on adsorption of Li and K for use in energy conversion applications. <b>2022</b> , 54, 1	0
795	Semi-oxidized phosphorene under uniaxial strain. <b>2022</b> ,	
794	Homogeneous Palladium Diselenide pn-Junction Diodes for Reconfigurable Circuit Applications. 2101282	0
793	Ultrafast and selective gas transport through highly ordered black phosphorene nanochannels. <b>2022</b> , 288, 120629	0
792	Metal doped black phosphorene for gas sensing and catalysis: A first-principles perspective. <b>2022</b> , 586, 152743	2
791	Nanostructured Materials and Architectures for Advanced Optoelectronic Synaptic Devices. 2110976	13
790	Second-order topological insulator state in hexagonal lattices and its abundant material candidates. <b>2021</b> , 104,	2
789	Magneto-Thermoelectric Transport of Bilayer Phosphorene: A Generalized Tight-Binding Model Study.	
788	Prediction of atomically thin two-dimensional single monolayer SnGe with high carrier mobility: a DFT study. <b>2022</b> , 46, 5368-5373	0

787	Layered MoS <sub>2</sub> for photocatalytic dye degradation. <b>2022</b> , 53, 10-14	2
786	Formation of stable polonium monolayers with tunable semiconducting properties driven by strong quantum size effects.. <b>2022</b> ,	
785	Electronic and optical properties of a novel two-dimensional semiconductor material TIPTs: a first-principles study.. <b>2022</b> ,	2
784	Semiconductor-to-metal transition from monolayer to bilayer blue phosphorous induced by extremely strong interlayer coupling: a first-principles study.. <b>2022</b> ,	0
783	Nanoscale metal oxides 2D materials heterostructures for photoelectrochemical water splitting 3 review.	5
782	Metallic semiconducting properties of quasi-one-dimensional tantalum selenide van der Waals nanoribbons.. <b>2022</b> ,	3
781	Effect of ion irradiation on thermal conductivity of phosphorene and underlying mechanism. <b>2022</b> , 71, 056101	0
780	DNA/RNA sequencing using germanene nanoribbons two dimensional molecular electronic spectroscopy: an study.. <b>2022</b> ,	
779	Directional effects in plasmon excitation and transition radiation from an anisotropic 2D material induced by a fast charged particle.. <b>2022</b> ,	
778	Gas Sensing Properties of Alkali Metal Decorated Pristine and Defect Free Monolayer Toward Acid So <sub>2</sub> and Alkaline Nh <sub>3</sub> Molecules.	
777	Defects in two-dimensional elemental materials beyond graphene. <b>2022</b> , 43-88	
776	New progress and prospects of mechanical exfoliation technology of two-dimensional materials. <b>2022</b> ,	
775	Wse <sub>2</sub> /Bp Heterostructure with Tunable Electronic Properties Via External Electric Field and Biaxial Strain.	
774	Construction and physical properties of low-dimensional structures for nanoscale electronic devices.. <b>2022</b> ,	1
773	Nonlinear optical properties of PtTe <sub>2</sub> based saturable absorbers for ultrafast photonics. <b>2022</b> , 10, 5124-5133	2
772	Prediction of high Curie-temperature intrinsic ferromagnetic semiconductors and quantum anomalous Hall states in XBr <sub>3</sub> (X = Cu, Ag, Au) monolayers.	1
771	2D material based heterostructures for solar light driven photocatalytic H <sub>2</sub> production.	4
770	The Elemental Phosphorus for Recent Sustainable Processes: Rules and Strategies in Preparation and Applications.	0

769	The exchange between anions and cations induced by coupled plasma and thermal annealing treatment for room-temperature ferromagnetism.. <b>2022</b> ,	0
768	Advances in Ultrathin 2D Materials. <b>2022</b> , 11-29	
767	Lower Limits of Contact Resistance in Phosphorene Nanodevices with Edge Contacts.. <b>2022</b> , 12,	0
766	Room-Temperature Non-Local Spin Transport in Few-Layer Black Phosphorus Passivated with MgO. 2101048	1
765	Performance analysis of broadband Mid-IR graphene-phototransistor using strained black phosphorus sensing gate: DFT-NEGF investigation. <b>2022</b> , 107187	1
764	Realization of In-Plane Polarized Light Detection Based on Bulk Photovoltaic Effect in A Polar Van Der Waals Crystal.. <b>2022</b> , e2200011	3
763	2D Cairo Pentagonal PdPS: Air-Stable Anisotropic Ternary Semiconductor with High Optoelectronic Performance. 2113255	5
762	Magnetoexcitons in phosphorene monolayers, bilayers, and van der Waals heterostructures. <b>2022</b> , 4,	0
761	Stopping and image forces on a charged particle moving parallel to an anisotropic two-dimensional material. <b>2022</b> , 105,	1
760	Two-dimensional Materials for all-solid-state Lithium Batteries.. <b>2021</b> , e2108079	8
759	Edge modified phosphorene nanoribbon heterojunctions: promising metal-free photocatalysts for direct overall water splitting. <b>2022</b> , 57, 5482-5496	0
758	Tunable metal contacts at layered black-arsenic/metal interface forming during metal deposition for device fabrication. <b>2022</b> , 3,	1
757	Structural, electronic, and transport properties of 1D Ta <sub>2</sub> Ni <sub>3</sub> Se <sub>8</sub> semiconducting material. <b>2022</b> , 120, 073101	0
756	Stable Two-dimensional Nanoconfined Ionic Liquids with Highly Efficient Ionic Conductivity.. <b>2022</b> , 18, e2108026	1
755	Thermal conductivity of two stable bilayer phosphorene stackings: A computation study. <b>2022</b> , 131, 075101	
754	Liquid-Phase Exfoliation of TaNiS and Its Application in Near-Infrared Mode-Locked Fiber Lasers with Evanescent Field Interactions and Passively Q-Switched Bulk Laser.. <b>2022</b> , 12,	2
753	Nanotube-based heterostructures for electrochemistry: A mini-review on lithium storage, hydrogen evolution and beyond. <b>2022</b> ,	1
752	Two-Dimensional Violet Phosphorus: A p-Type Semiconductor for (Opto)electronics.. <b>2022</b> ,	6

751	Evidence of $p$ -like Hybridization of Silicon Valence Orbitals in Thin and Thick Si Grown on $\beta$ -Phase Si(111) $\sqrt{3}\times\sqrt{3}$ -Bi. <b>2022</b> , 15,	1
750	Visualizing Line Defects in non-van der Waals BiOSe Using Raman Spectroscopy. <b>2022</b> ,	1
749	Self-Driven High Performance Broadband Photodetector Based on SnSe/InSe van der Waals Heterojunction. 2102068	2
748	Layer-Dependent Raman Spectroscopy and Electronic Applications of Wide-Bandgap 2D Semiconductor $\alpha$ -ZrNCl. <b>2022</b> , e2107490	0
747	Direct comparison of ohmic contact properties between graphene and metal source/drain electrodes. 1	0
746	Structures, properties, and challenges of emerging 2D materials in bioelectronics and biosensors.	2
745	Temperature-Dependent Growth and Evolution of Silicene on Au Ultrathin Films-LEEM and LEED Studies. <b>2022</b> , 15,	2
744	Tuning the band gap and effective mass of black arsenic phosphide monolayer by in-plane strain. <b>2022</b> , 9, 025009	3
743	The half-metallity induced by out-of-plane electric field on phosphorene nanoribbons.	
742	High-Performance MoS <sub>2</sub> Complementary Inverter Prepared by Oxygen Plasma Doping. <b>2022</b> , 4, 955-963	2
741	Black Phosphorus Quantum Dot-Engineered Tin Oxide Electron Transport Layer for Highly Stable Perovskite Solar Cells with Negligible Hysteresis. <b>2022</b> ,	2
740	Symmetry-protected bound states in the continuum in graphene nanoribbons.	1
739	2D arsenenes. <b>2022</b> , 43, 030201	1
738	A Strong Two-Dimensional Semiconductor I-B4C with High Carrier Mobility. <b>2022</b> , 126, 6036-6046	0
737	Stability and Passivation of 2D Group VA Elemental Materials: Black Phosphorus and Beyond. <b>2022</b> ,	0
736	Hard-templated engineering of versatile 2D amorphous metal oxide nanosheets. <b>2022</b> ,	1
735	How can the unstable two-dimensional Sn <sub>2</sub> Bi be experimentally realized on Si(111)? <b>2022</b> , 24, 1	
734	Optical Properties and Dynamic Extrinsic Chirality of Structured Monolayer Black Phosphorus. <b>2022</b> , 9,	1



733	First-Principles Calculations on Semiconducting $\alpha$ -GeS and $\beta$ -SnS Monolayer Nanosheets with Photocatalytic Activity for Sunlight-Driven Water Splitting. <b>2022</b> , 5, 3900-3912	2
732	The resurrection of tellurium as an elemental two-dimensional semiconductor. <b>2022</b> , 6,	5
731	Density functional theory study of nitrogen-doped black phosphorene doped with monatomic transition metals as high performance electrocatalysts for N <sub>2</sub> reduction reaction.. <b>2022</b> ,	1
730	2D Materials for Wearable Energy Harvesting. 2101623	1
729	Size-dependent osteogenesis of black phosphorus in nanocomposite hydrogel scaffolds.. <b>2022</b> ,	0
728	Visualized SERS Imaging of Single Molecule by Ag/Black Phosphorus Nanosheets.. <b>2022</b> , 14, 75	6
727	Recent advances in two-dimensional layered and non-layered materials hybrid heterostructures.	0
726	$\alpha$ -Arsenene Monolayer: A Promising Electrocatalyst for Anodic Chlorine Evolution Reaction. <b>2022</b> , 12, 296	0
725	Highly anisotropic mechanical and optical properties of 2D NbOX <sub>2</sub> (X=Cl, Br, I) revealed by first-principle.. <b>2022</b> ,	1
724	Challenges and opportunities in 2D heterostructures for electronic and optoelectronic devices.. <b>2022</b> , 25, 103942	4
723	2D Ultrawide Bandgap Semiconductors: Odyssey and Challenges.. <b>2022</b> , e2101348	2
722	In-situ STS studies and first principles calculations on bare and Sn adsorbed UHV exfoliated WS <sub>2</sub> layers. <b>2022</b> , 1221, 012046	
721	Visible Out-of-plane Polarized Luminescence and Electronic Resonance in Black Phosphorus.. <b>2022</b> ,	0
720	Arsenene nanotubes adsorbed with various non-metallic atoms: Chemical bonding, odd-even effect, and electronic transport. <b>2022</b> , 207217	
719	Perspective of 2D Integrated Electronic Circuits: Scientific Pipe Dream or Disruptive Technology?. <b>2022</b> , e2201082	4
718	Detecting the Knowledge Domains of Compound Semiconductors.. <b>2022</b> , 13,	
717	Theoretical design of two-dimensional visible light-driven photocatalysts for overall water splitting. <b>2022</b> , 3, 011310	1
716	Low-Power Magnetron Sputtering Deposition of Antimonene Nanofilms for Water Splitting Reaction.. <b>2022</b> , 13,	0

715	Lithography-free and high-efficiency preparation of black phosphorous devices by direct evaporation through shadow mask.. <b>2022,</b>	1
714	Sub-ppb-Level Detection of Nitrogen Dioxide Based on High-Quality Black Phosphorus.. <b>2022,</b>	2
713	Programmable black phosphorus image sensor for broadband optoelectronic edge computing.. <b>2022, 13, 1485</b>	10
712	Effects of the pseudo-Chern-Simons action for strongly correlated electrons in a plane. <b>2022, 105,</b>	
711	Analyzing Anisotropy in 2D Rhenium Disulfide Using Dichromatic Polarized Reflectance.. <b>2022, e2108028</b>	3
710	Elucidating the Ambient Stability and Gas Sensing Mechanism of Nickel-Decorated Phosphorene for NO Detection: A First-Principles Study.. <b>2022, 7, 9808-9817</b>	1
709	Recent advance on machine learning of MXenes for energy storage and conversion.	1
708	Manipulating Strain in Transistors: From Mechanically Sensitive to Insensitive. 2101288	
707	Tuning electronic properties and ferromagnetism of CrI3 monolayers with doped transition-metal atoms.	
706	Electronic Tuning in WSe/Au via van der Waals Interface Twisting and Intercalation.. <b>2022,</b>	1
705	Stability, optoelectronic and thermal properties of two-dimensional janus $\text{WTe}_2$ .. <b>2022,</b>	4
704	Analysis of schottky barrier heights and reduced fermi-level pinning in monolayer CVD-grown MoS2 field-effect-transistors.. <b>2022,</b>	2
703	The marriage of two-dimensional materials and phase change materials for energy storage, conversion and applications. <b>2022, 4, 100071</b>	3
702	Surface and interface control of black phosphorus. <b>2022, 8, 632-662</b>	2
701	Floating Gate Carbon Nanotube Dual-Gate Field-Effect Transistor for Reconfigurable AND/OR Logic Gates.	0
700	Recent Progress of Two-Dimensional Transition Metal Dichalcogenides for Thermoelectric Applications. 10,	
699	Scattering of edge-state electrons from a two-level atom located near the zigzag edge of a phosphorene nanoribbon. <b>2022, 345, 114687</b>	0
698	Strongly Tunable Raman Resonance in InSe under Pressure.	

697	Effect of fully functionalization on carrier mobility of two-dimensional BN. <b>2022</b> , 346, 114698	
696	Mo <sub>2</sub> CS <sub>2</sub> /MXene Supported Single-Atom Catalysts for Efficient and Selective CO <sub>2</sub> Electrochemical Reduction. <b>2022</b> , 153339	2
695	The sensitive energy band structure and the spiral current in helical graphenes. <b>2022</b> , 35, 105351	0
694	Formation of black phosphorus quantum dots via shock-induced phase transformation. <b>2022</b> , 120, 141902	1
693	Enhanced Linear Dichroism of Flattened-Edge Black Phosphorus Nanoribbons.. <b>2022</b> ,	0
692	Effects of Mechanical Strain on Electronic Properties of Phosphorene Structure in the Presence of Spin-Orbit Coupling.	
691	Realizing Ferromagnetism in a Field-Effect Transistor Based on VSe <sub>2</sub> Thin Flakes. 2101383	0
690	Zigzag phosphorene antidot nanoribbons (ZPANRs) for the detection of nucleobases: A DFT based study. <b>2022</b> , 131, 144301	0
689	Electronic and optical properties of Janus black arsenic-phosphorus AsP quantum dots under magnetic field.. <b>2022</b> ,	0
688	Electronic properties and optical absorption of multi-layer phosphorene quantum rings. <b>2022</b> , 12, 045303	
687	Exploring a high-carrier-mobility black phosphorus/MoSe <sub>2</sub> heterostructure for high-efficiency thin film solar cells. <b>2022</b> , 236, 576-585	0
686	A high sensitivity lossy mode resonance refractive index sensor based on SBS structure. <b>2022</b> , 36, 105454	0
685	A DFT investigation on the mechanical and structural properties of halogen- and metal-adsorbed silicene nanosheets. <b>2022</b> , 283, 126029	1
684	Mono-elemental saturable absorber in near-infrared mode-locked fiber laser: A review. <b>2022</b> , 122, 104103	0
683	Photocatalytic hydrogen evolution reaction with high solar-to-hydrogen efficiency driven by the Sb <sub>2</sub> S <sub>3</sub> monolayer and RuI <sub>2</sub> /Sb <sub>2</sub> S <sub>3</sub> heterostructure with solar light. <b>2022</b> , 532, 231352	3
682	Layer structured materials for ambient nitrogen fixation. <b>2022</b> , 460, 214468	1
681	Single-Walled Black Phosphorus Nanotube as a NO <sub>2</sub> Gas Sensor. <b>2022</b> , 31, 103434	
680	MXene films: Toward high-performance electromagnetic interference shielding and supercapacitor electrode. <b>2022</b> , 157, 106935	1

- 679 Stability, tunneling characteristics and thermoelectric properties of TeSe<sub>2</sub> allotropes. **2022**, 280, 115692 1
- 678 Ordered and disordered two-dimensional tellurium-selenium binary compounds from swarm intelligence and first principles. **2022**, 31, 103409
- 677 An emerging direct monolayer  $\alpha$ -AlP<sub>3</sub>: High stability, desirable carrier mobility, NO<sub>2</sub>-sensitive sensing performance, and superior catalytic properties toward the nitrogen reduction reaction. **2022**, 591, 153191 1
- 676 Anisotropic exciton states and excitonic absorption spectra in a freestanding monolayer black phosphorus. **2022**, 141, 115238 0
- 675 Enhanced magnetic anisotropy in two-dimensional 2H-TaS<sub>2</sub> by self-intercalation: A DFT study. **2022**, 553, 168988 0
- 674 The Effect of Compressive and Tensile Strains on the Electron Structure of Phosphorene. **2021**, 63, 1690-1694
- 673 Modulation of strain on electronic structure and contact type of BP/SnS van der waals heterostructure. **2022**, 55, 125102 1
- 672 A review of terahertz phase modulation from free space to guided wave integrated devices. **2022**, 11, 415-437 5
- 671 Structural stabilities, electronic structures, photocatalysis and optical properties of  $\alpha$ -GeN and  $\beta$ -SnP monolayers: a first-principles study. **2021**, 8, 125010
- 670 Bandstructure and Size-Scaling Effects in the Performance of Monolayer Black Phosphorus Nanodevices.. **2021**, 15, 1 1
- 669 Honeycomb Lattice in Metal-Rich Chalcogenide Fe<sub>2</sub>Te. **2021**, 38, 116801 1
- 668 General Synthesis of Two-Dimensional Porous Metal Oxides/Hydroxides for Microwave Absorbing Applications.. **2021**, 1 0
- 667 Phosphorene Nanoribbon-Augmented Optoelectronics for Enhanced Hole Extraction.. **2021**, 143, 21549-21559 11
- 666 Ultrahigh Anisotropic Transport Properties of Black Phosphorus Field Effect Transistors Realized by Edge Contact. **2022**, 8, 2100988 3
- 665 Surface functionalization of phosphorene via P-H bond for ambient protection and robust photocatalytic H<sub>2</sub> evolution. **2022**, 65, 1245-1251 0
- 664 Memory effects in black phosphorus field effect transistors. **2022**, 9, 015028 3
- 663 Theoretical study of stability, epitaxial formation, and phase transformations of two-dimensional pnictogen allotropes. **2021**, 104, 1 0
- 662 Charged vacancy defects in monolayer phosphorene. **2021**, 5, 1 0

661	Optical absorption of phosphorene structure in the presence of spin-orbit coupling: mechanical strain effects. <b>2022</b> , 137, 1	0
660	A wafer-scale van der Waals dielectric made from an inorganic molecular crystal film. <b>2021</b> , 4, 906-913	16
659	Enhanced Absorption in the Wide Wavelength Range: Black Silicon Decorated with Few-Layer PtS <sub>2</sub> . <b>2021</b> , 125, 27335-27343	1
658	SiCP Monolayer with a Direct Band Gap and High Carrier Mobility for Photocatalytic Water Splitting.. <b>2021</b> , 190-197	2
657	Recent progress in optoelectronic applications of hybrid 2D/3D silicon-based heterostructures. <b>2022</b> , 65, 876-895	0
656	Emerging Phases of Layered Metal Chalcogenides.. <b>2021</b> , e2105215	1
655	Next-generation machine vision systems incorporating two-dimensional materials: Progress and perspectives. <b>2022</b> , 4,	7
654	High-performance thermoelectric properties of strained two-dimensional tellurium. <b>2021</b> , 5,	0
653	Perspectives of 2D Materials for Optoelectronic Integration. <b>2022</b> , 32, 2110119	9
652	Epitaxial growth of black phosphorene enabled on black-phosphorene-like group IV-VI substrates. <b>2021</b> , 104,	0
651	Molecular Engineering of 2D Nanomaterial Field-Effect Transistor Sensors: Fundamentals and Translation across the Innovation Spectrum.. <b>2021</b> , e2106975	0
650	2D Mg-Cu Intermetallic Compounds with Nontrivial Band Topology and Dirac Nodal Lines. <b>2022</b> , 8, 2100927	0
649	Quantum transport simulation of the two-dimensional GaSb transistors. <b>2021</b> , 42, 122001	0
648	Polarization-Induced Band-Alignment Transition and Nonvolatile p-n Junctions in 2D Van der Waals Heterostructures. <b>2022</b> , 8, 2101022	0
647	Designing Direct Z-Scheme Heterojunctions Enabled by Edge-Modified Phosphorene Nanoribbons for Photocatalytic Overall Water Splitting.. <b>2021</b> , 1-11	5
646	Monoelemental two-dimensional iodine nanosheets: a first-principles study of the electronic and optical properties. <b>2022</b> , 55, 135104	
645	Direct evidence of two-dimensional electron gas-like band structures in hafnene. <b>2022</b> , 15, 3770-3774	
644	2D layered black arsenic-phosphorus materials: Synthesis, properties, and device applications. <b>2022</b> , 15, 3737-3752	3

- 643 Stabilities of Isomers of Phosphorus on Transition Metal Substrates. **2021**, 33, 9447-9453 1
- 642 RF Performance Investigation of NiO Pocket on Ga<sub>2</sub>O<sub>3</sub>-Based Hetero-MOSFET. **2021**, 55, S14-S21
- 641 Effect of stress regulation on electronic structure and optical properties of TiOCl<sub>2</sub> monolayer. **2022**, 71, 077101 0
- 640 Two-Dimensional Field-Effect Transistor Sensors: The Road toward Commercialization.. **2022**, 9
- 639 Magneto-thermoelectric transport of bilayer phosphorene: A generalized tight-binding model study. **2022**, 107294 0
- 638 NbCX (X=F, Cl, Br, I) with Highly Anisotropic Fermi Velocity, Optical, Mechanical and Electric Transport Properties. **2022**, 111551 0
- 637 Analysis of Low-Frequency 1/f Noise Characteristics for MoTe Ambipolar Field-Effect Transistors.. **2022**, 12, 1 1
- 636 Tunable Properties of the Stable SiSeS Janus Monolayer Under Biaxial Strain: First-principles Prediction. **2022**, 169123 0
- 635 Recent advances in solid-state supercapacitors: From emerging materials to advanced applications. 1
- 634 Investigating the high field transport properties of Janus WSSe and MoSSe by DFT analysis and Monte Carlo simulations. **2022**, 131, 144303 1
- 633 Electric Metal Contacts to Monolayer Blue Phosphorus: Electronic and Chemical Properties. **2022**, 153450
- 632 Performance Enhancement of SnS/-BN Heterostructure p-Type FET via the Thermodynamically Predicted Surface Oxide Conversion Method.. **2022**, 0
- 631 Photoelectronic properties and devices of 2D Xenes. **2022**,
- 630 Optothermal Raman Spectroscopy of Black Phosphorus on a Gold Substrate.. **2022**, 12, 1
- 629 A Multi-Layered Borophene-Silica-Silver Based Refractive Index Sensor for Biosensing Applications Operated at the Infrared Frequency Spectrum. **2022**, 9, 279
- 628 Crossed Andreev reflection in zigzag phosphorene nanoribbon based ferromagnet/superconductor/ferromagnet junctions.. **2022**, 12, 6079 1
- 627 Strong quantum-confined excitation and emission from violet phosphorus quantum dots. **2022**, 120, 151904 0
- 626 Sensing properties of nonmetal doped blue phosphorene toward NO and NO<sub>2</sub> molecules: A first-principles study. 0

- 625 Growth of Tellurium Nanobelts on h-BN for p-type Transistors with Ultrahigh Hole Mobility.. **2022**, 14, 109 2
- 624 Stabilization of Black Phosphorene by Edge-Selective Adsorption of C60 Molecules. **2022**, 126, 6874-6879 0
- 623 Hydrogen storage on flat land materials, opportunities, and challenges: A review study. 0
- 622 2D materials-enabled optical modulators: From visible to terahertz spectral range. **2022**, 9, 021302 2
- 621 A first-principles study on the adsorption properties of phosphorene oxide for pollutant removal from water. **2022**, 357, 119103 0
- 620 Data\_Sheet\_1.pdf. **2019**,
- 619 Designing a Perfect Phosphorene-Plasmon Adsorbent and Investigating its Geometric Irregularity Effects: A Simulation Study.
- 618 Enhancement of Gas Sensing by Doping of Transition Metal in Two-Dimensional As2c3 Nanosheet.
- 617 Role of Channel Inversion in Ambient Degradation of Phosphorene FETs. **2022**, 1-6
- 616 Exploring the emerging applications of the advanced 2-dimensional material borophene with its unique properties.. **2022**, 12, 12166-12192 0
- 615 FeP2 monolayer: Isoelectronic analogue of MoS2 with excellent electronic and optical properties. 0
- 614 Electrical and magneto transport in 2D semiconducting MXene Ti2CO2.
- 613 Experimental synthesis of borophene. **2022**, 0
- 612 Extending the Scaling Limit of Silicon Channel Transistors Through hhk-Silicene Monolayer: A Computational Study. **2022**, 1-5 0
- 611 Anisotropy of thermal transport in phosphorene: A comparative first-principles study using different exchange-correlation functional.
- 610 Recent Advances in SnSe Nanostructures beyond Thermoelectricity. 2200516 2
- 609 Computational Study of the C2P4 Monolayer as a Stable Two-Dimensional Material with High Carrier Mobility: Implications for Nanoelectronic Devices. 1
- 608 Aharonov-Bohm oscillations in phosphorene quantum rings: Mass anisotropy compensation by confinement potential. **2022**, 105, 0

607	Stable Al <sub>2</sub> O <sub>3</sub> Encapsulation of MoS <sub>2</sub> -FETs Enabled by CVD Grown h-BN. 2200123	1
606	Engineering Plasmonic Environments for 2D Materials and 2D-Based Photodetectors.. 2022, 27,	1
605	Compressive soliton in phosphorene at finite temperature. 2022,	
604	Modulating of electronic states and magnetic polarization in monolayered 1T-HfSe <sub>2</sub> under non-metal atom and transition metal atom doping. 2022, 413977	
603	The anisotropic plasmon dispersion and damping in multilayer 8-Pmmn borophene structures.	
602	Room-Temperature Infrared Photodetectors with Zero-Dimensional and New Two-Dimensional Materials. 2022, 12, 609	1
601	Electronic Self-Passivation of Single Vacancy in Black Phosphorus via Ionization.. 2022, 128, 176801	0
600	High-Speed and High-Responsivity Silicon/Black-Phosphorus Hybrid Plasmonic Waveguide Avalanche Photodetector.	2
599	Q-switched fiber laser using a polysulfone membrane enhanced with biosynthesized zinc oxide and titanium dioxide nanoparticles for use as saturable absorber. 2022, 32, 065101	0
598	Mechanical, optical, and thermoelectric properties of semiconducting ZnIn <sub>2</sub> X <sub>4</sub> (X=S, Se, Te). 2022, 105,	1
597	Band structure of molybdenum disulfide: from first principle to analytical band model. 1	1
596	Programmable van-der-Waals heterostructure-enabled optoelectronic synaptic floating-gate transistors with ultra-low energy consumption.	4
595	Optoelectronic Properties of HfMoO Tuned by H Dopant in Different Concentration.. 2022, 15,	
594	The trend of 2D transistors toward integrated circuits: Scaling down and new mechanisms.. 2022, e2201916	4
593	Near-zero Poisson's ratio and suppressed mechanical anisotropy in strained black phosphorene/SnSe van der Waals heterostructure: a first-principles study. 2022, 43, 627-636	
592	Twisted black phosphorus-based van der Waals stacks for fiber-integrated polarimeters.. 2022, 8, eabo0375	3
591	HgCdTe/black phosphorus van der Waals heterojunction for high-performance polarization-sensitive midwave infrared photodetector.. 2022, 8, eabn1811	8
590	Theoretical investigation on the electronic structure of new InSe/CrS <sub>2</sub> van der Waals heterostructure. 1	0



- 589 Revisiting Solution-Based Processing of van der Waals Layered Materials for Electronics. 0
- 588 Non-asymptotic quantum scattering theory to design high-mobility lateral transition-metal dichalcogenide heterostructures. **2022**, 131, 174302 0
- 587 Benchmarking Noise and Dephasing in Emerging Electrical Materials for Quantum Technologies.. **2022**, e2109671 1
- 586 Anisotropic behavior of thermoelectric power in zigzag and armchair 2D Phosphorene.
- 585 Effect of non-magnetic doping on magnetic state and Li/Na adsorption and diffusion of black phosphorene.. **2022**, 0
- 584 Microscopic optical nonlinearities and transient carrier dynamics in indium selenide nanosheet. **2022**, 30, 17967 1
- 583 Phosphorene - an emerging two-dimensional material: recent advances in synthesis, functionalization, and applications. 2
- 582 Observation of nontrivial topological electronic structure of orthorhombic SnSe. **2022**, 6,
- 581 First-principles prediction of stable Janus BiSbC3 monolayer with tunable electronic and optical properties under strain. **2022**, 31, e00687 0
- 580 Pentagon-based 2D materials: Classification, properties and applications. **2022**, 964, 1-42 3
- 579 First-principles calculations to investigate strain-tunable electronic bandgap of black phosphorus-structured nitrogen with desirable optical and elastic properties. **2022**, 281, 115745 0
- 578 Poly(dimethyl siloxane)-grafted black phosphorus nanosheets as filler to enhance moisture-resistance and flame-retardancy of thermoplastic polyurethane. **2022**, 286, 126189 1
- 577 Runge-Kutta FIE-FDTD formulations for analyzing optical transmission through periodic array of magnetically-biased graphene micro-patch structures. **2022**, 261, 169225
- 576 High thermoelectric figure of merit for GeS/phosphorene 2D heterostructures: A first-principles study. **2022**, 281, 115737 0
- 575 One-step co-precipitation method to construct SnO quantum dots modified black phosphorus nanosheets for room-temperature trace NH3 sensing. **2022**, 365, 131910
- 574 Tunneling effect in phosphorene through double barriers. **2022**, 351, 114777
- 573 Facile synthesis of black phosphorene via a low melting media assisted ball milling. **2022**, 444, 136593 1
- 572 Atomic-scale friction of black phosphorus from first-principles calculations: Insensitivity of friction under the high-load. **2022**, 172, 107590 0

- 571 Biaxial strain tuned electronic structure, lattice thermal conductivity and thermoelectric properties of MgI<sub>2</sub> monolayer. **2022**, 148, 106791 ○
- 570 Nano-labeled materials as detection tags for signal amplification in immunochromatographic assay. **2022**, 154, 116673 ○
- 569 Chemical Vapor Deposition Synthesis of Two-dimensional Bi<sub>2</sub>O<sub>2</sub>Se on Silicon Substrate and its Photodetecting Application. **2022**,
- 568 Strain engineering of lateral heterostructures based on group-V enes (As, Sb, Bi) for infrared optoelectronic applications calculated by first principles. **2022**, 12, 14578-14585
- 567 Electric field- and strain-induced bandgap modulation in bilayer C<sub>2</sub>N. **2022**, 120, 203101 2
- 566 Strain dependent magnetic properties of 1T-VSe<sub>2</sub> monolayer. ○
- 565 Gadolinium Halide Monolayers: A Fertile Family of Two-Dimensional 4f Magnets. ○
- 564 Quasi-Fermi-Level Phase Space and its Applications in Ambipolar Two-Dimensional Field-Effect Transistors. **2022**, 17,
- 563 Scalable production of p-MoTe<sub>2</sub>/n-MoS<sub>2</sub> heterostructure array and its application for self-powered photodetectors and CMOS inverters.
- 562 Two-Dimensional Materials and their Hetero-Superlattices for Photocatalytic Hydrogen Evolution Reaction.
- 561 The transverse magnetic electromagnetic bound mode in a black phosphorene inserted multilayer dielectric structure.
- 560 Integrated Optoelectronics with Two-Dimensional Materials. **2022**, ○
- 559 Recent Advances in Two-dimensional Material/Conducting Polymer Composites for Thermoelectric Energy Conversion. 2200107 ○
- 558 Topological Field-Effect Transistor Based on Quasi-Two-Dimensional Tellurium Flakes. **2022**, 17,
- 557 Rail-to-Rail MoS<sub>2</sub> Inverters.
- 556 Insights into controllable electronic properties of 2D type-II Twin-Graphene/g-CN43 and type-I Twin-Graphene/hBN vertical heterojunctions via external electric field and strain engineering. **2022**, 128216
- 555 Transport properties of blue phosphorene nanoribbons in the presence of pollutant molecules. **2022**, 207257
- 554 Electronic and thermoelectric properties of group IV/VI van der Waals heterostructures.

- 553 Enhanced Optoelectronic Properties of Solution-Processed Metal-Chalcogenide Devices Via Hydrogen-Driven Post-Annealing.
- 552 Two-dimensional  $\text{BiAs}/\text{BiAsP}$  van der Waals heterostructure for photovoltaic applications. 0
- 551 Extraordinary lattice thermal conductivity of gold sulfide monolayers.
- 550 Synthesis, Modification, and Application of Black Phosphorus, Few-Layer Black Phosphorus (FLBP), and Phosphorene: A Detailed Review. 0
- 549 A steep-slope tellurium transistor with a native voltage amplifying threshold switch. **2022**, 120, 223502 1
- 548 Approaching multi-band and broadband high absorption based on one-dimensional layered structures containing monolayer  $\text{MoS}_2$ . **2022**, 97, 065510
- 547 Lattice dynamics and elastic properties of black phosphorus. **2022**, 105, 0
- 546 Highly Sensitive Photodetector Based on the n-Si/p-GaSe Vertical Heterojunction. 0
- 545 Engineered 2D materials for optical bioimaging and path toward therapy and tissue engineering. 2
- 544 Monolayer  $\text{Sc}_2\text{I}_2\text{S}_2$ : An Excellent n-Type Thermoelectric Material with Significant Anisotropy. 2
- 543 Exfoliation of 2D van der Waals crystals in ultrahigh vacuum for interface engineering. **2022**, 1
- 542 Electrochemical exfoliation of two-dimensional phosphorene sheets and its Energy application.
- 541 Enhanced photodetector performance of black phosphorus by interfacing with chiral perovskite. 2
- 540 New 2D material: Two-dimensional black phosphorus (2D BP).
- 539 Chemically exfoliated inorganic nanosheets for nanoelectronics. **2022**, 9, 021313 0
- 538 Bioactive 2D nanomaterials for neural repair and regeneration. **2022**, 114379 0
- 537 A DFT study of two-dimensional  $\text{P}_2\text{Si}$  monolayer modified by single transition metal (Sc-Cu) atoms for efficient electrocatalytic  $\text{CO}_2$  reduction. **2022**, 0
- 536 Intrinsic ferromagnetic Janus  $\text{Cr}_2\text{PAs}$  monolayer with controllable magnetic anisotropy. **2022**, 128239 0

535	Casting Light on Black Phosphorus-Based Catalysts for Water Electrolysis: Approaches, Promotion Manners, and Perspectives. <b>2022</b> , 108018	1
534	Theoretical design of BAs/WX <sub>2</sub> (X = S, Se) heterostructures for high-performance photovoltaic applications from DFT calculations. <b>2022</b> , 153865	0
533	Metamaterial Perfect Absorbers and Performance. <b>2022</b> , 29-91	0
532	Chemically functionalized phosphorenes and their use in the water splitting reaction.	0
531	Gram-Scale Preparation of Black Phosphorus Nanosheets via Shock-Induced Phase Transformation.	1
530	Enhanced Thermal Transportation of Flexible Composite Films Across Electrostatic Self-assembly of Black Phosphorene and Boron Nitride Nanosheets.	0
529	The role of permanent and induced electrostatic dipole moments for Schottky barriers in Janus MX <sub>2</sub> /graphene heterostructures: a first-principles study.	1
528	Improving performance of monolayer arsenene tunnel field-effect transistors by defects.	
527	Research progress of tuning correlated state in two-dimensional system by organic molecule intercalation. <b>2022</b> , 71, 127403	0
526	Engineering van der Waals Materials for Advanced Metaphotonics.	2
525	Entropy stabilization of two-dimensional transition metal dichalcogenide alloys: A density functional theory study. <b>2022</b> , 131, 234302	0
524	High Thermoelectric Performance in 2D Technetium Dichalcogenides TcX <sub>2</sub> (X = S, Se, or Te).	1
523	Effect of MoO <sub>3</sub> buffer layer on the electronic structure of Al-BP interface.	0
522	Titanium dioxide, black phosphorus and bimetallic layer-based surface plasmon biosensor for formalin detection: numerical analysis. <b>2022</b> , 54,	0
521	Emerging two-dimensional magnetism in nonmagnetic electriles Hf <sub>2</sub> X (X=S, Se, Te. <b>2022</b> , 105,	1
520	Understanding random telegraph noise in two-dimensional BP/ReS <sub>2</sub> heterointerface. <b>2022</b> , 120, 253507	0
519	Detection of Blood Plasma Concentration Theoretically Using SPR-Based Biosensor Employing Black Phosphor Layers and Different Metals.	3
518	Electron transport properties of a narrow-bandgap semiconductor Bi <sub>2</sub> O <sub>2</sub> Te nanosheet. <b>2022</b> , 120, 233102	1

517	Synthesis of a monolayer fullerene network. <b>2022</b> , 606, 507-510	12
516	1D van der Waals Nb <sub>2</sub> Pd <sub>3</sub> Se <sub>8</sub> -Based n-Type Field-Effect Transistors Prepared by Liquid Phase Exfoliation. 2200620	
515	Ga <sub>3</sub> Te <sub>3</sub> I: novel 1D and 2D semiconductor materials with promising electronic and optical properties.	0
514	The rise of 2D materials/ferroelectrics for next generation photonics and optoelectronics devices. <b>2022</b> , 10, 060903	3
513	Direct mapping of edge states in bilayer zigzag phosphorene nanoribbons into a SSH ladder model and optimizing their thermoelectric performance via edge state engineering. <b>2022</b> , 137,	0
512	2D Material and Perovskite Heterostructure for Optoelectronic Applications. <b>2022</b> , 12, 2100	4
511	Improving Harsh Environmental Stability of Few-Layer Black Phosphorus by Local Charge Transfer. 2203967	0
510	Strong Spin-Phonon Coupling in Two-Dimensional Magnetic Semiconductor CrSBr.	1
509	Interfacial Thermal Conductance of BP/MoS <sub>2</sub> van der Waals Heterostructures: an Insight from the Phonon Transport. <b>2022</b> , 102119	0
508	A Black Phosphorus-Based Fabry-Pérot Cavity and Its Application for Reversible Color Switching. 2200137	
507	Metal-phosphorus network on Pt(111). <b>2022</b> , 9, 045002	0
506	2D Oxides for Electronics and Optoelectronics. 2200008	3
505	Doping of Carbon Nanotubes with Encapsulated Phosphorus Chains.	1
504	Strong bulk-surface interaction dominated in-plane anisotropy of electronic structure in GaTe. <b>2022</b> , 5,	0
503	High Anisotropic Optoelectronics in Monolayer Binary M <sub>8</sub> X <sub>12</sub> (M = Mo, W; X = S, Se, Te). <b>2022</b> , 14, 27056-27062	1
502	Recent advances in field-effect transistors for heavy metal ion detection.	
501	Preparation, synthesis, properties and characterization of graphene-based 2D nano-materials for biosensors and bioelectronics. <b>2022</b> , 19, 2657-2694	3
500	Enhancement of gas sensing by doping of transition metal in two-dimensional As <sub>2</sub> C <sub>3</sub> nanosheet: A density functional theory investigation. <b>2022</b> , 599, 153941	1

- 499 Phosphorene. **2022**, 121-148
- 498 The structural and electronic richness of buckled honeycomb AsP bilayers. 0
- 497 Selenene and Tellurene. **2022**, 197-224 1
- 496 Integration paths for Xenon. **2022**, 405-438
- 495 The  $\alpha$ - $\text{In}_2\text{Se}_3$  THz Photodetector. **2022**, 1-6
- 494 Modulating the Photoelectrocatalytic Conversion of  $\text{CO}_2$  to methanol and/or  $\text{H}_2\text{O}$  to Hydrogen at Phosphorene modified Ti/TiO<sub>2</sub> electrode.
- 493 Black phosphorene/NP heterostructure as a novel anode material for Li/Na-ion batteries. 0
- 492 Metal oxides for optoelectronic and photonic applications: A general introduction. **2022**, 3-31
- 491 Strain-tunable magnetic and electronic properties of a  $\text{CuCl}_3$  monolayer.
- 490 Computational discovery of  $\text{In}_2\text{XY}_2$  (X, Y = S, Se, and Te;  $X \neq Y$ ) monolayers as multifunctional energy conversion materials. 1
- 489 Magnetoplasmonic coupling in graphene nanodisk dimers: An extended coupled-dipole model for circularly polarized states. **2022**, 105, 1
- 488 One-dimensional excitons in long phosphorene atomic chains. **2022**, 105, 0
- 487 Two-dimensional diamonds from  $\text{sp}^2$ -to- $\text{sp}^3$  phase transitions. 7
- 486 Graphene-Based Electrochemical Sensors for Psychoactive Drugs. **2022**, 12, 2250 3
- 485 The Interfacial Properties of Monolayer MX<sub>2</sub>/Metal Contacts. 0
- 484 High-Performance and Low-Power Transistors Based on Anisotropic Monolayer  $\text{TeO}_2$ . **2022**, 17, 4
- 483 Straightforward strategy for selecting and tuning substrates for two-dimensional material epitaxy. **2022**, 6, 0
- 482 Regulation of electronic and optical properties of monolayer black phosphorus by co-doping B and Si. **2022**, 12, 065031

- 481 Adsorption Mechanism of SO<sub>2</sub> on Transition Metal (Pd, Pt, Au, Fe, Co and Mo)-Modified InP<sub>3</sub> Monolayer. **2022**, 10, 279
- 480 Excimer formation in non-van der Waals 2D semiconductor Bi<sub>2</sub>O<sub>2</sub>Se. 2204227 0
- 479 Magnetic phase transition of monolayer chromium trihalides investigated with machine learning: Toward a universal magnetic Hamiltonian.
- 478 Facile Synthesis of Monodispersed Titanium Nitride Quantum Dots for Harmonic Mode-Locking Generation in an Ultrafast Fiber Laser. **2022**, 12, 2280 2
- 477 Mid-Infrared Optoelectronic Devices Based on Two-Dimensional Materials beyond Graphene: Status and Trends. **2022**, 12, 2260 2
- 476 Far-infrared anisotropic optical properties of Si<sub>3</sub>N<sub>4</sub> microsphere arrays based on black phosphorus-like structures. **2022**, 128,
- 475 Large-Scale Multilayer MoS<sub>2</sub> Nanosheets Grown by Atomic Layer Deposition for Sensitive Photodetectors. 0
- 474 Anisotropic optical transitions of gated β<sub>12</sub>-borophene.
- 473 Enhanced acidic gas adsorption performance of arsenene by Pt mediation. **2022**, 12, 075108
- 472 Transition metal dichalcogenides (TMDCs) heterostructures: Optoelectric properties. **2022**, 17, 1
- 471 The effect of different dopants and their positions on the magnetic properties of an armchair antimonene nanoribbon: comprehensive theoretical investigation. **2022**, 97, 085808
- 470 Quasi-1D ZrS<sub>3</sub> as an Anisotropic Nano-Reflector for Manipulating Light-Matter Interactions. 2201030 1
- 469 Approaches to Enhancing Electrical Conductivity of Pristine Metal-Organic Frameworks for Supercapacitor Applications. 2203307 3
- 468 Cr<sub>2</sub>XTe<sub>4</sub> (X = Si, Ge) monolayers: a new type of two-dimensional high-T<sub>C</sub> Ising ferromagnetic semiconductors with a large magnetic anisotropy. **2022**, 34, 384001 2
- 467 Enhanced Spin Thermopower in Phosphorene Nanoribbons via Edge-State Modifications. **2022**, 12, 2350 1
- 466 Tuning the electronic and magnetic properties of O Vacancy and nonmetallic atoms doped monolayer SnO: A first-principles study. **2022**, 114884 0
- 465 Effects of the Tc, Ru, Rh and Cd substitution doping on the structural, electronic, magnetic and optical properties of blue P monolayer. **2022**, 756, 139386 1
- 464 Black phosphorus quantum dots and Ag nanoparticles co-modified TiO<sub>2</sub> nanorod arrays as powerful photocatalyst for tetracycline hydrochloride degradation: Pathways, toxicity assessment, and mechanism insight. **2022**, 297, 121454 1

- 463 Highly selective simultaneous determination of isoniazid and acetaminophen using black phosphorus nanosheets electrochemical sensor. **2022**, 426, 140775 ○
- 462 Investigation of carrier transport behavior for cubic  $\text{CH}_3\text{NH}_3\text{SnX}_3$  and  $\text{CH}_3\text{NH}_3\text{PbX}_3$  (X=Br and I) using Boltzmann transport equation. **2022**, 213, 111609 ○
- 461 Strain enhanced electronic and optical properties in Janus monolayers  $\text{AsMC}_3$  (M: Sb, Bi). **2022**, 642, 414143 ○
- 460 Revealing and modeling of fire products in gas-phase for epoxy/black phosphorus-based nanocomposites. **2022**, 305, 135504 1
- 459 Mechanical strain and electric field tunable electronic structure of black/violet phosphorene van der Waals heterostructure: From type I to Z-scheme system. **2022**, 169, 110863
- 458 Two-dimensional V-shaped  $\text{PdI}_2$ : Auxetic semiconductor with ultralow lattice thermal conductivity and ultrafast alkali ion mobility. **2022**, 601, 154176 1
- 457 The effect of edge passivation of phosphorene nanoribbons with different atoms and arrangements on their electronic and transport properties. **2022**, 601, 154216
- 456 Ferroelectricity and Piezoelectricity in 2D Van der Waals  $\text{CuInP}_2\text{S}_6$  Ferroelectric Tunnel Junctions. **2022**, 12, 2516 ○
- 455 The First-Principles Study of External Strain Tuning the Electronic and Optical Properties of the 2D  $\text{MoTe}_2/\text{PtS}_2$  van der Waals Heterostructure. 10, ○
- 454 Strain-tunable pure H- conduction in one-atom-thick hexagonal boron nitride for high-energy-density fuel cells. **2022**, 138223 ○
- 453 Evolution of the Electronic and Optical Properties of Meta-Stable Allotropic Forms of 2D Tellurium for Increasing Number of Layers. **2022**, 12, 2503 1
- 452 Investigation of black phosphorus anodic catalyst for electrolysis: Degradation of organics via a perchlorate-free oxidant activation. **2022**, 135765
- 451 Device Simulation of 5.1 nm High-Performance Field-Effect Transistors Based on Two-Dimensional Boron Phosphide. **2022**, 126, 12091-12099 ○
- 450 First-principle studies of twisted bilayer black phosphorus. ○
- 449 Electronic structure and optical properties of B-, N-, and BN-doped black phosphorene using the first-principles. **2022**, 28,
- 448  $\text{SnSe}$  nanosheet arrays film for trace  $\text{NO}_2$  detection at room temperature. **2022**, 370, 132407 ○
- 447 Linear and nonlinear optical propagation in 2D materials. **2021**, 2021, 19-37
- 446 Tunable Schottky and Ohmic contacts in  $\text{Ti}_2\text{NF}_2/\text{Te}$  van der Waals heterostructure.



- 445 Two-Dimensional Sic Schottky Junctions with Symmetrical and Asymmetrical Metal Electrode Contacts.
- 444 High electron mobility and wide-bandgap properties in a novel 1D PdGeS<sub>3</sub> nanochain. **2022**, 24, 18868-18876 ○
- 443 First-principles study on the structure prediction and electronic properties of two-dimensional SiP<sub>2</sub> allotropes. **2022**, 0
- 442 Isolated Ni atoms induced edge stabilities and equilibrium shapes of CVD-prepared hexagonal boron nitride on Ni(111) surface. 5
- 441 Development Trend of 3D Printing Bone Tissue Engineering Scaffold Based on Black Phosphorus Nanosheets. **2022**,
- 440 Elastic response of monolayer Si<sub>1-x</sub>Ge<sub>x</sub>. **2022**, 106,
- 439 A DFT investigation on the mechanical and structural properties of silicene nanosheets under doping of transition metals. **2022**, 128, 1
- 438 Solution-Processed Two-Dimensional Materials for Scalable Production of Photodetector Arrays. **2022**, 31, 228-237
- 437 Selective substitution induced anomalous phonon stiffening within quasi-one-dimensional PB chains in SiP<sub>2</sub>.
- 436 Progress, Challenges, and Opportunities in Oxide Semiconductor Devices: A Key Building Block for Applications Ranging from Display Backplanes to 3D Integrated Semiconductor Chips. 2204663 4
- 435 Effect of stacking order on the vibration properties of bilayer black phosphorus. **2022**, 478,
- 434 Black Phosphorus: Fundamental Properties and Influence of Impurities Induced by Its Synthesis. **2022**, 14, 34867-34874 1
- 433 Recent progress in the edge reconstruction of two-dimensional materials. **2022**, 55, 414003 1
- 432 Black phosphorous nanomaterials as a new paradigm for postoperative tumor treatment regimens. **2022**, 20, 1
- 431 Phosphorus-Based Materials for High-Performance Alkaline Metal Ion Batteries: Progress and Prospect. 2201808 ○
- 430 An Investigation of Monolayer As<sub>1-x</sub>P<sub>x</sub> Solid Solutions: From a Theoretical Perspective. 2200747
- 429 Effects of edge defects on  $\pi^2$  borophene nanoribbon conductance. **2022**, 128388 1
- 428 Multilayer Ti<sub>3</sub>C<sub>2</sub>T<sub>x</sub>: From microwave absorption to electromagnetic interference shielding. **2022**, ○

427	BTE-Barna: An extension of almaBTE for thermal simulation of devices based on 2D materials. <b>2022</b> , 108504	
426	Theoretical studies of valleytronic and optical properties in monolayer MoP <sub>2</sub> X <sub>2</sub> Y <sub>2</sub> (XY=BTe,AlS,. <b>2022</b> , 106,	
425	Heat transfer in transversely coupled qubits: Optically controlled thermal modulator with common reservoirs.	0
424	2D semiconductors for specific electronic applications: from device to system. <b>2022</b> , 6,	3
423	Ultratough Hydrogen-Bond-Bridged Phosphorene Films. 2203332	1
422	Two-dimensional complementary gate-programmable PN junctions for reconfigurable rectifier circuit.	0
421	Generation of cost-effective MXene@polydopamine-decorated chitosan nanofibrous wound dressing for promoting wound healing. <b>2022</b> , 213055	2
420	Distinct optical and acoustic phonon temperatures in nm-thick suspended WS <sub>2</sub> : direct differentiating via acoustic phonon thermal field invariant. <b>2022</b> , 100816	
419	Two-dimensional CP <sub>2</sub> and Li <sub>x</sub> CP <sub>2</sub> (x=1 and 2) m. <b>2022</b> , 106,	0
418	Realization of unpinned two-dimensional dirac states in antimony atomic layers. <b>2022</b> , 13,	0
417	Strain modulated electronic and optical properties of laterally stitched MoSi <sub>2</sub> N <sub>4</sub> /XSi <sub>2</sub> N <sub>4</sub> (X=W, Ti) 2D heterostructures. <b>2022</b> , 115471	1
416	First principles study of biaxially deformed hexagonal buckled XS (X=Ge and Si) monolayers with light absorption in the visible region. <b>2022</b> , 139457	
415	Advances in Two-Dimensional Materials for Optoelectronics Applications. <b>2022</b> , 12, 1087	3
414	Polymorphic Phosphorus Applied to Alkali-Ion Battery Electrodes. 2200735	
413	Ultra-tough, photothermal healing and fire safety polystyrene/hydroxylated black phosphorus-triazine COF composites. <b>2022</b> , 244, 110166	1
412	New insights into the covalent functionalization of black and blue phosphorene. <b>2022</b> , 1215, 113839	1
411	Emerging exotic properties of two-dimensional ternary tetrahedral BCN: Tunable anisotropic transport properties with huge excitonic effects for nanoelectronics and optoelectronics. <b>2022</b> , 27, 100792	1
410	Self-powered anisotropic photo-responsive properties of tin mono-selenide (SnSe) photodetector. <b>2022</b> , 132, 112756	1

409	Structure design and properties investigation of Bi <sub>2</sub> O <sub>2</sub> Se/graphene van der Waals heterojunction from first-principles study. <b>2022</b> , 33, 102289	1
408	Half-metallicity in strained phosphorene nanoribbons. <b>2022</b> , 449, 128363	0
407	Liquefaction of water on the hydrophobic surface of black phosphorene: A reactive molecular dynamics simulation. <b>2022</b> , 364, 119947	0
406	Strain-tunable optical properties of the promising infrared detector AsP monolayer: A first-principles study. <b>2022</b> , 354, 114898	0
405	Black phosphorus analogue- 0D/2D multistructure of Tin(II) monosulfide for improved photocatalytic hydrogen evolution and pollutant removal. <b>2022</b> , 8, 119-128	
404	Impurity properties in phosphorene: First-principles calculations and comparisons. <b>2022</b> , 151, 107006	
403	Recent advancements in bismuth vanadate photoanodes for photoelectrochemical water splitting. <b>2022</b> , 26, 101060	0
402	Designing a perfect Phosphorene-Plasmon absorber and investigating its geometric irregularity effects: A simulation study. <b>2022</b> , 156, 108519	
401	Enhanced optoelectronic properties of solution-processed metal-chalcogenide devices via hydrogen-driven post-annealing. <b>2022</b> , 926, 166780	
400	Optical spectra of bilayer borophene synthesized on Ag(1 1 1) film. <b>2022</b> , 282, 121711	0
399	Unravelling the regulating role of stacking pattern on the tunable dipole, mechanical behavior and carrier mobility for asymmetric Janus SnSSe bilayer. <b>2022</b> , 33, 104191	
398	Synthesis and polymorphism of a new phase 1D chalcogenide M <sub>2</sub> N <sub>3</sub> X <sub>8</sub> structure based on the periodic table: Ta <sub>2</sub> Ni <sub>3</sub> S <sub>8</sub> with a tetragonal structure. <b>2022</b> , 926, 166752	0
397	Mid-Infrared Dual-Wavelength Passively Q-Switched Er: SrF <sub>2</sub> Laser by CsPbCl <sub>3</sub> Quantum Dots Absorber. <b>2022</b> , 12, 1265	1
396	Two-Dimensional Black Phosphorus: Preparation, Passivation and Lithium-Ion Battery Applications. <b>2022</b> , 27, 5845	1
395	First-principles study of divacancy defect in arsenene nanoribbon. <b>2022</b> , 170, 207376	0
394	Piezoelectricity and optical properties of janus MXY (M = Sb, As; X = Te, Se; Y = Br, I) monolayers. <b>2022</b> , 170, 207396	1
393	Adsorption of CO, NO, and SO <sub>2</sub> gases on pristine and single Ni <sub>3</sub> cluster doped arsenene monolayer for its potential application as sensor or adsorbent by density functional theory study. <b>2022</b> , 1217, 113871	0
392	A Type-II WSe <sub>2</sub> /BP heterostructure with adjustable electronic properties under external electric field and biaxial strain. <b>2022</b> , 251, 119256	0

- 391 Black phosphorus biomaterials for photo-controlled bone tissue engineering. **2022**, 246, 110245 ○
- 390 Tunable electronic structures of covalent triazine frameworks/GaS van der Waals heterostructures via a perpendicular electric field and parallel strain. **2022**, 806, 140069 1
- 389 Electric field- and polarisation-dependent two-photon absorption in bilayer black phosphorus. **2022**, 133, 112996 ○
- 388 Two-dimensional SiC Schottky junctions with symmetrical and asymmetrical metal electrode contacts. **2022**, 605, 154699 ○
- 387 SiC<sub>2</sub>/BP<sub>5</sub>: A pentagonal van der Waals heterostructure with tunable optoelectronic and mechanical properties. **2022**, 606, 154857 ○
- 386 The structure and electronic properties of the MoSe<sub>2</sub>/PtS<sub>2</sub> van der Waals heterostructure. **2022**, 24, 19853-19864 ○
- 385 A new phosphorene allotrope: the assembly of phosphorene nanoribbons and chains. **2022**, 24, 22572-22579 ○
- 384 Chapter 1. Introduction. **2022**, 1-32 ○
- 383 The magnetic anisotropy and spin filtering effect in ferromagnetic phosphorene. **2022**, 67, 931-934 ○
- 382 The structural, electronic and optical properties of four H<sub>2</sub>Se-based heterostructures with hyperbolic characteristics. **2022**, 24, 21674-21687 ○
- 381 Abnormally weak intervalley electron scattering in MoS<sub>2</sub> monolayer: insights from the matching between electron and phonon bands. **2022**, 14, 12007-12012 ○
- 380 Oxidation behavior of layered FeGeTe<sub>2</sub> (n = 3, 4, 5) and Cr<sub>2</sub>Ge<sub>2</sub>Te<sub>6</sub> governed by interlayer coupling. **2022**, 14, 11452-11460 ○
- 379 Quantum Dots: Applications in Environmental Remediation. **2022**, 1-22 ○
- 378 Chapter 6. Next Generation Electronics Based on Anisotropic 2D Materials. **2022**, 168-187 ○
- 377 Multi-functional O<sub>2</sub>/H<sub>2</sub> electrochemistry by an abundant mineral: a novel and sustainable alternative for noble metals in electrolyzers and metal-air batteries. 1
- 376 Several semiconducting two-dimensional silicon nanosheets assembled from zigzag silicene nanoribbons. **2022**, 14, 14038-14045 ○
- 375 It takes two: advances in employing the interactions between black phosphorous and metals in various applications. **2022**, 10, 18490-18508 ○
- 374 A two-dimensional Sb/InS van der Waals heterostructure for electronic and optical related applications. **2022**, 24, 22000-22006 ○


- 373 Non-equilibrium spin-transport properties of Co/phosphorene/Co MTJ with non-collinear electrodes under mechanical bending. 0
- 372 Black phosphorus-based nanohybrids for energy storage, catalysis, sensors, electronic/photonic devices, and tribological applications. **2022**, 10, 14053-14079 2
- 371 Design and Analysis of GO Coated High Sensitive Tunable SPR Sensor for OATR Spectroscopic Biosensing Applications. **2022**, 10, 103496-103508 0
- 370 Industrial applications of MXene nanocomposites. **2022**, 481-503 1
- 369 Enhanced performance of a n-Si/p-GaTe heterojunction through interfacial passivation and thermal oxidation. **2022**, 10, 11747-11754 0
- 368 A tellurium short-wave infrared photodetector with fast response and high specific detectivity. **2022**, 14, 13187-13191 1
- 367 Flake Size Limits for Growth of Vertically Stacked Two-Dimensional Materials by Analytical Diffusion-Based Kinetic Model. **2022**, 22, 5264-5271 0
- 366 Thickness Dependent Ultrafast Charge Transfer in BP/MoS<sub>2</sub> Heterostructure. 2206952 0
- 365 Infrared Light Emission Devices Based on Two-Dimensional Materials. **2022**, 12, 2996 2
- 364 Van der Waals imprinting of black-phosphorus-like binary alloyed monolayers with tunable band gaps and moiré superstructures. **2022**, 106, 0
- 363 Black Phosphorus: Mid-Infrared Light-Emitting Properties and Devices. **2022**, 0
- 362 Blue phosphorene/MoSi<sub>2</sub>N<sub>4</sub> van der Waals type-II heterostructure: Highly efficient bifunctional materials for photocatalytics and photovoltaics. 0
- 361 Covalent functionalization of black phosphorus nanosheets via insensitive glycidyl azide polymer with durable stability. 0
- 360 Synthesis of two-dimensional materials: How computational studies can help?. 0
- 359 First-principles Investigations on the Magnetic, Electronic, and Optical Properties of Honeycomb-Kagome-Structured Fe<sub>2</sub>O<sub>3</sub> Monolayer. 0
- 358 Chemical vapor deposition: a potential tool for wafer scale growth of two-dimensional layered materials. **2022**, 55, 473001 1
- 357 Transparent, Multivalued Transistors Enabled By Area-Selective Optical Doping on Ga-Doped IZTO Thin Films. 2200771 0
- 356 First-principles study of O-functionalized two-dimensional AsP monolayers: Electronic structure, mechanical, piezoelectric, and optical properties. 0

- 355 Black Phosphorus/Carbon Nanoframes for Efficient Flexible All-Solid-State Supercapacitor. **2022**, 12, 3311 0
- 354 The marriage of Xenes and Hydrogels: Fundamentals, Applications, and Outlook. **2022**, 100327 0
- 353 Emerging low-dimensional materials for nanoelectromechanical systems resonators. **2023**, 11, 21-52 0
- 352 Sumanene Monolayer of Pure Carbon: A Two-Dimensional Kagome-Analogy Lattice with Desirable Band Gap, Ultrahigh Carrier Mobility, and Strong Exciton Binding Energy. **2022**, 18, 2203274 0
- 351 Electronic and optical properties of the buckled and puckered phases of phosphorene and arsenene. 0
- 350 Integration and Applications of Nanomaterials for Ultrafast Photonics. 2200386 3
- 349 Metallic B2C3P Monolayer as Li-Ion Battery Materials: A First-Principles Study. **2022**, 10, 1809 1
- 348 2D Xenes: Optical and Optoelectronic Properties and Applications in Photonic Devices. 2206507 0
- 347 One-Pot Covalent Functionalization of 2D Black Phosphorus by Anionic Ring Opening Polymerization. 2201245 1
- 346 Electronic and Optical Properties of BP, InSe Monolayer and BP/InSe Heterojunction with Promising Photoelectronic Performance. **2022**, 15, 6214 0
- 345 Ultra-Narrow Phosphorene Nanoribbons Produced by Facile Electrochemical Process. 2203148 1
- 344 Scanning tunneling microscopy study of natural black arsenic. **2022**, 106, 0
- 343 Phonon-limited transport of two-dimensional semiconductors: Quadrupole scattering and free carrier screening. **2022**, 106, 1
- 342 Bandgap engineering in BP/PtO<sub>2</sub> van der Waals (vdW) hetero-bilayer using first-principles study. **2022**, 12, 095312 0
- 341 High-Temperature Nodal Ring Semimetal in 2D Honeycomb-Kagome Mn<sub>2</sub>N<sub>3</sub> Lattice. 0
- 340 Field Enhancement for the Composite MXene/Black Phosphorus-Based Metasurface. **2022**, 12, 3155 0
- 339 Review on recent advances in two-dimensional nanomaterials-based cathodes for lithium-sulfur batteries. 0
- 338 2D Structures Based Field-Effect Transistors (Review). **2022**, 67, 1134-1151 0

337	High-yield aqueous synthesis of partial-oxidized black phosphorus as layered nanodot photocatalysts for efficient visible-light driven degradation of emerging organic contaminants. <b>2022</b> , 134228	3
336	Novel two-dimensional PdSe phase: A puckered material with excellent electronic and optical properties. <b>2022</b> , 17,	1
335	Charge carrier dynamics in 2D materials probed by ultrafast THzspectroscopy. <b>2023</b> , 8,	0
334	Termolecular EleyRideal pathway for efficient CO oxidation on phosphorene-supported single-atom cobalt catalyst.	0
333	High-throughput design of functional-engineered MXene transistors with low-resistive contacts. <b>2022</b> , 8,	5
332	Experimental Realization of Semiconducting Monolayer Si <sub>2</sub> Te <sub>2</sub> Films. 2208281	0
331	Black-Phosphorus-Nanosheet-Reinforced Coating of Implants for Sequential Biofilm Ablation and Bone Fracture Healing Acceleration.	0
330	Phosphorus based hybrid materials for green fuel generation.	0
329	Raman tensor studies on defective non-van der Waals Bi <sub>2</sub> O <sub>2</sub> Se. <b>2022</b> , 12, 105105	0
328	Investigation of two-dimensional HfS <sub>2</sub> /PtSSe heterostructure with strong visible light adsorption and strain tunable bandgap. <b>2022</b> , 55, 475301	0
327	Rational Design of Black Phosphorus-Based Direct Z-Scheme Photocatalysts for Overall Water Splitting: The Role of Defects. 9363-9371	2
326	Gas sensing properties of alkali metal decorated pristine and defect $\delta$ -AsP monolayer toward acid SO <sub>2</sub> and alkaline NH <sub>3</sub> molecules. <b>2022</b> , 356, 114962	0
325	The zoology of two-dimensional van der Waals materials. <b>2022</b> ,	0
324	Ultrahigh thermoelectric performance of Janus $\delta$ Te <sub>2</sub> and $\delta$ SeTe <sub>2</sub> monolayers.	0
323	Two-dimensional van der Waals heterostructures (vdWHs) with band alignment transformation in multi-functional devices. <b>2022</b> , 12, 31456-31465	0
322	Electronic structure and interfacial contact with metallic borophene of monolayer ScSX (X=I, Br, and Cl).	0
321	Solid-phase sintering and vapor-liquid-solid growth of BP@MgO quantum dot crystals with a high piezoelectric response.	1
320	Exploring 2D Energy Storage Materials: Advances in Structure, Synthesis, Optimization Strategies, and Applications for Monovalent and Multivalent Metal-Ion Hybrid Capacitors. 2205101	0

319	2D Layers of Group VA Semiconductors: Fundamental Properties and Potential Applications. 2203956	2
318	Bioinspired interactive neuromorphic devices. <b>2022</b> ,	1
317	Charge and Spin Current Rectification through Functionalized Boron Nitride Bilayers. <b>2022</b> , 126, 18383-18392	0
316	Formation of One-Dimensional van der Waals Heterostructures via Self-Assembly of Blue Phosphorene Nanoribbons to Carbon Nanotubes.	0
315	Characterization of the electric transport properties of black phosphorous back-gated field-effect transistors. <b>2022</b> , 2353, 012005	1
314	Biological Effects of Black Phosphorus Nanomaterials on Mammalian Cells and Animals.	0
313	Ambipolar Nonvolatile Memory Behavior and Reversible Type-Conversion in MoSe <sub>2</sub> /MoSe <sub>2</sub> Transistors with Modified Stack Interface. 2205567	0
312	Polarization-sensitive infrared photodetectors based on van der Waals heterojunction with the unilateral depletion region. <b>2022</b> , 55, 495106	0
311	Highly insulating phase of Bi <sub>2</sub> O <sub>2</sub> Se thin films with high electronic performance.	0
310	Deciphering the Effects of 2D Black Phosphorus on Disrupted Hematopoiesis and Pulmonary Immune Homeostasis Using a Developed Flow Cytometry Method.	0
309	P-Type 2D Semiconductors for Future Electronics. 2206939	0
308	Enhanced Thermoelectric Performance in Black Phosphorene via Tunable Interlayer Twist. 2204197	0
307	Electronic structures and NIR-II optical properties of black phosphorus using first principles. <b>2022</b> , 18, 595-600	0
306	Biological Effects of Black Phosphorus Nanomaterials on Mammalian Cells and Animals.	0
305	Challenges for Nanoscale CMOS Logic Based on Two-Dimensional Materials. <b>2022</b> , 12, 3548	1
304	Tunable Electronic Property and Robust Type-II Feature in Blue Phosphorene/MoSi <sub>2</sub> N <sub>4</sub> Bilayer Heterostructure. <b>2022</b> , 12, 1407	0
303	An overview on room-temperature chemiresistor gas sensors based on 2D materials: Research status and challenge. <b>2022</b> , 110378	0
302	Fully Encapsulated and Stable Black Phosphorus Field-Effect Transistors. 2200546	1



301	Energy band alignment of 2D/3D MoS <sub>2</sub> /4H-SiC heterostructure modulated by multiple interfacial interactions. <b>2023</b> , 18,	0
300	2D tribotronic transistors.	0
299	Effect of surface Se concentration on stability and electronic structure of monolayer Bi <sub>2</sub> O <sub>2</sub> Se. <b>2022</b> , 155528	1
298	The Advanced Applications of 2D Materials in SERS. <b>2022</b> , 10, 455	0
297	Research progress of two-dimensional nano black phosphorous and fabrication methods. <b>2022</b> ,	0
296	Achieving metal-like malleability and ductility in Ag <sub>2</sub> Te <sub>1</sub> -S inorganic thermoelectric semiconductors with high mobility. <b>2022</b> , 3, 100341	2
295	Mixed Insulating State for van der Waals CoPS <sub>3</sub> . 10486-10493	1
294	M-cymene and m-xylene adsorption studies on hex-star arsenene nanosheets  DFT investigation.	1
293	Intrinsic and engineered properties of black phosphorus. <b>2022</b> , 28, 100895	0
292	Defect engineered Ti <sub>3</sub> C <sub>2</sub> T <sub>x</sub> MXene electrodes by phosphorus doping with enhanced kinetics for supercapacitors. <b>2022</b> , 435, 141372	0
291	2D Materials towards sensing technology: From fundamentals to applications. <b>2022</b> , 38, 100540	1
290	Photo-dynamics in 2D materials: Processes, tunability and device applications. <b>2022</b> , 993, 1-70	0
289	MXenes: An exotic material for hybrid supercapacitors and rechargeable batteries. <b>2022</b> , 56, 105914	0
288	Charge density, atomic bonding and band structure of two-dimensional Sn, Sb, and Pb semimetals. <b>2022</b> , 808, 140124	0
287	Effectiveness of the analytical models used in standard techniques for mechanical property characterization of 2D materials. <b>2022</b> , 33, 104802	0
286	Application of graphdiyne oxide in photoelectrochemical-type photodetectors and ultrafast fiber lasers. <b>2022</b> , 47, 101653	0
285	The half-metallicity induced by non-magnetic adatoms on phosphorene nanoribbons. <b>2023</b> , 648, 414406	0
284	Compressive solitary waves in black phosphorene. <b>2023</b> , 146, 115519	0

283	Epitaxial growth of elemental 2D materials. <b>2022</b> ,	0
282	Sensitivity Enhancement of Surface Plasmon Resonance (SPR) Sensor Assisted by BlueP/MoS <sub>2</sub> Based Composite Heterostructure. <b>2022</b> , 10, 116152-116159	0
281	Controlled hydrophilization of black phosphorene: a reactive molecular dynamics simulation approach.	1
280	Charge transmission of MoS <sub>2</sub> /MoTe <sub>2</sub> vertical heterojunction and it's modulation. <b>2023</b> , 0	0
279	Progress in the preparation, application, and recycling of black phosphorus. <b>2023</b> , 311, 137161	0
278	Prediction of new 2D Hf <sub>2</sub> Br <sub>2</sub> N <sub>2</sub> monolayer as a promising candidate for photovoltaic applications. <b>2023</b> , 294, 126979	0
277	First-principles calculations to investigate electronic structures and magnetic regulation of non-metallic elements doped BP with point defects. <b>2023</b> , 118, 108370	0
276	Ab initio Methods for Electronic Transport in Semiconductors and Nanostructures. <b>2023</b> , 1515-1558	0
275	Review on the Energy Transformation Application of Black Phosphorus and Its Composites. <b>2022</b> , 12, 1403	1
274	Controlled p-type Doping of Black Phosphorus Using AuCl <sub>3</sub> Molecules and Its Diode Applications.	0
273	Emerging Two-Dimensional Metal Oxides: From Synthesis to Device Integration. 2207774	0
272	Black phosphorus quantum dots: Nonlinear optical modulation material with ultraviolet saturable absorption. 10,	0
271	Anisotropic magneto-optical transport properties in black phosphorus induced by in-plane magnetic field.	0
270	Water adsorption and dynamics on graphene and other 2D materials: computational and experimental advances. <b>2023</b> , 8,	0
269	Mechanical cleavage of non-van der Waals structures towards two-dimensional crystals.	1
268	Two-dimensional Cr-based ferromagnetic semiconductor: Theoretical simulations and design. 10,	0
267	Emerging low-dimensional black phosphorus: from physical-optical properties to biomedical applications.	0
266	Electrochemically exfoliated phosphorene nanosheet thin films for wafer-scale near-infrared phototransistor array. <b>2022</b> , 6,	1

- 265 Two-Dimensional Half-Metallic and Semiconducting Lanthanide-Based MXenes. **2022**, 7, 40929-40940 ○
- 264 Optical redshift and blueshift spectra in monolayer  $\Gamma$ 12 -borophene: Inversion symmetry breaking effects. **2022**, 106, ○
- 263 MgXN<sub>2</sub> (X = Hf/Zr) Monolayers: Auxetic Semiconductor with Highly Anisotropic Optical/Mechanical Properties and Carrier Mobility. **2022**, 13, 10534-10542 1
- 262 Theoretical study on the electronic and transport properties of top and edge contact MoSiN<sub>4</sub>/Au heterostructure. **2022**, 128535 ○
- 261 Recent progress in black phosphorus nanosheets for improving the fire safety of polymer nanocomposites. **2022**, 110404 1
- 260 Magnetic Field-Controlled Bandgap of a Phosphorene-Based PN-Device for Sensing Application. ○
- 259 Vacancy-Regulated Charge Carrier Dynamics and Suppressed Nonradiative Recombination in Two-Dimensional ReX<sub>2</sub> (X = S, Se). **2022**, 13, 10656-10665 1
- 258 Evolution of Low-Dimensional Phosphorus Allotropes on Ag(111). ○
- 257 Progress, challenges, and opportunities of two-dimensional layered materials based electrochemical sensors and biosensors. **2022**, 26, 101235 ○
- 256 Electrical Transport Properties of Layered Black Phosphorus grown by Chemical Vapor Transport. 2200164 ○
- 255 Strong Interlayer Interaction for Engineering Two-Dimensional Materials. ○
- 254 Multidirectional strain-induced thermoelectric figure of merit enhancement of zigzag bilayer phosphorene nanoribbons. ○
- 253 MoO<sub>3</sub> Interlayer Modification on the Electronic Structure of Co/BP Interface. **2022**, 14, 2448 ○
- 252 Wigner molecules in phosphorene quantum dots. **2022**, 106, 1 1
- 251 Nonlinear optical properties and laser modulation of gold non-covalently doped all-inorganic perovskite. **2023**, ○
- 250 High-throughput analysis of tetragonal transition metal Xenes. **2022**, 24, 29406-29412 1
- 249 A first-principles study of the adsorption mechanism of NO<sub>2</sub> on monolayer antimonide phosphide: a highly sensitive and selective gas sensor. ○
- 248 Quantum manifestations in electronic properties of bilayer phosphorene nanoribbons. ○

- 247 Insights into the regulation of energy storage behaviors of antimonene in aqueous electrolytes. **2023**, 439, 141585 ○
- 246 Ultrathin Ti<sub>3</sub>C<sub>2</sub>T<sub>x</sub> MXene-based electrochemical transistor for highly sensitive determination of nitrite. **2023**, 928, 117012 ○
- 245 High performance 1D/2D CuO/MoS<sub>2</sub> photodetectors enhanced by femtosecond laser-induced contact engineering. ○
- 244 Tunable absorbance by the magnetic field in multilayer black phosphorene dielectric structures. **2023**, 457, 128569 ○
- 243 Effects of tilted Dirac cones and in-plane electric field on the valley-dependent magneto-optical absorption spectra in monolayer 8Bmmn borophene. **2023**, 457, 128578 ○
- 242 Analysis of 1/f and GB noise in Phosphorene FETs. **2023**, 200, 108530 ○
- 241 High-activity black phosphorus quantum dots/Au/TiO<sub>2</sub> ternary heterojunction for efficient levofloxacin removal: Pathways, toxicity assessment, mechanism and DFT calculations. **2023**, 307, 122838 ○
- 240 Theoretical study on the photocatalytic potential of BSe nanotubes for water splitting under visible light. **2023**, 566, 111771 ○
- 239 Two-dimensional nanomaterials: A critical review of recent progress, properties, applications, and future directions. **2023**, 165, 107362 1
- 238 A novel black-P/blue-P heterostructure for the photovoltaic applications. **2023**, 812, 140242 ○
- 237 Frontiers and recent developments on supercapacitor's materials, design, and applications: Transport and power system applications. **2023**, 58, 106104 ○
- 236 Bi<sub>2</sub>O<sub>3</sub> monolayer: A promising material as field-effect phototransistor and out-of-plane piezoelectric device. **2023**, 614, 156198 ○
- 235 Adsorption behavior of small molecule on monolayered SiAs and sensing application for NO<sub>2</sub> toxic gas. **2023**, 613, 156010 ○
- 234 Positive and negative Goos-Hänchen shifts in anisotropic two-dimensional atomic crystals. **2023**, 530, 129174 ○
- 233 Efficient carbon monoxide electroreduction on two-dimensional transition metal phosphides: A computational study. **2023**, 613, 156025 ○
- 232 Electrical and optical properties of Black Phosphorus under Strain effects: A First-principles Study. **2022**, ○
- 231 Ultrathin origami accordion-like structure of vacancy-rich graphitized carbon nitride for enhancing CO<sub>2</sub> photoreduction. ○
- 230 Anisotropy of the Optical Properties of Pentacene:Black Phosphorus Interfaces. **2022**, 126, 20694-20701 ○

229	Decorating InSe Surface by Gold Species for Improved Carrier Transport and Efficient Sunlight Harvesting Toward High-Performance Flexible Photodetectors. 2201685	2
228	DFT Coupled with NEGF Study of N-Type MOSFET Based on 2D Planar B2S3 Semiconductor. <b>2022</b> , 126, 20613-20619	0
227	The Application of Black Phosphorus Nanomaterials in Bone Tissue Engineering. <b>2022</b> , 14, 2634	0
226	Two-dimensional superconducting MoSi <sub>2</sub> N <sub>4</sub> (MoN) <sub>4n</sub> homologous compounds.	1
225	Interface Engineering and Device Applications of 2D Ultrathin Film/Ferroelectric Copolymer P(VDF-TrFE).	0
224	Progress and future of relative humidity sensors: a review from materials perspective. <b>2022</b> , 45,	2
223	Breathing Mode Temperature Coefficient Estimation and Interlayer Phonon Scattering Model of Few-Layer Phosphorene. <b>2022</b> , 7, 43462-43467	0
222	Tunable circular polarization responses of twisted black phosphorus metamaterials. <b>2022</b> , 30, 47690	0
221	Perspective and Outlook. <b>2022</b> , 295-316	0
220	The VdW Heterostructure Interface Physics. <b>2022</b> , 125-156	0
219	MXenes for Sulfur-Based Batteries. 2202860	0
218	Strong interlayer transition in a staggered gap GeSe / MoTe <sub>2</sub> heterojunction diode for highly efficient visible and near-infrared photodetection and logic inverter.	0
217	Width and split effects on effective spin flip through armchair phosphorene nanoribbons. <b>2022</b> , 137,	0
216	Waveguide integrated high-speed black phosphorus photodetector on a thin film lithium niobate platform. <b>2023</b> , 13, 272	0
215	Forming Hexagonal and Triangular Ultrathin WS <sub>2</sub> Shapes by Controlling the Flow of Vapor. 421, 149-160	0
214	Electron-scattering-induced entanglement between two atoms placed near the zigzag edge of a phosphorene ribbon. <b>2023</b> , 22,	0
213	The 2D Semiconductor Library. <b>2022</b> , 1-31	0
212	High-performance junction-free field-effect transistor based on blue phosphorene. <b>2022</b> , 6,	0

- 211 Double-layer stretching broadens the absorption range of the solar spectrum in XSi<sub>2</sub>N<sub>4</sub>. **2022**, 414583 ○
- 210 High-performances ultraviolet photodetector based on vertical van der Waals heterostructures. **2022**, 2383, 012037 ○
- 209 Robust and Enhanced Short-Wave Near-Infrared Light Emission in Phosphorene through Photon-Activated Oxidation. **2022**, 9, 3935-3942 ○
- 208 Tuning the Electronic and Mechanical Properties of Kagome Graphene via Hydrogenation. **2022**, 126, 21426-21437 ○
- 207 Nanomaterial-Based Electrically Conductive Hydrogels for Cardiac Tissue Repair. Volume 17, 6181-6200 ○
- 206 Recent progress in two-dimensional nanomaterials of graphene and MXenes for thermal camouflage. **2022**, ○
- 205 Gate-Controlled Metal to Insulator Transition in Black Phosphorus Nanosheet-Based Field Effect Transistors. **2022**, 5, 18376-18384 ○
- 204 Graphene and Two-Dimensional Materials-Based Flexible Electronics for Wearable Biomedical Sensors. **2023**, 12, 45 ○
- 203 Boost solar-to-hydrogen efficiency by constructing heterostructures with the pristine and Se/Te-doped AgInP<sub>2</sub>S<sub>6</sub> monolayers. **2022**, 156254 ○
- 202 A Theoretical Study on Adjustment of Negative Differential Resistance Effect in Monolayer GeS via Substitutional Doping. 2200499 ○
- 201 Identification of a Magnetic Phase via a Raman Spectrum in Single-Layer MnSe: An ab Initio Study. ○
- 200 Mechanical properties characterization of 2D materials via pressure bulge testing. ○
- 199 Heterogeneous complementary field-effect transistors based on silicon and molybdenum disulfide. ○
- 198 Progress in the synthesis of 2D black phosphorus beyond exfoliation. **2022**, 9, 041318 1
- 197 Recent progress of two-dimensional heterostructures for thermoelectric applications. **2023**, 35, 073001 1
- 196 Electronic and optical properties of the buckled and puckered phases of phosphorene and arsenene. **2022**, 12, ○
- 195 Sliding induced multiple polarization states in two-dimensional ferroelectrics. **2022**, 13, ○
- 194 Impaired barrier integrity of endothelial cells induced by PEGylated black phosphorus nanosheets. **2022**, 160645 ○

- 193 Black phosphorous-based biomaterials for bone defect regeneration: a systematic review and meta-analysis. **2022**, 20, 0
- 192 Nanomaterial-mediated Photoporation For Intracellular Delivery. **2022**, 0
- 191 Unique low-energy line defects and lateral heterostructures in phosphorene. **2023**, 98, 015815 0
- 190 High-throughput screening of 2D van der Waals crystals with plastic deformability. **2022**, 13, 0
- 189 Interlayer Doping of Cu on Bilayer Black Phosphorus for Enhanced Charge Transfer and Transport Properties. **2022**, 13, 11489-11495 0
- 188 Strongly Anisotropic Quasi-1D BaTiS<sub>3</sub> Chalcogenide Perovskite for Near-Infrared Polarized Photodetection. 2201859 0
- 187 Zero to Three Dimension Structure Evolution from Carbon Allotropes to Phosphorus Allotropes. 2201941 1
- 186 Low dimensional nanomaterials for treating acute kidney injury. **2022**, 20, 0
- 185 Measuring the Bandgap of Ambipolar 2D Semiconductors using Multilayer Graphene Contact. 2200075 0
- 184 High-Throughput Computational Screening of Two-Dimensional Semiconductors. **2022**, 13, 11581-11594 1
- 183 Recent Advances in Surface Modifications of Elemental Two-Dimensional Materials: Structures, Properties, and Applications. **2023**, 28, 200 0
- 182 Solvent-stabilized few-layer violet phosphorus and its ultrafast nonlinear optics. 1
- 181 Two/Quasi-two-dimensional Perovskite-based Heterostructures: Construction, Properties and Applications. 0
- 180 Controllable Synthesis of 2D Materials by Electrochemical Exfoliation for Energy Storage and Conversion Application. 2206702 0
- 179 Borophene-based materials for energy, sensors and information storage applications. **2023**, 0
- 178 Recent Progress in Emergent Two-dimensional Silicene. 0
- 177 Engineered Two-Dimensional Nanostructures as SERS Substrates for Biomolecule Sensing: A Review. **2023**, 13, 102 1
- 176 Room-Temperature Self-Powered Terahertz Photodetection in Ge-Intercalated Topological Insulator GeBi<sub>4</sub>Te<sub>7</sub>. 2200484 0

- 175 Record-high Work-function p-Type CuBiP 2 Se 6 Atomic Layers for High-photoresponse van der Waals Vertical Heterostructure Phototransistor. 2209995 ○
- 174 First-principles study on GeC/AsP heterostructure with type-II band alignment for photocatalytic water splitting. **2023**, 156298 ○
- 173 Preparation and characterization of SbAs nanorods for opto-electronics applications. **2023**, 46, ○
- 172 Disorder effects on the ballistic transport of gated phosphorene superlattices. **2023**, 107, ○
- 171 Printed Electronics Based on 2D Material Inks: Preparation, Properties, and Applications toward Memristors. 2201156 ○
- 170 Effect of 3d Transition Metal Atom Intercalation Concentration on the Electronic and Magnetic Properties of Graphene/MoS<sub>2</sub> Heterostructure: A First-Principles Study. **2023**, 28, 509 ○
- 169 Band gap anomaly in single-layer Nb<sub>2</sub>SiTe<sub>4</sub>-based compounds. **2023**, 0 ○
- 168 Investigation of the thermoelectric properties of the perfect and defective (3,7) boron nitride nanosheets by DFT. **2023**, 97, ○
- 167 O-doping effects on the adsorption and detection of acetaldehyde and ethylene oxide on phosphorene monolayer: A DFT investigation. **2023**, 140315 ○
- 166 Ionic liquid passivated black phosphorus for stabilized compliant electronics. ○
- 165 Highly sensitive detection of infected red blood cells (IRBCs) with plasmodium falciparum using surface plasmon resonance (SPR) nanostructure. **2023**, 55, 9
- 164 Optoelectronic properties of monolayer and bilayer AgI: role of many-body interactions. ○
- 163 Discovery of Clustered-P1 Borophene and Its Application as the Lightest High-Performance Transistor. **2023**, 15, 3182-3191 ○
- 162 Electrical Contacts With 2D Materials: Current Developments and Future Prospects. 2206550 ○
- 161 Theoretical prediction of type-II BP/SiH heterostructure for high-efficient electronic devices. ○
- 160 Thermoelectric properties of C2P4 monolayer: A first principle study. **2023**, 133, 015102 ○
- 159 An ultra-high vacuum system for fabricating clean two-dimensional material devices. **2023**, 94, 013903 ○
- 158 Temperature-dependent synthesis of SnO<sub>2</sub> or Sn embedded in hollow porous carbon nanofibers toward customized lithium-ion batteries. ○



157	Stability and electronic properties of two-dimensional Ga <sub>2</sub> O <sub>3</sub> and (M <sub>x</sub> Ga <sub>1-x</sub> ) <sub>2</sub> O <sub>3</sub> (M = Al, Ga) alloys. <b>2023</b> , 156439	0
156	Ultrathin high-temperature ferromagnetic rare-earth films: GdScGe and GdScSi monolayers. <b>10</b> ,	0
155	Spin Polarization in Ferromagnetic Barrier Phosphorene Superlattice Under an Exterior Magnetic Field.	0
154	Optical angular transparency and broadband absorption based on photonic topological transition in black phosphorus/aluminum oxide hyperbolic metamaterial. <b>2023</b> , 13, 015301	0
153	Graphene Oxide for Nonlinear Integrated Photonics. 2200512	3
152	Revealing the biotoxicity of phosphorene oxide nanosheets based on the villin headpiece.	0
151	Benchmarking fundamental gap of Sc <sub>2</sub> C(OH) <sub>2</sub> MXene by many-body methods.	0
150	Carrier and Phonon transport in 2D InSe and its Janus structures.	0
149	Graphene oxide for photonics, electronics and optoelectronics.	4
148	Synthesis of Two-Dimensional Metal, Metal Oxide and Metal Hydroxide Nanomaterials for Biosensing. <b>2023</b> , 161-185	0
147	Electric field modulated valley- and spin-dependent electron retroreflection and Klein tunneling in a tilted n-p-n junction of monolayer 1T'-Mo. <b>2023</b> , 107,	0
146	Two-dimensional H <sub>2</sub> and FBX (X = O, S, Se, and Te) photocatalysts with ultrawide bandgap and enhanced photocatalytic performance for water splitting. <b>2023</b> , 13, 2301-2310	0
145	Polarization-dependent excitons in Borophene-Black phosphorus heterostructures. <b>2023</b> , 291, 122372	0
144	Electrochemically Exfoliated Two-Dimensional Nanomaterials for Electronics. <b>2022</b> , 25, 427-436	0
143	Anisotropic Carrier Mobility and Spectral Fingerprints of Two-Dimensional $\alpha$ -Phosphorus Carbide with Antisite Defects. <b>2023</b> , 14, 214-220	1
142	Thermal Transport in 2D Materials. <b>2023</b> , 13, 117	0
141	Graphene Bridge Heterostructure Devices for Negative Differential Transconductance Circuit Applications. <b>2023</b> , 15,	0
140	Electric-Field-Tunable Spin Polarization and Carrier-Transport Anisotropy in an A-Type Antiferromagnetic van der Waals Bilayer. <b>2022</b> , 18,	0

- 139 2D heterostructures for advanced logic and memory devices. **2023**, 141-167 ○
- 138 Highly Specific Antibiotic Detection on Water-Stable Black Phosphorus Field-Effect Transistors. ○
- 137 Recent advances in single crystal narrow band-gap semiconductor nanomembranes and their flexible optoelectronic device applications: Ge, GeSn, InGaAs, and 2D materials. ○
- 136 Dimension-dependent magnetic anisotropy for tunable anomalous Hall effect in transition metal dichalcogenides. **2023**, 107, ○
- 135 Self-Powered and Broadband Bismuth Oxyselenide/p-Silicon Heterojunction Photodetectors with Low Dark Current and Fast Response. **2023**, 15, 5411-5419 1
- 134 Covalent Organic Frameworks: Recent Progress in Biomedical Applications. 1
- 133 Black phosphorus unipolar transistor, memory, and photodetector. **2023**, 58, 2689-2699 2
- 132 Two-dimensional MX<sub>2</sub>Y<sub>4</sub> systems: ultrahigh carrier transport and excellent hydrogen evolution reaction performances. **2023**, 25, 4519-4527 ○
- 131 Exploring the oxidation mechanisms of black phosphorus: a review. **2023**, 58, 2068-2086 ○
- 130 Unipolar barriers in near-broken-gap heterostructures for high-performance self-powered photodetectors. **2023**, 122, 043505 ○
- 129 2D materials for flexible electronics. **2023**, 169-206 ○
- 128 Exact Relationship between Black Phosphorus Thickness and Behaviors of Field-Effect Transistors. **2023**, 13, 1736 1
- 127 MXenes for energy applications. **2023**, 475-502 ○
- 126 Tuning electronic properties and contact type in van der Waals heterostructures of bilayer SnS and graphene. **2023**, 616, 156489 ○
- 125 Kubo conductivity in phosphorene. **2023**, 176, 111257 ○
- 124 Quantitative Characterization of the Anisotropic Thermal Properties of Encapsulated Two-Dimensional MoS<sub>2</sub> Nanofilms. ○
- 123 Energy spectrum and light absorption of arsenene quantum dots. **2023**, 35, 105542 ○
- 122 Optical properties and polaritons of low symmetry 2D materials. **2023**, 2, R03 ○

- 121 Enabling triferroics coupling in breathing kagome lattice Nb<sub>3</sub>X<sub>8</sub> (X = Cl, Br, I) monolayers. ○
- 120 Preparation and formation mechanism of few-layer black phosphorene through liquid pulsed discharge. **2023**, 11, 3652-3660 ○
- 119 Advances in the understanding of the structure-performance relationships of 2D material catalysts based on electron microscopy. ○
- 118 Two Dimensional Heterostructures for Optoelectronics: Current Status and Future Perspective. **2023**, 28, 2275 ○
- 117 Gate-defined two-dimensional hole and electron systems in an undoped InSb quantum well. **2023**, 5, ○
- 116 Black Phosphorous and Cytop Nanofilm-Based Long-Range SPR Sensor with Enhanced Quality Factor. **2023**, 2023, 1-10 ○
- 115 Energy Storage Mechanism of C12-3-3 with High-Capacity and High-Rate Performance for Li/Mg Batteries. ○
- 114 The Controllable Synthesis of High-Quality Two-Dimensional Iron Sulfide with Specific Phases. 2207325 ○
- 113 Sub-5 nm 2D Semiconductor-Based Monolayer Field-Effect Transistor: Status and Prospects. ○
- 112 Narrowing the optical gap of CdPS<sub>3</sub> single crystal via chemical intercalation using liquid ammonia method. **2023**, 363, 115116 ○
- 111 Effects of Electric Field and Strain on the BP/GeTe van der Waals Heterojunction. ○
- 110 General rules and applications for screening high phonon-limited mobility in two-dimensional semiconductors. **2023**, 107, ○
- 109 Ultrabroadband Imaging Based on Wafer-Scale Tellurene. ○
- 108 A review of enhanced electrocatalytic composites hydrogen/oxygen evolution based on quantum dot. **2023**, 121, 27-39 ○
- 107 Electronic transport properties of GeS single crystals grown by vapor transport from molten GeS source. **2023**, 609, 127153 ○
- 106 2D Mg<sub>2</sub>M<sub>2</sub>X<sub>5</sub> (M' = B, Al, Ga, In, Tl; X' = S, Se, Te) monolayers: Novel stable semiconductors for water splitting photocatalysts. **2023**, 621, 156892 ○
- 105 Injectable thermosensitive black phosphorus nanosheet- and doxorubicin-loaded hydrogel for synergistic bone tumor photothermal-chemotherapy and osteogenesis enhancement. **2023**, 239, 124209 ○
- 104 Visible light response in 2D QBi (Q=Si, Ge and Sn) monolayer semiconductors: A DFT based study. **2023**, 35, 105886 ○

- 103 Intrinsic ferromagnetic half-metal: Non-equivalent alloying compounds CrMnI<sub>6</sub> monolayer. **2023**, 623, 157084 ○
- 102 Fabrication, energy band engineering, and strong correlations of two-dimensional van der Waals moiré superlattices. **2023**, 50, 101829 ○
- 101 Insight into the growth mechanism of black phosphorus. **2023**, 18, ○
- 100 Structural and electronic properties of hexagonal MXH (M = C, Si, Ge and Sn; X = N, P, As and Sb) monolayers: A first-principles prediction. **2023**, 115710 ○
- 99 Recent advancements review in zinc oxide and titanium dioxide saturable absorber for ultrafast pulsed fiber laser. **2023**, 170855 ○
- 98 Effects of hexagonal boron nitride encapsulation on the electronic properties of Cu, Li, and O-doped black phosphorus monolayer. **2023**, 660, 414880 ○
- 97 Iron oxyhalides monolayers with excellent optical anisotropic properties and large anisotropic carrier mobility. **2023**, 949, 169832 ○
- 96 Electro- and magneto- optical properties of edge states in bilayer black phosphorene quantum dots. **2023**, 362, 115081 ○
- 95 Pristine and X-doped (X = B, N) phosphorene as platform materials to the removal of phenol: A theoretical insight. **2023**, 374, 121280 ○
- 94 Adhesive tapes: From daily necessities to flexible smart electronics. **2023**, 10, 011305 ○
- 93 Prediction of superconductivity in Li, K, Ca, and Sr-intercalated blue phosphorene bilayer using first-principle calculations. **2023**, 35, 135601 ○
- 92 Adsorption of 3d transition-metal atoms on two-dimensional penta-graphene: A first-principles study. **2023**, 27, 101611 ○
- 91 Research progress on black phosphorus hybrids hydrogel platforms for biomedical applications. **2023**, 17, ○
- 90 Design of a triple-band black phosphorus-based perfect absorber and full-wave analysis using the semi-analytical method of lines. **2023**, 53, 101112 ○
- 89 Investigating the stability of an explicit ADE-FDTD scheme for modeling graphene: Avoiding erroneous conclusions. **2023**, 275, 170608 ○
- 88 Emerging Two Dimensional Channel Materials for MOSFETs: A Review. **2022**, ○
- 87 Monolayer group IV monochalcogenides T-MX (M = Sn, Ge; X = S, Se) with fine piezoelectric performance and stability. **2023**, 122, 062903 ○
- 86 Black Phosphorus Nanosheets in Field Effect Transistors with Ni and NiCr Contacts. 2200537 ○

- 85 Electronic structure and layer-dependent magnetic order of a new high-mobility layered antiferromagnet KMnBi. **2023**, 35, 155801 ○
- 84 Ferromagnetism Induced by Magnetic Dilution in Van der Waals Material Metal Thiophosphates. **2023**, 6, 2200105 ○
- 83 A Review of Phosphorus Structures as CO<sub>2</sub> Reduction Photocatalysts. 2207840 ○
- 82 Graphene-Like Monoelemental 2D Materials for Perovskite Solar Cells. **2023**, 13, 2204074 ○
- 81 Heavy Ion Displacement Damage Effect in Carbon Nanotube Field Effect Transistors. **2023**, 15, 10936-10946 ○
- 80 Highly anisotropic and ultra-diffusive vacancies in Antimonene. **2023**, 15, 4821-4829 ○
- 79 Uniaxial Strain-Induced Tunable Mid-infrared Light Emission from Thin Film Black Phosphorus. **2023**, 14, 2092-2098 ○
- 78 Emerging Two-Dimensional Materials-Based Electrochemical Sensors for Human Health and Environment Applications. **2023**, 13, 780 ○
- 77 Dirac Fermions in Blue Phosphorene Monolayer. 2213664 ○
- 76 Two-Dimensional Semiconductors with High Intrinsic Carrier Mobility at Room Temperature. **2023**, 130, ○
- 75 Temperature dependent black phosphorus transistor and memory. **2023**, 4, 014001 ○
- 74 Towards an accurate description of one-dimensional pnictogen allotropes in nano-confinements. **2023**, 25, 9256-9263 ○
- 73 Injectable FHE+BP composites hydrogel with enhanced regenerative capacity of tendon-bone interface for anterior cruciate ligament reconstruction. 11, ○
- 72 The phonon thermal Hall angle in black phosphorus. **2023**, 14, ○
- 71 Nonlinear Hall effect in monolayer phosphorene with broken inversion symmetry. **2023**, 35, 165701 ○
- 70 Hydrogen-assisted growth of one-dimensional tellurium nanoribbons with unprecedented high mobility. **2023**, 63, 50-58 ○
- 69 Atomically Thin Twisted Heterostructure Optoelectronics Enhanced via vdW Interface Engineering. 2202396 ○
- 68 Structural properties of Bi/Au(110). **2023**, 34, 235601 ○

- 67 Direct Imaging of Band Structure for Powdered Rhombohedral Boron Monosulfide by Microfocused ARPES. **2023**, 23, 1673-1679 ○
- 66 Electrocatalytic reduction of N<sub>2</sub> on FeRu dual-atom catalyst anchored in N-doped phosphorene. **2023**, 539, 113032 ○
- 65 Percolation-Based Metal/Insulator Transition in Black Phosphorus Field Effect Transistors. **2023**, 15, 13299-13306 ○
- 64 Review of the role of ionic liquids in two-dimensional materials. **2023**, 18, ○
- 63 Trends in the Preparation and Passivation Techniques of Black Phosphorus Nanostructures for Optoelectronics Applications: A Review. **2023**, 6, 3159-3183 ○
- 62 Solution-Processed 2D Materials for Electronic Applications. **2023**, 5, 1335-1346 ○
- 61 hBN Encapsulation Effects on the Phonon Modes of MoS<sub>2</sub> with a Thickness of 1 to 10 Layers. **2023**, 10, ○
- 60 Spin-dependent tunnelling time in phosphorene superlattice. 1-14 ○
- 59 Two-Dimensional AMgB (A = Na, K; B = P, As, Sb, Bi) with Promising Optoelectronic and Thermoelectric Performances. **2023**, 5, 1405-1419 ○
- 58 Fluorine-Stabilized Defective Black Phosphorene as a Lithium-Like Catalyst for Boosting Nitrogen Electroreduction to Ammonia. ○
- 57 Fluorine-Stabilized Defective Black Phosphorene as a Lithium-Like Catalyst for Boosting Nitrogen Electroreduction to Ammonia. ○
- 56 2D material-based sensing devices: an update. **2023**, 11, 6016-6063 ○
- 55 High-Performance Photodetectors With Polarization Sensitivity Based on p-n and p-p+ Black Phosphorus/Germanium Heterojunctions. **2023**, 70, 1739-1744 ○
- 54 From highly oriented bulk black arsenic phosphorus to well-crystallized exfoliated flakes with enhanced anti-oxidation: precise control upon chemical vapor transport. **2023**, 11, 4683-4693 ○
- 53 WS<sub>2</sub> Transistors with Sulfur Atoms Being Replaced at the Interface: First-Principles Quantum-Transport Study. **2023**, 8, 10419-10425 ○
- 52 Chemical Sensors Based on Graphene and 2D Graphene Analogs. 2200057 ○
- 51 Computational Analysis of Metal Contact on Bi<sub>2</sub>O<sub>2</sub>Se with Se Surface Vacancies. 2201221 ○
- 50 2D-Material-Based Volatile and Nonvolatile Memristive Devices for Neuromorphic Computing. **2023**, 5, 1109-1135 ○

- 49 2D Layered Nanomaterials as Fillers in Polymer Composite Electrolytes for Lithium Batteries. **2023**, 13, ○
- 48 Preparation, properties, and applications of Bi<sub>2</sub>O<sub>2</sub>Se thin films: A review. **2023**, 44, 031001 ○
- 47 Structural Reconstruction Modulated Physical Properties of Titanium Oxide at the Monolayer Limit. **2023**, 127, 5631-5639 ○
- 46 Silver-ion-passivated black phosphorus photodetectors to improve the response time. **2023**, 47, 7432-7437 ○
- 45 Physics-based bias-dependent compact modeling of 1/f noise in single- to few-layer 2D-FETs. **2023**, 15, 6853-6863 ○
- 44 Soft Electronics for Health Monitoring Assisted by Machine Learning. **2023**, 15, 1 ○
- 43 Theoretical design of a photodetector based on a two-dimensional SnSe<sub>2</sub>/GaP type-II heterostructure. **2023**, 25, 2326-2338 ○
- 42 Two-Dimensional Nanocrystal Assemblies for Photocapacitive Devices. **2023**, 5, 1770-1777 ○
- 41 Epitaxial growth of borophene on substrates. **2023**, 100704 ○
- 40 Construction of A Novel 2D/1D/-2D RP/BP-Bi<sub>2</sub>WO<sub>6</sub> Composite with In Situ Junction and Z-scheme System for Enhanced Photocatalytic H<sub>2</sub> and H<sub>2</sub>O<sub>2</sub> Production. **2023**, 8, ○
- 39 Growth of single-crystal black phosphorus and its alloy films through sustained feedstock release. ○
- 38 Structural transition at the subsurface of few-layer Bi(110) film during the growth. **2023**, 7, ○
- 37 High-performance metal electrode-enhanced double parallel p-n heterojunctions photodetector. **2023**, 133, 124502 ○
- 36 Polarization Modulation on Charge Transfer and Band Structures of GaN/MoS<sub>2</sub> Polar Heterojunctions. **2023**, 13, 563 ○
- 35 Black Phosphorus Degradation during Intercalation and Alloying in Batteries. **2023**, 17, 6220-6233 ○
- 34 Step-guided epitaxial growth of blue phosphorene on vicinal Ag(111). **2023**, 7, ○
- 33 Two-dimensional C<sub>6</sub>X (X = P<sub>2</sub>, N<sub>2</sub>, NP) with ultra-wide bandgap and high carrier mobility. **2023**, 10, 045602 ○
- 32 Large-Area Black Phosphorus/PtSe<sub>2</sub> Schottky Junction for High Operating Temperature Broadband Photodetectors. ○

- 31 Efficient Non-Destructive Detection of Interface Adhesion State by Interfacial Thermal Conductance: A Molecular Dynamics Study. **2023**, 11, 1032 ○
- 30 Sequential hydrogen storage in phosphorene nanotubes: A molecular dynamics study. **2023**, ○
- 29 Covalent bonded bilayers from germanene and stanene with topological giant capacitance effects. **2023**, 7, ○
- 28 Antimonene quantum dots as bifunctional fluorescent sensors for rapid detection of cation (Fe<sup>3+</sup>) and anions (CrO<sub>4</sub><sup>2-</sup>/Cr<sub>2</sub>O<sub>7</sub><sup>2-</sup>). **2023**, 11, 041101 ○
- 27 Theoretical Study on the Electronic Properties of Two-Dimensional Covalent Triazine Frameworks/As van der Waals Heterostructures. **2023**, 2023, 1-8 ○
- 26 Two-dimensional TiCl<sub>2</sub>: a high-performance anode material for Na-ion batteries with high capacity and fast diffusion. ○
- 25 First principles study in two-dimensional antiferromagnetic Mn<sub>2</sub>Cl<sub>8</sub> with strain-controllable and hydrogenation. **2023**, 10, 046102 ○
- 24 Realizing a Superconducting Square-Lattice Bismuth Monolayer. ○
- 23 Strain-Modulated Electronic and Thermal Transport of Monolayer Black Arsenic Phosphorus. **2023**, 2463, 012042 ○
- 22 Terahertz Spectroscopy and DFT Analysis of Phonon Dynamics of the Layered Van der Waals Semiconductor Nb<sub>3</sub>X<sub>8</sub> (X = Cl, I). **2023**, 8, 14190-14196 ○
- 21 Gate-controlled photoresponse improvement in b-AsP/WSe<sub>2</sub> heterostructures with type-I band alignment. **2023**, 122, 151105 ○
- 20 Tunable hydrogen evolution activity of black antimony phosphorus monolayers via strain engineering: a first-principles calculation. **2023**, 129, ○
- 19 Ultra-high photo responsivity and self-powered photodetector in broad spectral range based on non-layered MnSe/WSe<sub>2</sub> heterojunction. 10, ○
- 18 Gate-Tunable van der Waals Photodiodes with an Ultrahigh Peak-to-Valley Current Ratio. ○
- 17 Recent Advances, Properties, Fabrication and Opportunities in Two-Dimensional Materials for their Potential Sustainable Applications. **2023**, 102780 ○
- 16 Epitaxial growth of 2D gallium selenide flakes for strong nonlinear optical response and visible-light photodetection. **2023**, 18, ○
- 15 Enhanced quantum capacitance in Ti, V, Cr, Fe, Ga, Ge, Se, and Br doped arsenene: A first principles investigation. **2023**, 823, 140500 ○
- 14 Advances in the Field of Two-Dimensional Crystal-Based Photodetectors. **2023**, 13, 1379 ○



- 13 Theoretical Study of Intercalation Effects: Graphene and hBN Layers in Metal and Monolayer Black Phosphorus Contacts. ○
- 12 MatHub-2d: A database for transport in 2D materials and a demonstration of high-throughput computational screening for high-mobility 2D semiconducting materials. ○
- 11 Casimir interaction with black phosphorus sheets. **2023**, 31, 15204 ○
- 10 Hydrogenation-induced interfacial bonding effects on the structural, electronic, and optical properties of GaN bilayer. **2023**, 112080 ○
- 9 Long-range electrostatic contribution to electron-phonon couplings and mobilities of two-dimensional and bulk materials. **2023**, 107, ○
- 8 Emerging monoelemental 2D materials (Xenes) for biosensor applications. ○
- 7 Development of in situ characterization of two-dimensional materials grown on insulator substrates with spectroscopic photoemission and low energy electron microscopy. **2023**, 264, 147318 ○
- 6 Chemistry of two-dimensional pnictogens: emerging post-graphene materials for advanced applications. ○
- 5 Thickness-dependent piezoelectricity of black arsenic from few-layer to monolayer. **2023**, 115175 ○
- 4 Controlled Bipolar Doping of One-Dimensional van der Waals Nb<sub>2</sub>Pd<sub>3</sub>Se<sub>8</sub>. ○
- 3 Direct gas phase synthesis of high-purity black arsenic phosphorus with non-metallic mineralizer. **2023**, 956, 170256 ○
- 2 Near-unity broadband infrared absorption in a graphene-black phosphorus bimodal triple-layer structure. **2023**, 13, 1535 ○
- 1 Hydrogen-Terminated Two-Dimensional Germanane/Silicane Alloys as Self-Powered Photodetectors and Sensors. ○